# Part V
## Applications in product development

# 18
## Biomechanical engineering of jeans

X. ZHANG[1,2], Y. LI[1], AND A. WONG[1]
[1]The Hong Kong Polytechnic University, China
[2]Xian University of Engineering Science & Technology, China

## 18.1    Introduction

### 18.1.1 Need for numerical simulation of jeans' mechanical performance

Jeans have become more and more popular in the world because they provide a satisfactory level of comfort and durability for consumers. Their fitness and pressure comfort have been identified as important attributes of mechanical comfort to satisfy the wearer's physiological and psychological needs. To quickly respond to the jeans market, it is necessary to predict jeans' mechanical performance at the design stage by using engineering design technology, for the optimal design of jeans in terms of functional performance and pressure comfort. This engineering design application involves two aspects of development: (i) the need to develop a mechanical model that is able to describe the dynamic mechanical interaction between jeans and the human body in the design stage with satisfactory accuracy; (ii) the need to develop a computational methodology to solve the model and to visualize the 3D distribution of the mechanical performances of the jeans.

The mechanical comfort of a garment during wear is determined by a complex process, in which the human body interacts dynamically with the garment on large surface contact areas. The interaction force generated during the dynamic interactions between the clothing and the human body induces the perception of various mechanical sensations. Therefore, the engineering design of jeans' mechanical performance based on the development of the mechanical model requires interdisciplinary knowledge and technologies mainly in four aspects: human physiology and psychology, clothing mechanics, contact mechanics and advanced computing technologies. Extensive research has been carried out experimentally on garment mechanical comfort, such as garment pressure. However, very little has been reported on the theoretical inverstigation of jeans' mechanical performance during wear by integration of the knowledge and technologies

for the development of advanced engineering design technology for jeans products.

## 18.1.2  Biomechanical features of body parts covered by jeans

Jeans cover the hip, the lower abdomen and the lower limbs of the human body. The abdomen consists of the abdominal cavity, of which the volume changes with respiration, and the digestion of food and drink. The lower limbs play an important role in supporting the whole body and in walking and other movements. Like other body parts, the lower limbs consist of skin, tissue, fat, bones, and so on. They also consist of muscles. The thicknesses of skin, fat, and muscles vary greatly among the abdomen, hip, thigh and shank, and even among different regions of the same part. For example, the hip and thigh have a much thicker layer of fat than the shank; and the thigh has a skin layer of different thickness at the front, the back, and the side, the skin at the side being the thickest. Actually, the skin elasticity also varies among different regions. All these differences lead to different sensibilities about pressure at different positions.

When the body is subjected to small external force, such as garment pressure during wearing, the bone can be considered as a stiff material without deformation. The skin may have tensile, shearing and bending deformations. The soft tissue, which consists of the adipose tissue and the skeletal muscles in passive condition, can be regarded as incompressed rubber, indicating that its shape distortion is much easier than its volume change. Therefore, to describe the interactive mechanics between a deformable human body and a garment, it is assumed that the human body consists of three major components: skin, soft tissue and bone.

## 18.1.3  Sensory perceptions and preference in jeans' wearing

Generally, by their nature, jeans are perfect-fitting or tight-fitting; at least they have close contact with the waist and thigh of the body. The mechanical interaction stimulates neurophysiological impulses of touch and pressure through the mechanical receptors in the deep layer of the skin, which further induces subjective perceptions and relevant pressure discomfort sensations of the human body. Growther[1] pointed that classic jeans are characterized by body-hugging or tight fitting, which may result not only in a sculptured form, but also in possible body malfunction in the long-term. The author suggests that (i) the fabric construction and the chosen angle of bias along the back-rise seam of a pair of jeans may directly contribute to clothing fit and body comfort, and (ii) that cotton denim may be pre-

shaped to accommodate body contours and so reduce the compressive forces of the fabric on the body in the jeans with close-fit styling.

The results reported by Makabe *et al.*[2] indicated that the pressure at the waist is influenced by the area covered, respiration and the ability of the garment to follow bodily movements. The subjective evaluation of clothing pressure at the waist showed that no sense of discomfort is perceived when the pressure is in the range of $0$–$15\,gf/cm^2$. Negligible or only slight discomfort is perceived when the pressure is in the range of $15$–$25\,gf/cm^2$, and extreme discomfort is perceived when the pressure exceeds $25\,gf/cm^2$. Through their study on girdle pressure,[3] they found that subjects complained of discomfort when the clothing pressure reached more than $40$~$54\,gf/cm^2$, and the discomfort areas are at the waistline, the thigh base, and the thigh front. The relation between waistband-pressure and wearing time was examined by a series of subjective experiments.[4] The results show that both the waist girth and the clothing pressure changed according to the time of day and increased significantly after eating. A linear relation between the increment of waist girth and the increment of waistband-pressure was observed.

## 18.2  Biomechanical modeling

Denton[5] pointed out that the level of garment pressure is a mechanical parameter that mainly depends on four factors: (i) design and fit of the garment; (ii) the different radii of curvature of body parts; (iii) the mechanical properties of the underlying tissue and (iv) the extensibility of the garment. Therefore, it is possible to predict garment pressure in terms of the geometrical and mechanical parameters of individual people wearing garments. The basic work is to develop a mechanical model of garment pressure for optimizing the design of a garment in terms of functional performance and pressure comfort at the design stage. Numerical simulation of garment pressure based on the model will help designers and consumers to see the pressure distribution of the garment on a body before the actual garment is produced. There is also a need for quick response to the changes of clothing marketing. This simulation has two objectives. The first is to predict jeans' mechanical performance on a human body in a 3D display by development of a jeans–body dynamic contact model. The second one is to study the mechanical interaction of the contact interface between the jeans and the human body.

### 18.2.1 Model description

During the process of wearing a garment, the human body deforms the garment and, in return, the pressure induced from the garment deforms the

skin and soft tissue of the body. The interactive deformations between the human body and the garment can be disintegrated into three deformation components. First, the garment is stretched to fit the human body, which induces pressure on the body. Secondly, the pressure compresses the elastic components of the body and makes the soft tissue flow or redistribute, and the skin is stretched accordingly. Thirdly, the rigid bone restrains the deformation of the skin and the soft tissue. The pressure distribution is changing dynamically with the garment stretch that accommodates the body shape and the body deformation during the wearing process.

Garment pressure is closely related to specific shapes of individual human bodies and garment styles. To obtain simulation results that are able to represent actual situations, a specific 3D geometric model for a particular individual female body needs to be developed and a specific 3D geometric model for a particular garment. For this simulation, 3D models of a female human body and jeans were generated by using commercial graphic software. The body is modeled with three layers of materials that have different properties, representing the bone, the soft tissue and the skin respectively.

As the basis of the analysis, there are the following assumptions:

(i)    The human model consists of three components: the bone, the soft tissue and the skin. The bone is regarded as a stiff shell, the skin as a thin elastic shell and the soft tissue as an incompressible rubber shell.

(ii)   The displacements of the skin and the soft tissue are the same when subjected to compression from the garment and the displacements cannot be permeated to the bone.

(iii)  The mechanical performances of the skin and the soft tissue are assumed to be of material linearity and geometrical non-linearity.

(iv)   The garment is regarded as a thin elastic shell of material linearity and geometric non-linearity, and the stress in its thickness direction is assumed to be negligible.

(v)    The garment is moving up along the human body from the foot to the waist without friction while the human body stands still during the wearing process.

(vi)   The contact between the human body and the garment is a dynamic process of coordinated contact, which is related to the overall stress distribution in the contacting objects.

The time-dependent contact system involves four objects (the garment, the skin, the soft tissue and the bone) and the three contact interfaces (between the garment and the skin, between the skin and the soft tissue, and between the soft tissue and the bone). At time $t = 0$, the garment occupies domain ${}^0\Omega^1$ and the human body occupies domains of ${}^0\Omega^2$ for the skin, ${}^0\Omega^3$ for the soft tissue and ${}^0\Omega^4$ for the bone, respectively. From time $t = 0$,

the garment starts to move from foot to waist to fit the body, during which it is occupying new domains $'\Omega^1$ and contacting the domain $'\Omega^2$ of the skin that corresponds to the domain $'\Omega^3$ and $'\Omega^4$ at any time $t > 0$.

## 18.2.2 Contact modeling

*Contact interfaces inside the body*

Shell elements are used in the discretization of the 3D human body. Figure 18.1a shows a schematic diagram of the constraint methods used in the contact interfaces inside the body. The method of merging matched nodes is used in the geometrical structure of the contact between skin and soft tissue. As the shell elements have no true thickness, the mid-surfaces of the skin and the soft tissue are regarded as coincident, as shown in Fig. 18.1a. Then, the elements of the skin and the soft tissue can be tied by merging the matched nodes at the mid-interfaces, which are marked with the circles shown in Fig. 18.1a. The merged nodes on the mid-surfaces will have the same degrees of freedom during the wearing process but have different stress–strain distributions due to their different mechanical properties, such as Young's modulus $E_t$ for the soft tissue and $E_s$ for the skin.

The method of offset tying is used in the geometrical structure of the contact between soft tissue and bone, to make the soft tissue and the skin both deform and show no penetration through the bone during the wearing process. A geometrical control distance $d_c$ between the mid-surfaces of the bone and the soft tissue is constructed, as shown in Fig. 18.1b, where the soft tissue is defined as the master surface and the bone as the slave surface. This $d_c$ can be regarded as the maximum compressive allowance of the skin and the soft tissue against the normal direction of the bone. The tying will work if the surfaces are close to each other. Therefore, a distance $d$ is used to determine whether a slave node is tied down or not. The distance $d$ is defined as 1 mm in the simulation, with consideration of the size of the shell
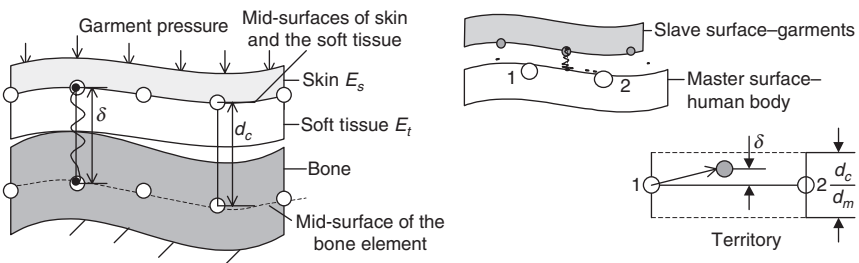


(a) Contact interfaces in the body model          (b) Contact between body and garment

*18.1* Contact interface.

elements used. The soft tissue must be tied to the bone if $\delta \leq d$, where $\delta$ is the distance between the slave node and the master segment.

The penalty constraint method[6] is used in the contact interface between the soft tissue and the bone. The contact constraint consists of placing normal interface springs between all penetrating nodes and the contact point, as shown in Fig. 18.1b. In the constraint, a contact force $q_{ci}$ applied between the slave node and its contact point is represented as $q_{c1} = -k_i\delta$, where $k_i$ is the stiffness factor for the master surface as spring stiffness. This $k_i$ is given in terms of its bulk modulus, the element volume, the segment area, and the penalty scale factor. Because the element sizes in the three layers are similar, each master node on the soft tissue can coincide with a slave node on the bone to ensure complete displacement compatibility along the interface. Therefore, no nodes on the bone interpenetrate through the surface of the soft tissue in the numerical simulation.

*Contact between body and garment*

Contact between the human body and the garment is modeled as a dynamic sliding interface. In the sliding contact algorithm, the human body is defined as a master surface with a target boundary and the garment is defined as a slave surface with hitting boundary, as shown in Fig. 18.1b. A slave node on the slave surface is assumed to be in contact with a master segment if $-d_m \leq \delta \leq d_c$. Here, $\delta$ is the distance between the slave node and the master segment, $d_c$ is control distance, and $d_m$ is the maximum penetration allowed. The equation defines a domain, which may be referred as a contact territory as shown in Fig. 18.1b. Thus, a node is considered as a contacting node if it is within the contact territory. In explicit analysis with the penetration method, it is natural to set $d_c$ to zero. Thus, the value of $\delta$ is equal to the penetration ${}^t p^1$ as a slave node passing through a master segment. The penalty constraint method consists of placing normal interface springs between all penetrating nodes and the contact surface, as shown in Fig. 18.1b. If the slave node does not penetrate, nothing is done. If it does penetrate, a contact force ${}^t q_{ci}$ is applied between the slave node and its contact point: ${}^t q_{c1} = -k_i {}^t p^1$, where, $k_i$ is the stiffness factor for the master surface, such as a spring stiffness, which is given in terms of the human body's bulk modulus $K_i$, its element volume $V_i$, its segment area $A_i$ and the penalty scale factor *fsi* that can be controlled. The spring stiffness matrix must be assembled into the global stiffness matrix.

Since the penetration ${}^t p^1$ depends only on the displacement of the contact system at time $t$ and $k_i$ as a chosen parameter, the normal contacting force ${}^t q_{ci}$ can be calculated by knowing the configuration of the contact system at $t$ time. Therefore, the contact force vector ${}^t Rc$ can be evaluated as a function of the displacement $U$.

## 18.2.3 Numerical solution

The solution of the mechanical contact system is complicated by (i) dynamic balance on space domain and on time domain; (ii) geometry non-linearity of the garment deformation; (iii) contact non-linearity due to the unknown contacting boundaries prior to the solution of the problem. Therefore, the model needs to be solved numerically using the finite element method in the space domain and the finite difference method in the time domain. The mechanical analysis of the model is performed using LS-Dyna Finite Element Method (FEM) software. The Belytschko–Lin–Tsay shell element[6] is used in the discretization of the 3D human body and the jeans, because of the large displacements and large rotations of the elastic objects. The total element number of the human body is 13362 (7221 elements for the bone, 3145 for the soft tissue, 2996 for the skin) and 1585 for the garment. Since the simulation is a non-linear problem, dynamic explicit analysis is carried out.

## 18.3    Computational experiments

### 18.3.1  Material properties

To validate the model, it is applied to simulate mechanical performance during wearing jeans of two different materials. Table 18.1 shows the mechanical parameters of the materials used in the simulation.

For lifting the trousers, the top of the trousers is given a speed 100 mm/s for moving from foot to the waist. The termination time is 6.5 seconds to make the garment fit to the body. The time step size is 3.5E-4 second, which can be adjusted according to the needs of computing stability.

*Table 18.1* Mechanical parameters of the materials used in the simulation

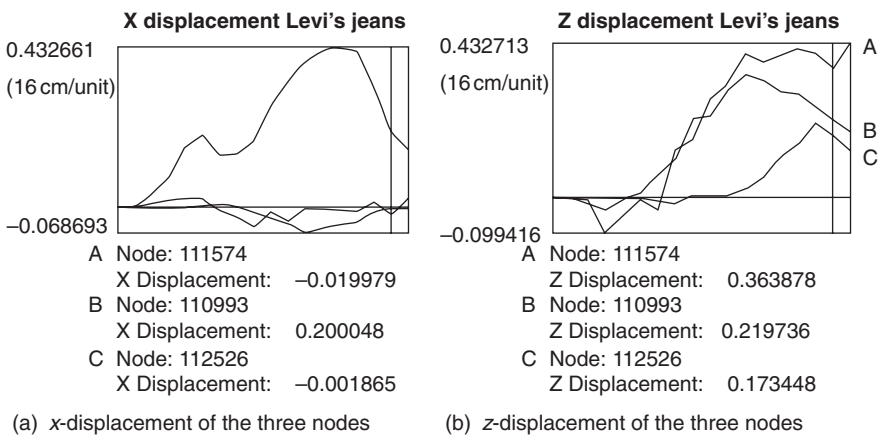| | | |
|---|---|---|
| The soft tissue | Density (kg/m³) | *937 |
| | Shear modulus (kg/m²) | ^3300 |
| | Poisson's ratio | 0.49 |
| The skin | Density (kg/m³) | *1060 |
| | Tensile modulus (kg/m²) | ^2000 |
| | Poisson's ratio | 0.3 |
| Denim A | Density (kg/m³) | 492 |
| | Tensile modulus (kg/m²) | 54000 |
| | Poisson's ratio | 0.48 |
| Denim B | Density (kg/m³) | 370 |
| | Tensile modulus (kg/m²) | 42000 |
| | Poisson's ratio | 0.40 |

*[7, 8]

## 18.3.2 Mechanical performance of jeans

*Jeans' deformation*

The simulation indicates the jeans stretch and recover during the wearing process. Also, the simulation shows the jeans wrinkle in the wearing process. To describe the process of the dynamic deformation, three nodes were selected on the jeans (A at the center front waist, B at the pelvis and C at the knee). Figure 18.2 shows the curves of the displacements of the three nodes, (a) for the displacement at $x$-direction of the body wide direction and (b) for the displacement at $z$-direction of the body thickness direction. The scale in the graphs is presented in the unit used in the finite element model, which is transformed into centimeters by multiplying by 16. The positive and negative values of the displacement are relative to the $x$-axis and $z$-axis. For the three nodes, the displacements at the $x$- and $z$-directions are all increasing to a maximum value and then decreasing, indicating the jeans stretch-recovery on passing the hips and finally fitting to the body. For node A at the center front waist, the positive value at the $z$-direction indicates that the jeans stretch; this increases to a value around 5.7 cm on passing the hips, then to 6.8 cm when finally fitted to the waist. For node B at the pelvis, a maximum stretch of 6.8 cm is observed in the $x$ direction when passing the hips. This decreases to 3.2 cm in the $x$-direction and 3.3 cm in the $z$-direction when finally fitted to the waist. For node C at the knee part, the maximum stretch is observed in the $z$-direction, finally recovering to 2.7 cm. Small displacements in the $x$-direction are observed at nodes A and C, as shown in Fig. 18.2a, due to their center positions on the jeans.
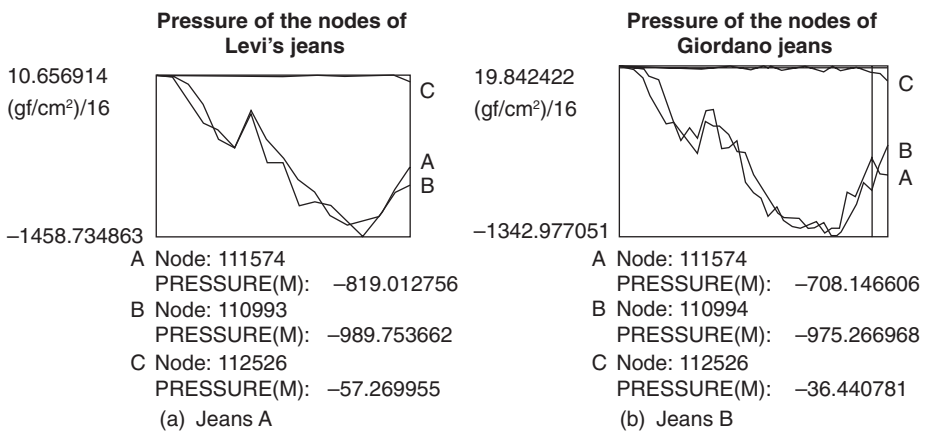


**X displacement Levi's jeans**

0.432661

(16 cm/unit)

−0.068693

A  Node: 111574
   X Displacement:    −0.019979
B  Node: 110993
   X Displacement:    0.200048
C  Node: 112526
   X Displacement:    −0.001865

(a) *x*-displacement of the three nodes

**Z displacement Levi's jeans**

0.432713

(16 cm/unit)

A

B
C

−0.099416

A  Node: 111574
   Z Displacement:    0.363878
B  Node: 110993
   Z Displacement:  0.219736
C  Node: 112526
   Z Displacement:    0.173448

(b) *z*-displacement of the three nodes

*18.2* Displacements at the three nodes of jeans A.

*Jeans' pressure distributions*

The pressure distribution of the two pairs of jeans was visualized. Negative values of pressure showed the pressure on the body induced by the garment; positive values of pressure showed the force in the garment to move it towards the skin when the garment did not contact the body at a specific point. From the pressure contour plots of the two pairs of jeans, it could be seen that the pressure does not distribute uniformly over different parts of the body. The pressure on most of the front waist area and the pelvis area covered by the clothing was in the range of 20 to 60 gf/cm². The pressure on most of the leg area and knees is in the range of 2 to 20 gf/cm². The pressure distribution on the front waist area and the upper leg area covered by jeans A showed some difference with the pressure distribution on the same areas by jeans B.

   Figures 18.3a and b show the dynamic pressure changes at the three nodes of jeans A and jeans B, respectively. For the two pairs of jeans, the pressure on node A at the center front waist and node B at the pelvis is increasing until the garment passes the hip area, and then decreasing as they fit to the waist. The pressure on node C arises when fitting to the waist. When jeans A are fitted the body, a high-pressure value of 62 gf/cm² is observed on node B, followed by a value of 51 gf/cm² on node A and 3.5 gf/cm² on node C at the knee. When jeans B are fitted to the body, a high-pressure value of 61 gf/cm² is observed on node B, followed by a value of 44 gf/cm² on node A and 2.3 gf/cm² on node C at the knee. The results indicate that the pressure distribution is different for the two pairs of jeans, but high pressure is observed at the pelvis and lower pressure at the knees



**Pressure of the nodes of Levi's jeans**

10.656914 (gf/cm²)/16

−1458.734863

A Node: 111574
  PRESSURE(M):  −819.012756
B Node: 110993
  PRESSURE(M):  −989.753662
C Node: 112526
  PRESSURE(M):  −57.269955

(a) Jeans A

**Pressure of the nodes of Giordano jeans**

19.842422 (gf/cm²)/16

−1342.977051

A Node: 111574
  PRESSURE(M):  −708.146606
B Node: 110994
  PRESSURE(M):  −975.266968
C Node: 112526
  PRESSURE(M):  −36.440781

(b) Jeans B

*18.3* Pressure change.

for the two pairs of jeans. It corresponds to the fact that the two pairs of jeans in the simulation are of the same style but different material properties. The pressure on the waist area and the pelvis area exceeds 25 gf/cm², which may cause extreme discomfort sensations according to the report by Makabe *et al.*[2]

### 18.3.3  Mechanical behavior of the human body

*Displacement of the skin*

In the wearing process, the human body is deformed under pressure from the garment. The displacements did not distribute uniformly over different parts of the body. Most of the areas covered by the jeans had displacements in the range 0.3 to 2.8 mm. High-deformation zones of 8 mm were observed on the front of the thigh. The distribution of the displacement was different for the two pairs of jeans, especially at the front of right thigh. The results indicated that the jeans have a different trimming function for the human body.

*Skin pressure distributions*

The distributions of the skin pressure in wearing the two pairs of jeans was visualized. A positive value of pressure showed that the skin pressure was towards the normal direction of the skin and the interface or against the garment pressure on the skin. A negative value showed the areas subject to the pressure from the garment or the areas not subject to pressure. The pressure distributions were similar to the distribution of skin displacement in the $z$-direction as observed for skin displacement, suggesting that the skin deformation induces pressure on the soft tissues (defined as the skin pressure).

In the case of wearing jeans A, many areas show a pressure value in the range 0.25 to 2.8 gf/cm², and values higher than 8 gf/cm² are observed at the front of the thigh and the hip back. In the case of wearing jeans B, many areas show pressure values in the range 0.75 to 3.6 gf/cm², and values higher than 9.4 gf/cm² are observed at the front of the thigh and the hip back. Compared with Fig. 18.3a and b, the trends of pressure change correspond to the jeans pressure changes, respectively. A high skin pressure of 6.8 gf/cm² is observed when wearing jeans B, and a lower skin pressure of 2.7 gf/cm² is observed at the node when wearing jeans A, while the garment pressure at node B shows similar values of 61 gf/cm² and 62 gf/cm² for the two pairs of jeans. It suggests that the skin pressure is not only induced by local contact but also by the overall contact situation. The results illustrate how the skin deformation induces the inner pressure on the soft tissues during wearing.

## 18.3.4 Model validation

From the simulation results, it is clear that the biomechanical human body provides quantitative descriptions of the mechanical interaction between the human body and the garment during wear, which can be neither simulated by using a rigid model of the human body nor easily measured by experimental methods. The mechanical interaction induces two pressure components: the pressure on the skin by the garment deformation and the pressure on the soft tissue due to the skin deformation, which determine the perception of pressure related comfort sensations.

To validate the simulation results, the predicted jeans pressures at the three nodes have been compared with the objective measurements at corresponding nodes on the Levi's jeans and Giordano jeans in a wearing experiment by Kwok *et al.* (private correspondence) where the geometrical model of the jeans used in the finite element analysis was constructed similar to the jeans styles in the experiment. Figure 18.4 shows comparisons with the two pairs of jeans respectively. The trends of the nodes' pressure show good agreement between the prediction and the experimental measurement; node B at the pelvis had high pressure, followed by node A at the center of the front of the waist, and C at the knee had lower pressure. However, for the two pairs of jeans, the predictions show nearly five times the measurement at node A, twice the measurement at node B, and four times the measurement at node C.

The factors influencing the deviation between the prediction and the measurements need examination. From previous experience in measuring garment pressure, the authors found that there are two major factors influencing the validation method. The first one is the difference between the wearer's actual body shape in the experiment and the geometrical model of the female human body used in the simulation. The second one is the distortion degree of the sensor insertion and the accurate degree of the sensor used that influences the level of garment pressure measured.
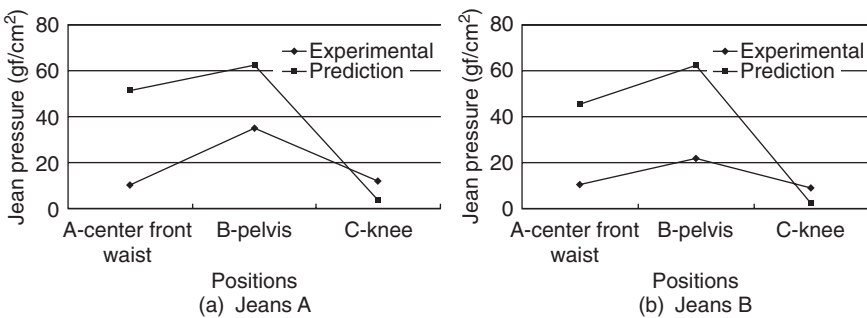


18.4 Pressure comparison between predicted and measured results.

Therefore, development of an experimental method is needed to obtain a map of the deformation of the garment and the pressure contours on the body and the garment. Also, the geometric models of a human body and a garment should be generated from the 3D measurements of the human body and the garment for individuals. All of those will be further work in this research direction.

## 18.4   Application in jeans' design

Numerical simulation on the basis of the biomechanical human model is able to generate quantitative descriptions of mechanical behaviors such as the garment deformation process, the garment pressure distribution, the human body deformation and the inner stress of the skin. The simulation results based on the model can help the design and evaluation of a garment at the design stage and in e-business use before it is manufactured.

From the simulations of garment deformation in the fitting process, the fit of a garment on a body can be evaluated. The quantitative description of the displacement of garment 3D directions, as shown in Fig. 18.2, may give designers a guide to adjust the garment size.

The predicted pressure distribution of a garment provides a map of the mechanical function of the jeans on a body. It helps to optimize the design of jeans in terms of functional performance and pressure comfort. With the numerical data from the solution of the model, visualization of mechanical sensory perceptions can be achieved based on the investigation of the relationship between objective stimulus and subjective perceptions, and the investigation of the relationship between the predictions and the objective measurements. Designers can judge whether the jeans meet the comfort requirements by comparing the predictions with desirable values, such as desirable pressure distribution or subjective perception of comfort pressure.

The validation of the work has more limitations because jeans pressure varies with individual human situations and pressure comfort is a very subjective sensation. The authors have found that the type of jeans and body posture have a significant influence on the pressure comfort rating. Therefore, to model jeans of various types the dynamic change of body posture is necessary in the simulation to aid sensory engineering design.

## 18.5   Acknowledgement

## 18.6    References

1. Growther, E.M., Comfort and Fit in 100% Cotton-Denim Jeans. *Journal of the Textile Institute*, 1985: p. 323–338.
2. Makabe, H. *et al.*, Effect of Covered Area at the Waist on Clothing Pressure. *Sen'i-Gakkaishi*, 1991. **49**(10): p. 513–521.
3. Makabe, H. *et al.*, A Study of Clothing Pressure Developed by the Girdle. *Journal of the Japan Research Association for Textile End-uses*, 1991. **32**(9): p. 424–438.
4. Mitsuno, T., Changes in the waistband-pressure according to time of day – In special reference to diet and the phase of menstrual cycle. *Journal of Japan Research Association for Textile End-uses*, 1999. **40**(10): p. 57–66.
5. Denton, M.J., Fit, Stretch, and Comfort. *Textiles*, 1972. **1**(1): p. 12–17.
6. Hallquist, J.O., *LS-DYNA Theoretical Manual*. 1998: Livermore Software Technology Corporation.
7. Yamada, H., *Strength of Biological Materials*. 1970: The Williams & Wilkins Company Baltimore. 226.
8. Zheng, X.Y., *Advances in Sports Biomechanics*. 1998, Beijing: Guo Fang Gong Ye Press. p. 145–147.

# 19

## Biomechanical engineering of a sports bra

Y. LI[1], X. ZHANG[2], AND K. W. YEUNG[1]
[1]The Hong Kong Polytechnic University, China
[2]Xian University of Engineering Science & Technology, China

## 19.1 Designing a sports bra

### 19.1.1 Introduction

A bra is the most feminine of foundation garments, required to satisfy the aesthetic needs and physiological health and comfort of the wearer. Generally, sports activity puts tremendous stress on breasts and the tissue surrounding them. A good bra offers the best support and protection against damaging breast tissue. Most women wear their bras between 10 and 12 hours every day from puberty until death. Therefore, it is important to select and wear a bra that is a good fit with support and pressure comfort. To optimize the design of a bra with such properties, the mechanical mechanisms involved in the dynamic contact between breast and bra need to be studied experimentally and theoretically. There is a very limited amount of literature in this area, particularly in theoretical investigation. A number of papers have been published in Japan on the measurement of garment pressure and relevant subjective sensations in wear trials.[1–4] Makabe *et al.* studied the pressure of brassieres by letting subjects wear brassiere samples that were designed in different shapes, materials and patterns.[1] Pressures were measured at 6 points under the bra. The pressure of the most comfortable brassiere sample was $24\,mm\,Hg$ ($32.40\,gf/cm^2$) at the point where the strap and the shoulder line cross, and $11–16\,mm\,Hg$ ($14.85–21.60\,gf/cm^2$) at the points under bust line and lateral top areas of the cup.

To achieve design optimization, a thorough theoretical understanding of the mechanisms and processes concerning the physiology, psychology and physics of the breast and bra are needed as the foundation of engineering design, which involves a number of aspects of research. Firstly, the human body needs to be scanned and digitized as the actual shape and dimension of the body and breast have a critical influence on the garment–skin contact process. Secondly, biomechanical models of the body and breast need to be developed as different parts of the body have different structural and material features. Thirdly, mechanical models need to be developed to

describe the dynamic mechanical interaction between the body (breast) and garment with satisfactory accuracy. Finally, computational methodology to solve the models and computing technology needs to be developed to visualize the dynamic interactions.

### 19.1.2 Biomechanical characteristic of breasts

Breasts comprise a number of different structures, each with their own specific function. One-third of the breast is composed of fatty tissue. The other two-thirds are made up of structural components called ducts and lobules. Fat fills the spaces between lobules and ducts. There are no muscles in the breast, but muscles lie under each breast and cover the ribs. Each breast also contains blood vessels and vessels that carry lymph. The breast increases in volume during pregnancy and generally weighs between 400–600 grams, increasing up to 800 grams during lactation.[5] Very weak ligaments, which stretch easily, support the breasts. The overlying skin of the breast offers only secondary support.

During walking, breasts bounce with each foot-strike, and this repeated action accelerates permanent stretching of the skin and sagging. Easily stretched ligaments cause the breast to sag. Excessive breast motion is the most common cause of movement discomfort during physical activity. Therefore, the breast structures, lacking internal anatomical support, require some type of external support, including weight support, movement restriction and compression by flattening the breast against the body, depending on an individual's needs and shape.

### 19.1.3 Mechanical characteristics of a bra

A good design of a 3D structural bra is probably the most important factor influencing the bra's functional performance and dynamic comfort during wear. It needs to be constructed with an appropriate structure that induces basic load distribution in the bra. The front straps should be positioned so that they lie in a direct line of lift over the nipples, allowing for optimal vertical breast support. The strap fabric should also be wide to allow for greater force distribution to prevent the straps digging into the shoulders. Fasteners, hooks and wires should be covered to avoid irritation. A good bra does not chafe around the arms or ribcage. Actually, most sports bras come without wires as these can puncture the skin during physical activity. All of these factors should be considered in a 3D-structural design of a bra. The contact interface between the breast and bra can be regarded as a dynamic coordinated contact. It represents the contact feature that the magnitude of the contact interface is comparable to the effective surfaces of a woman's body and bra.

Fabric stretch is another important factor influencing the effectiveness of the support. A bra should have enough elasticity to accommodate upper torso movement but prevent breast movement. It should be sufficiently elastic in the horizontal plane to allow for chest expansion while breathing. However, elasticity in the vertical plane should be limited to minimize vertical breast movement. Straps should have limited elasticity for the same reason. Fabric-stretch in multi-directions and frictional slippage generate pressure from a bra over the skin surface. Generally, the mechanical properties of desirable bra fabrics are both lower tensile modulus with large deformation and effective elastic recovery, which can be regarded as the mechanical properties of material linearity but geometric non-linearity.

## 19.2   Biomechanical modeling

### 19.2.1  Mechanical interactions between breast and bra

To optimize sports bra design, a biomechanical model for numerical simulation of mechanical interactions of bra and breast during wear was developed.[6] Based on analyzing the mechanical characteristics of breast and bra, a mechanical model was developed based on the theory of contact mechanics. The finite element method is used in the time domain for deriving a numerical solution of the dynamic contact model. A female wearing a bra and walking at a constant speed is simulated. During walking, breasts may bounce with each foot-strike, causing mechanical deformation in the breast. Meanwhile, mechanical interaction occurs at the contact surface between the breast and bra that supports and compresses the breasts. The external forces on an element of the breast involve gravity $q_g$, the interactive contact force $q_c$ at the normal direction of the contact surface, the friction $q_f$ of the bra as it is slipping on the breast surface. Contact force $q_c$ and friction $q_f$ are interaction forces between breast and bra. The mechanical forces will cause the internal strain–stress and the inertia force $q_i$ within the breast and the bra respectively.

By analyzing the characteristics of the breast and bra, the authors developed a mechanical model to simulate the mechanical interaction as a female body wears a sport bra and walks at a constant speed $V_z$, which results in an up–down cycling motion of the body with speed $V_y$, according to analysis of the sports biomechanics during human walking.[7]

### 19.2.2  Model development

*Model assumptions*

On the basis of the analysis, the following assumptions are made:

(i)     The female body is assumed to be a bi-material body that consists of two material components within an object: elastic material for the breast part and rigid material for the other part.

(ii)    The bra is considered as a thin elastic shell with material linearity and geometric non-linearity; the stress in the fabric thickness is assumed to be zero.

(iii)   The body always keeps in contact with the highest point of the bra's shoulder strap.

(iv)    The contact between breast and bra is dynamic coordinated contact, due to the contact feature that the magnitude of the contact interface is comparable to the effective surfaces of the breast and bra.[8]

(v)     The friction between the human body and the garment is neglected.

*Model descriptions*

Figure 19.1 shows the time-dependent contact system between the female human and the bra in a fixed global coordinate system $\mathbf{x}$ $(x_1, x_2, x_3)$. In this system, the bra is regarded in a domain $\Omega^1$, and the human body in a domain $\Omega^2$ that consists of two connecting sub-domains of elastic breast $\Omega_e^2$ and rigid body $\Omega_r^2$, as shown in Fig. 19.1. At time $t = 0$, the bra and the human occupy domains $^0\Omega^1$ and $^0\Omega^2$ in their unreformed configuration respectively. The human body and the bra are all simply connected so that there is no interior boundary in any of them, satisfying physical constraint:

$$^t\Omega^1 \cap {}^t\Omega^2 = \varnothing \quad (t \geqslant 0),$$

where $\varnothing$ denotes a null space, indicating that $\Omega^1$ and $\Omega^2$ do not penetrate each other.
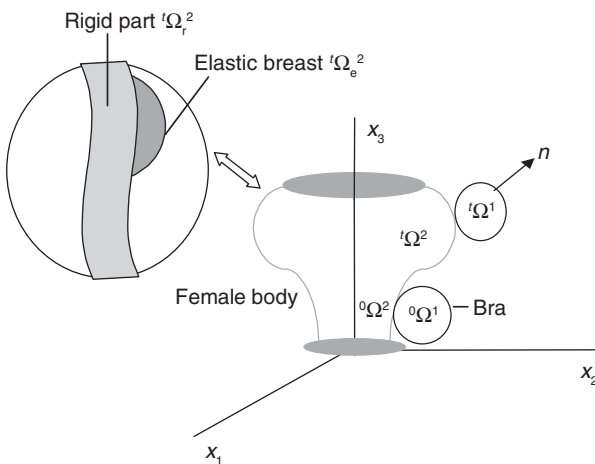


*19.1* Global coordinate system of the contact system.

From time $t = 0$, the human body moves to occupy new domain ${}^{t}\Omega^2$, contacting the domain ${}^{t}\Omega^1$ of the bra at any time $t > 0$. The boundaries of ${}^{t}\Omega^1$ and ${}^{t}\Omega^2$ are denoted by ${}^{t}\Gamma^1$ and ${}^{t}\Gamma^2$, respectively, which consists of three components:

$${}^{t}\Gamma^n = {}^{t}\Gamma_d^n \cup {}^{t}\Gamma_f^n \cup {}^{t}\Gamma_c^n \quad n = 1,$$

where $\Gamma_d$ denotes prescribed displacements boundary, $\Gamma_f$ denotes prescribed load boundary, and $\Gamma_c$ denotes the contact boundary where contact may occur, and $\cup$ denotes the union operator.

*Governing equations*

The motion equation of the bra at time $t$ is:

$$\frac{\partial {}^{t}\sigma_{ji}(x)}{\partial {}^{t}x_j} + {}^{t}q_{g_i}(x) = \rho {}^{t}a_i(x), x \in {}^{t}\Omega^1; i = 1 \text{ to } 3 \quad \text{and} \quad j = 1 \text{ to } 3$$

For the female body of bi-material, the motion equation is written in the two sub-domains of elastic breast $\Omega_e^2$ and rigid body $\Omega_r^2$ respectively:

$$\frac{\partial {}^{t}\sigma_{ji}(x)}{\partial {}^{t}x_j} + {}^{t}q_{g_i}(x) = \rho {}^{t}a_i(x), x \in {}^{t}\Omega_e^2; i = 1 \text{ to } 3 \quad \text{and} \quad j = 1 \text{ to } 3 \quad \text{and}$$

$${}^{t}q_{g_i}(x) = \rho {}^{t}a_i(x), x \in {}^{t}\Omega_r^2; i = 1 \text{ to } 3 \text{ and } j = 1 \text{ to } 3,$$

where $t$ denotes time; $x$ a position vector; $a(x)$ the acceleration field; ${}^{t}\sigma_{ij}(x)$ is the Cauchy stress components that give the actual traction on an imaginary plane at a point within an object; ${}^{t}q_{g_i}(x)$ is the $i$-th component of the gravity ${}^{t}q_g(x)$ on an object, $\rho$ is the mass density of an object which is assumed constant, and $a_i(x)$ is the $i$-th component of the acceleration vector of a material particle within an object.

For the bra and the breast of linear elasticity, the stress–strain relationship is given by the generalized Hooke's law,[9] i.e.,

$${}^{t}s_{ij} = c_{ijkl} {}^{t}\varepsilon_{kl}, \quad \text{on} \quad {}^{t}\Omega^1 \quad \text{and} \quad {}^{t}\Omega_e^2, k = 1 \text{ to } 3 \quad \text{and} \quad i = 1 \text{ to } 3,$$

where $c_{ijkl}$ are material constants; $s_{ij}$ is a component of the second Piola–Kirchhoff stress tensor that is related to the Cauchy stress component $\sigma_{ij}(x)$; $\varepsilon_{kl}$ is a component of the Green–Lagrange strain tensor to describe the deformation of geometric non-linearity, which consists of linear and non-linear components ${}^{t}e_{ij}$ and ${}^{t}\eta_{ij}$:

$${}^{t}\varepsilon_{ij} = {}^{t}e_{ij} + {}^{t}\eta_{ij}$$

$${}^{t}e_{ij} = ({}^{t}u_{i,j} + {}^{t}u_{i,j})/2, \qquad {}^{t}\eta_{ij} = {}^{t}u_{k,i} {}^{t}u_{k,j}/2,$$

where, $\quad {}^{t}u_{i,j} = \dfrac{\partial {}^{t}u_i}{\partial X_j}, \quad$ on ${}^{t}\Omega^1$ and ${}^{t}\Omega_e^2; \quad k = 1 \text{ to } 3$ and $i = 1 \text{ to } 3$.

*Various conditions*

*Initial speed*: Initial speed is exerted on the rigid body part, which consists of two components: horizontal motion with speed $V_z$ at $x_1$-direction and up–down motion with speed $V_y$ in $x_3$-direction, which are presented as:

$$^0V_1(x) = V_z \quad \text{and} \quad ^0V_3(x) = V_y \quad \text{on} \quad ^t\Gamma^2_d.$$

*Displacement boundary condition*: According to assumption (iii), the shoulder strap of the bra has the same movement as the body. The displacement boundary conditions on these contact points are represented as follows:

$$^tu_1(x^1) = {}^tu_1(x^2), \quad \text{and} \quad ^tu_3(x^1) = {}^tu_3(x^2), \quad \text{on} \quad ^t\Gamma^n_d, n = 1,2.$$

*External force*: Gravity exerted on the bra, the breast and the rigid body part is expressed as:

$$q^n_g = \rho^n g, \quad \text{on} \quad ^t\Omega^1, {}^t\Omega^2_e, {}^t\Omega^2_r, \text{where } g \text{ is gravity acceleration.}$$

*Contact conditions*: For the frictionless contact interfaces denoting the contact force $q^n_c$, then by Newton's third law, we have:

$$^tq^n_{c1} = -{}^tq^{n+1}_{c1}, \quad \text{on} \quad ^t\Gamma^1_c \cup {}^t\Gamma^2_c, n = 1,$$

where $^tq^n_{c1}$ is the component of contact force $^tq^n_c$ in the normal direction of contact points. The mechanical contact condition as a constraint on the normal contact force $^tq^n_{c1}$ is:

$$^tq^n_{c1} \leq 0, \quad \text{on} \quad ^t\Gamma^1_c \cup {}^t\Gamma^2_c, n = 1,2.$$

This means the interactive pressure is exerted on the object $n$ against its normal direction of the contact boundary points.

## 19.2.3 Numerical simulation

*3D geometrical models*

The 3D geometrical models are described by B-spline surfaces. The Belytschko–Lin–Tsay shell element[10] is used in the discretization of the 3D surfaces of the female body and the garment. The bi-material model of the female body is constructed by tying the nodes of the elastic breast to the rigid chest. The total element number of the female body is 24790 (5770 elements for the breast, 19120 for the rigid part), and 2386 for the bra.

*Table 19.1* Mechanical parameters of the materials

| | | |
|---|---|---|
| The bone | Density (kg/m³) | *1579 |
| | Compression modulus (kg/m²) | *489000 |
| | Poisson's ratio | 0.3 |
| The breast | Density (kg/m³) | 2250 |
| | Tensile modulus (kg/m²) | 2500 |
| | Poisson's ratio | 0.45 |
| Bra | Density (kg/m³) | 455 |
| | Tensile modulus (kg/m²) | 3500 |
| | Poisson's ratio | 0.32 |

*[11] and [7]

*Material properties*

The mechanical properties of the human body were estimated from the published data in the literature.[7,11] The breast density was estimated from its weight and volume. The tensile modulus of the fabrics were tested on an Instron tensile machine and the Poisson's ratio was estimated from the measurements of a Kawabata bi-tensile test. Table 19.1 shows the mechanical parameters of the materials used in the computing.

*Simulation conditions*

In the simulation, it is assumed that the female model is walking at an initial speed $V_z$, which results in a cycling motion of the body in the y-direction with speed $V_y$. The $V_z$ is specified as 10 cm/s and $V_y$ as 30 cm/s, and the time period of motion is 0.05 seconds. Thus, the movement amplitude of the human body in the y-direction is about 1.5 cm in the motion period. The time step size is 1.08E-4 second, which can be adjusted according to the needs of computing stability. The numerical computation is implemented by using the commercial finite element software, LS-DYNA.[10]

## 19.3    Biomechanical analysis
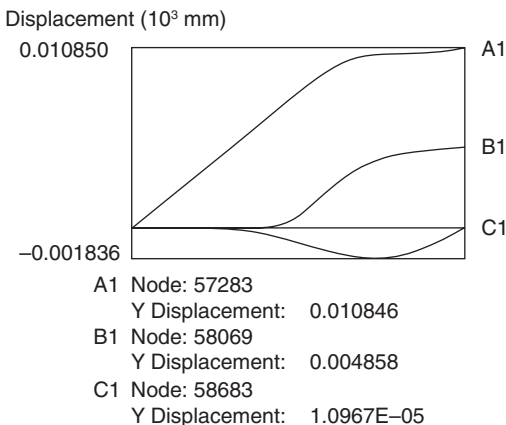
### 19.3.1  Breast bounce process

Simulation shows that during the dynamic deformation, the breast bounces with the body movement. The bra stretches to conform with the breast dynamic deformation. The displacements do not distribute uniformly over both breast and bra in the body movement.
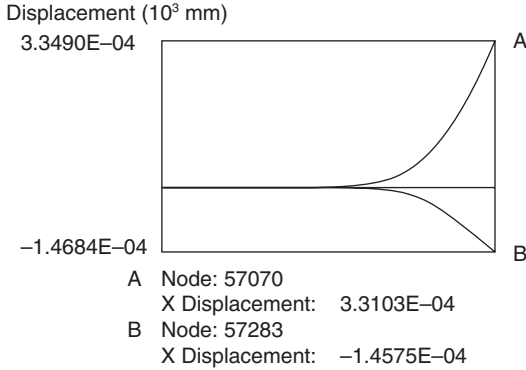
## 19.3.2  Mechanical behavior of the bra

*The displacement of the bra*

A bra will accommodate the breast deformation by fabric stretch and recovery. Figure 19.2 shows the bra displacement of three nodes ($A_1$, $B_1$, $C_1$). For node $A_1$ at the shoulder strap, the displacement appears increasing linearly with the body movement until reaching a level of steady slow increase. For the nodes $B_1$, $C_1$, the displacements are zero at the initial stage of the body movement, which is related to the bra accommodating the upward movement of the body, the downward movement of the breast and the space allowance between the breast and the bra. Then, the displacement of node $B_1$ is gradually increasing to accommodate the displacement of node B of the breast. The displacement of node $C_1$ is decreasing to $-1.8$ mm then recovering to zero value, indicating the stretch and recovery property of the bra in accommodating the bouncing process of node C of the breast.

Figure 19.3 shows the bra displacement of two nodes (at A position of right and left shoulder) in the shoulder straps' x-direction. One positive value and one negative value in the x-direction means that the shoulder straps of the bra are slipping on the skin surface during the movement of the body. In the initial stage of body movement, the displacements of the two nodes are zero, indicating that no slipping occurs between the bra and the shoulder. Comparing them with the displacement in the y-direction of node $A_1$, it is found that the slippage is a factor causing the slow displacement in the final stage of the movement as shown in Fig. 19.2.



Displacement ($10^3$ mm)

0.010850 — A1
— B1
— C1
−0.001836

A1  Node: 57283
    Y Displacement:   0.010846
B1  Node: 58069
    Y Displacement:   0.004858
C1  Node: 58683
    Y Displacement:   1.0967E−05

*19.2* Bra displacement at three nodes in *y*-direction.

Displacement ($10^3$ mm)

3.3490E–04 ⌐                                A

–1.4684E–04 └                              B

    A   Node: 57070
        X Displacement:    3.3103E–04
    B   Node: 57283
        X Displacement:    –1.4575E–04

*19.3* Displacement of the shoulder strap in *x*-direction.

*Bra pressure*

The stretch of the bra in multi-directions induces pressure on the human body. From a pressure contour plot, it could be seen that the pressure did not distribute uniformly over different parts of the bra. The pressure on most of the areas was in the range of 4 to 20 gf/cm². When the breast was falling, high-pressure zones were observed in the lower part of the bra with a value of about 14 gf/cm². When the breast was bouncing, high-pressure zones were observed in the upper part of the bra with a value of about 20 gf/cm².

*Bra stress*

Garment pressure is related to the strain–stress in the deformed fabric.[12] The effective stress is a scalar by integrating all the internal stress components, such as tension, shearing and bending, which are shown by positive values. Simulation suggests that the garment pressure distributions are directly related to the effective stress distributions in the garments. The effective stresses in the bra vary from 0 to 12 gf/cm² with the breasts falling, while with the breasts bouncing they vary in the range of 0 to 20 gf/cm². For the three nodes, the maximum value is observed at node $A_1$ with 18.7 gf/cm², followed by node $B_1$ and $C_1$, indicating that the front straps are subject to the maximum strain–stress in a vertical direction.

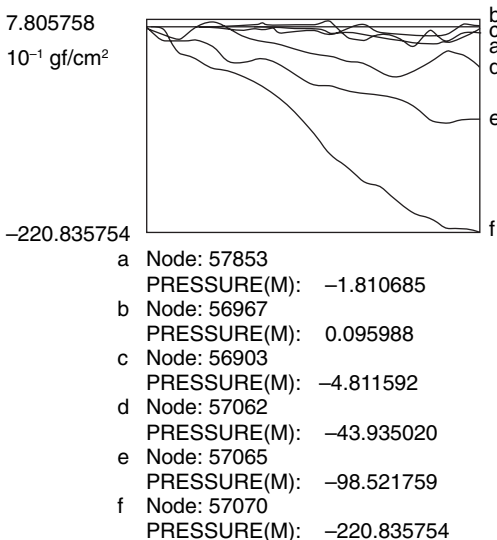## 19.3.3 Mechanical behavior of the breast

Responding to the dynamic movement and the bra pressure, there are stress–strain distributions in the breast. Simulation showed the distributions of effective stress in the breast during wearing the bra for the case of the

breast falling and for the case of the breast bouncing. In the case of the breast falling, a higher value of stress is observed in the root area around the breast. When the breast is bouncing, a higher value of stress appears at the upper area of the breast. Many areas with effective stress of about $1000\,gf/cm^2$ are observed.

## 19.4    Validation of the model

To validate the model, the simulation results were compared with the measurements from the experimental measurements of bra pressure reported by Makabe *et al.*[1] In their experiment, pressures were measured at six points under the bras that were of four styles and different material compositions. Six points were then selected on the simulation model which corresponded to the points used in the experiment: point a under bust line and mammary line cross, b under bust line and anterior axially line cross (seam), c under bust line and scapular line cross, d at the lateral area of cup and ribcage band cross, e at ribcage band and anterior axially line cross (seam), f at strap and shoulder line cross.

The corresponding pressure changes are shown in Fig. 19.4. For the points of d, e and f at the lateral area of cup and strap of bra, good agreement is observed between the simulation and the experiment. For the points of a, b and c that are all at under-bust line, the simulated values appear to be much smaller than the experimental measurements. The major reason causing the deviation is due to the difference in bra-styles used in the



```
7.805758

10⁻¹ gf/cm²
```

$$7.805758$$
$$10^{-1}\ gf/cm^2$$

b
c
a
d

e

f

$-220.835754$

a  Node: 57853
    PRESSURE(M):   −1.810685
b  Node: 56967
    PRESSURE(M):    0.095988
c  Node: 56903
    PRESSURE(M):  −4.811592
d  Node: 57062
    PRESSURE(M):  −43.935020
e  Node: 57065
    PRESSURE(M):  −98.521759
f  Node: 57070
    PRESSURE(M):  −220.835754

*19.4* Pressure changes of the six measuring points on the bra.

experiment and in the simulation. In Makabe's experiment, the bra was of a very tight-fitting style with a stiff ring along the underbust line, while in the current numerical model, only a one-piece style sportsbra can be simulated. Therefore, the pressure under the under-bust line is predicted to be small. The prediction of bra pressure at the upper parts of the bra is close to the magnitude of the measurements from the experiments of bra pressure, indicating that the model is able to predict and simulate bra pressure during wear with reasonable accuracy.

## 19.5    Conclusion

A 3D biomechanical model of a female body, which consists of an elastic breast and a rigid body, has been developed on the basis of analyzing the biomechanical characteristics of the human body. The bra is regarded as having material linearity and geometric non-linearity. The contact between the human body and the bra is modeled as a dynamic sliding interface based on the theory of contact mechanics. A finite element method is used in the time domain for deriving a numerical solution of the dynamic contact problem.

An example is presented to illustrate the simulation results of the computational model: a female human model is walking at a constant speed when wearing a bra. The computational model can simulate and characterize the dynamical mechanical behavior of the breast and bra during the body movement with the breast falling and bouncing, in terms of the bra deformation, pressure and stress distributions and breast stress distributions. With the distributions of the variables, the effects of the bra on the dynamic deformation of the breast during the body movement can be studied. Compared with the quantity of measured garment pressure reported in the literature, the predicted pressure is close to the magnitude of experimental measurements, indicating that the model is able to simulate bra pressure during wear with reasonable accuracy. The model can be used as an engineering design tool for optimizing the structure and material in the bra design process.

## 19.6    Acknowledgement

## 19.7    References

1. Makabe, H. *et al.*, A Study of Clothing Pressure Developed by the Brassiere. *Journal of the Japan Research Association for Textile End-uses*, 1991. **32**(9): p. 416–423.

2. Makabe, H. *et al.*, A Study of Clothing Pressure Developed by the Girdle. *Journal of the Japan Research Association for Textile End-uses*, 1991. **32**(9): p. 424–438.
3. Makabe, H. *et al.*, Effect of Covered Area at the Waist on Clothing Pressure. *Sen'i-Gakkaishi*, 1991. **49**(10): p. 513–521.
4. Mitsuno, T., Changes in the waistband-pressure according to time of day – In special reference to diet and the phase of menstrual cycle. *Journal of Japan Research Association for Textile End-uses*, 1999. **40**(10): p. 57–66.
5. http://mesomorphosis.com/home.htm. 2001.
6. Li, Y., Zhang, X. and Yeung, K.W., A 3D biomechanical model for numerical simulation of dynamic mechanical interactions of bra and breast during wear. *Sen'i-Gakkaishi*, 2003. **59**(1): p. 12–21.
7. Zheng, X.Y., *Advances in Sports Biomechanics*. 1998, Beijing: Guo Fang Gong Ye Press. p. 145–147.
8. Johnson, K.L., *Contact Mechanics*. 1992, Beijing: High Education Press.
9. Xu, X., Guo, Y.M. and Shen, Y.X., *Non-linear Finite Element and Program Design*. 1993, Hong Zhou, China: Zhejiang University Press.
10. Hallquist, J.O., *LS-DYNA Theoretical Manual*. 1998: Livermore Software Technology Corporation.
11. Yamada, H., *Strength of Biological Materials*. 1970: The Williams & Wilkins Company, Baltimore. p. 226.
12. Zhang, X., Yeung, K.W. and Li, Y., Numerical simulation of 3D dynamic garment pressure. *Textile Research Journal*, 2002. **72**(3): p. 245–252.

# 20
## Biomechanical engineering of compression stockings

X-Q. DAI[1,2], Y. LI[1], R. LIU[1] AND Y.L. KWOK[1]
[1]The Hong Kong Polytechnic University, China
[2]Soochow University, China

## 20.1 Introduction

### 20.1.1 Bio-functional requirement and classification of compression stockings

As introduced in Chapter 9, as a type of compression therapy, elastic compression stockings come into our daily life, and there is a wide range of them available commercially. Among them, Graduated Compression Stockings (GCSs), which provide graded compression with the greater pressure applied distally, have been reported as more effective in enhancing venous return, reducing stasis, etc.[1] Usually, the specification of a GCS only describes a range for the pressure exerted at ankle level. However, the pressure profile for a GCS has pressure ranges at several levels: ankle, calf, knee and maybe thigh. Figure 20.1 shows the pressure profile for GCS proposed by the European Normalization Committee (CEN). Depending on the pressure exerted at the ankle, the GCS is then classified into four compression classes, I being the weakest and IV the strongest. The choice of a stocking depends on both medical indication and the patient's tolerance and acceptance. According to the European Standardization Commission, there are classifications and indications for GCS.[1]

Compression stockings are available as different styles: full-length, thigh-length, and knee-length. Earlier research has shown that there is no increase in deep venous flow velocity when whole limb compression is applied, compared with below-knee compression.[2,3] Moreover, since thigh or full length stockings are more difficult to put on and less tolerated than knee-length ones, and maybe more easily ill-fitted, they may actually be inferior to knee-length ones.[4] So knee-length stockings are expected to replace thigh-length stockings for DVT treatment and prophylaxis, being equally effective, cheaper, more likely to fit correctly and better tolerated by patients.
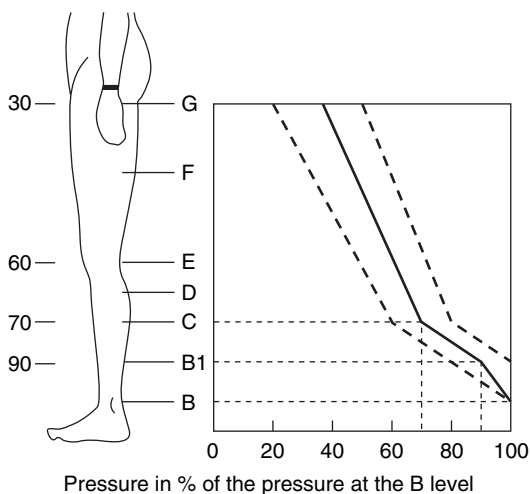
*20.1* Pressure profile for GCS fulfilling the CEN criteria.

## 20.1.2  Demand for a biomechanical model

GCS therapy has not been as effective in clinical practice as it has been in research studies, in part due to poor patient compliance due to painful, hot, and itchy reactions; and some potential complications such as impairment of subcutaneous tissue oxygenation, peroneal nerve damage, skin necrosis, pressure ulcer, induced arterial hypoxia, and even DVT.[5] Some investigations show that poor fit, and incorrect size are major causes for these negative effects.[6] Stocking fit is of utmost importance in order for the pressure gradient to be effective.

However, as a key factor in compression therapy, the pressure itself has not been investigated sufficiently. The pressure exerted by a GCS may vary among individuals, different leg levels, and also different regions at the same level. The size selection based on the simple measurement of leg length and circumference is insufficient to evaluate the pressure exerted on an individual leg. There are three major approaches for pressure determination of compression stockings. The early approach was to stretch a stocking on a tensile tester to a suitable size, and then calculate the pressure according to the fabric tension indirectly, based on Laplace's law.[7] Another approach is to determine pressure by using air-filled leg segments to counterbalance the stocking pressure.[7] A more common approach is to measure pressure *in situ*, based on the insertion of a pressure sensor in the form of a fluid or air filled balloon (connected to a manometer), or other pressure sensor.[8–10] All these techniques have several intrinsic defects. As the limb dimensions of humans are infinitely variable, the same stocking fitted to various individuals results in different pressures. To obtain the pressure, the measurement

must be carried out on each individual body. Accuracy is also a problem because the pressure sensors may themselves distort the limb dimensions and produce incorrect pressure measurements. Only the pressures at several measured points are obtained, not the overall pressure distribution.

Based on the above considerations, a mathematical model to simulate the mechanical interaction between a leg and a stocking is necessary to theoretically evaluate the pressure *in situ*, and further to fundamentally understand the mechanism of the compression therapy exerted by stockings. The design of GCS also demands a tool to evaluate what will be the overall pressure distribution exerted on a leg before the stockings are produced.

## 20.2    Biomechanical simulation

### 20.2.1  Mechanical modeling

A common way to obtain the final leg-fitting shape for a stocking is to simulate a dynamic wearing process. Two objects are involved in the simulation; one is the leg, which is solid, and the other is the stocking, which can be regarded as a sheet material. It is too difficult to include the foot in the wearing simulation due to the complex definition of boundary conditions. Since the focus is to investigate the pressure exerted on the leg, only the process of putting the stocking on from ankle to knee, or upper part was simulated. As boundary conditions, the body is assumed to stand still; the top welt of the stocking moves upwards at a constant speed until it reaches a fixed displacement. The dynamic contact takes place in a large space and period of the time domain. During the wear process, the stocking is slipping over the surface of the body with friction. To prevent the stocking interpenetrating the lower limb and generating a frictional effect, it is necessary to enforce a kinematical constraint in the normal direction as well as in the tangent direction of the contact surface. The simulation is performed using 'ABAQUS', a commercial Finite Element Method (FEM) software from ABAQUS Inc., Pawtucket, RI, USA.

### 20.2.2  Numerical simulation

*3-D geometric models of lower leg and stocking*

The lower leg consists of bones, cartilages, ligaments, soft tissue (muscle, fat, and skin), etc. A simplified model including soft tissue and two bones (the medial tibia and the lateral fibula) is used to model a lower leg during standing. The surfaces of a lower limb and inner bones are reconstructed from Magnetic Resonance Imaging (MRI) coronal images, and

then the solid bone and soft tissue are created using 'SolidWorks', a 3-D drawing tool.

Commercial knee-length stockings with medical effects to prevent and manage varicose veins were taken as samples and their dynamic wearing on a male and a female lower leg simulated. The stocking sizes were chosen properly according to the lower legs' geometrical shapes. The legging of the stocking was of cylindrical shape. A cylindrical tube was built as the initial geometry of the stocking, its size being taken from the actual sample.

### Material model

Even though both the materials for the lower limb and stockings may behave with material non-linearity when undergoing large deformation, to simplify the problem, it is assumed that there is material linearity for all materials involved. An assumption is made that the medial tibia and the lateral fibula do not deform due to wearing the stockings, so the bones are assumed to be rigid. The soft tissue material is assumed to be homogeneous, isotropic and linear elastic. For the soft tissue, the Young's modulus, Poisson ratio, mass density are taken as 0.01 MPa, 0.49, and $9.37 \times 10^{-10}$ tonne/mm$^3$, respectively.[11,12]

Since knitted fabrics often have significantly different mechanical properties in the wale and course directions, the material properties for stockings are defined as orthotropic and linearly elastic. Different kinds of knit stitches are used for the ankle part and the calf part of the sample stockings. Hence the two parts have different mechanical properties. All the parameters needed in the numerical analysis are listed in Table 20.1, where $E_1$ and $E_2$ denote the Young's moduli in the course and wale directions respectively, $G_{12}$ and $v_1$ are the shear modulus and Poisson ratio, and $t$ denotes the fabric thickness.

### Finite Element Analysis

The Finite Element Method was used for numerical analysis of the model due to its unique capability to analyze structures of complicated shape, loading and material behavior. The model was elaborated using the ABAQUS 6.4 FE software package (ABAQUS Inc., Pawtucket, RI, USA).

Table 20.1 Mechanical properties of the stocking materials

| Part | $W$ (tonne/mm$^3$) | $E_1$ (N/mm$^2$) | $E_2$ (N/mm$^2$) | $G_{12}$ (N/mm$^2$) | $v_1$ | $t$ (mm) |
|------|------|------|------|------|------|------|
| Ankle | 2.1E-10 | 0.098 | 0.147 | 0.052 | 0.113 | 0.8 |
| Calf | 2.0E-10 | 0.093 | 0.059 | 0.029 | 0.369 | 0.76 |

*Contact constraints*:  The interface between the stocking and the lower limb is considered as surface-to-surface contact; the surfaces can undergo finite sliding relative to each other. Finite sliding allows arbitrary motion of the surfaces forming the contact pair. A penalty method is employed to enforce a kinematical constraint that the slave surface nodes (inner surface of stocking) do not penetrate the master surface (lower limb surface).

*Boundary condition*: Since the medial tibia and the lateral fibula are assumed not to deform due to wearing the stockings, the displacements of all the nodes on the two bones are constrained in all directions as a boundary condition in the simulation. Thus, for the stockings along the lower leg length direction, the displacements of both the top and the bottom lines are defined while in the cross-sectional plane they can deform freely according to the shape of the lower leg.

*Numerical solution*: The dramatic change in contact pressure that occurs when a contact condition changes from open (a positive clearance) to closed (clearance equal to zero), may make it difficult to complete contact simulations. The geometric non-linearity due to the large deformation of the stocking, and the boundary non-linearity due to the discontinuous contact constraints make the mechanical simulation complicated. A nonlinear explicit dynamic analysis was performed for the numerical simulation using ABAQUS/Explicit.

## 20.2.3 Dynamic wearing simulation

The wearing simulation is set to complete within 10 seconds. Once the contact occurs, the interaction between the lower leg and the stocking stretches the stocking, meanwhile inducing pressure on the lower leg. As the contact area increases, the pressure also spreads. And as the stocking gets much more stretched, the pressure value increases. However, even at the final state, the pressure does not distribute uniformly over all the lower leg. Due to the complicated geometrical features of the lower leg surface, the stocking is not in contact with the underlying body everywhere. Only the surface of convex curvature supports the stocking, and the surface of concave curvature does not come into contact with the stocking.

## 20.2.4 Model validation

To validate the model, the wearing of two stockings on two legs was simulated respectively. Meanwhile, the two subjects whose lower limbs were scanned for the simulation participated in the wearing trial for pressure measurement. As with commercial stockings having medical effect to

prevent and manage varicose veins, the stocking sample used has a specified pressure value. It has graduated compression on the lower leg, the highest pressure of about 15–19 mmHg (1995–2527 Pa) being at the ankle level, and then while moving upward, the pressure decreases. The pressure at the maximum calf level will decrease to 65% of the specified value. The pressure was measured by using apparatus developed in the laboratory of the Institute of Textiles and Clothing at the Hong Kong Polytechnic University, in which the 'Flexiforce Sensor Model A201',[13] a piezoelectric sensor, was used for the compression receptors. The sensor is shaped as a thin ribbon. Air- or fluid-filled devices are not used because they may cause localized ballooning, raising the pressure spuriously.

The pressure was measured at the following positions, as illustrated in Fig. 20.2, showing where the maximum calf (Cf) contour is crossed by the front central line (F), inside line (I.S), back central line (B) and outside line (O.S) and where the minimum ankle (Ak) contour is crossed by F, I.S, B and O.S. The measurement results are given in Fig. 20.3, where 'M' and 'S' correspond to 'measured' and 'simulated', respectively. The peak pressures
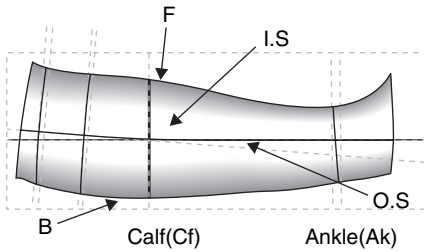


20.2 Pressure measurement position.
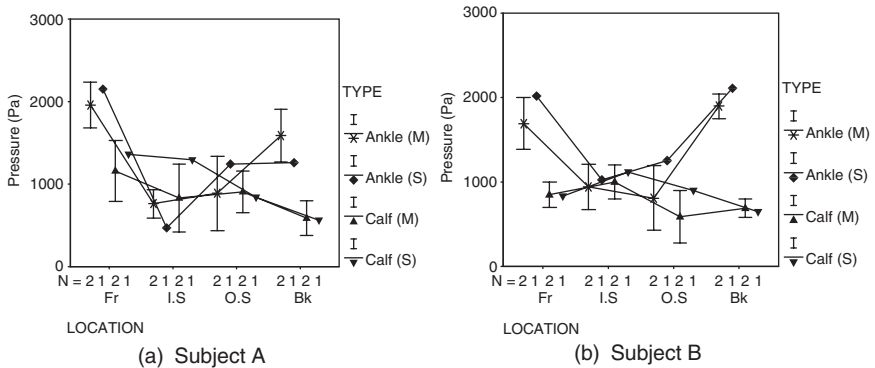


20.3 Pressure exerted on lower leg.

for both the male (1960 Pa) and female (1896 Pa) cases are close to the lower limits of the specified pressure ranges. And as the stocking moves upward, the pressure decreases. At the maximum calf level the peak pressure is 1160 Pa, which is 59.2% of the respective one at the ankle for subject A; and 998 Pa, which is 52.6% of the respective one at the ankle for subject B. These results generally agree with the specification for the stockings though the measured results are a little smaller than the specified values. This indicates that the pressure measurement is successful. Comparing the measured pressure values with the respective simulated results, good agreement is obtained as shown in Fig. 20.3a and b.

## 20.3   Analysis and discussion

### 20.3.1  Pressure induction

Figure 20.4 shows the dynamic changes of the mises stress and pressure of three nodes, which are at the top (995), middle (2478) and bottom (6554) on the front central line of the stocking. From these plots, observations and considerations were made as follows: (i) other than at the top node 995, which shows fabric stretch and recovery as it passes through the maximum calf, the stress curves show monotonic increases during the wearing process; (ii) the pressure curves show obvious rising and falling, due to the change of the contact interface; (iii) in Fig. 20.4b, for all the three curves, the peaks
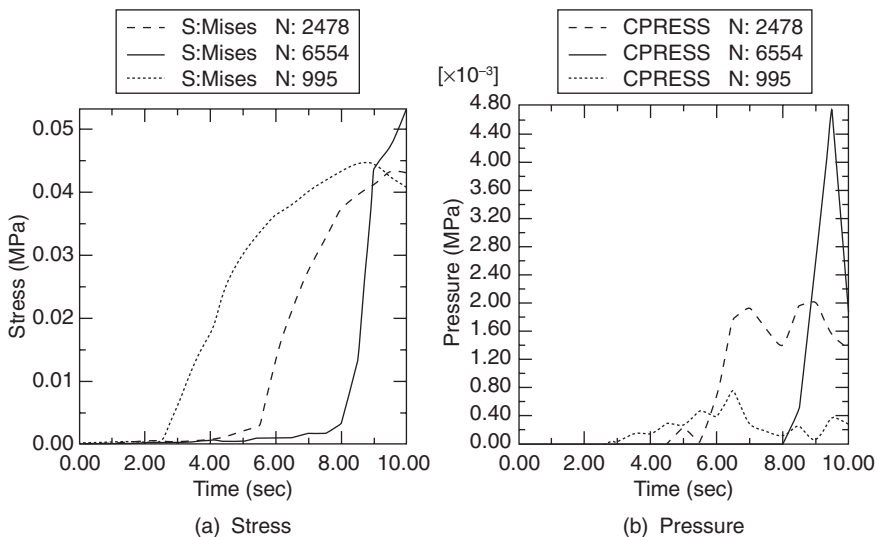


20.4 Dynamic changes of stress and pressure.

occur in the middle rather than at the end of the simulation, indicating that the dynamic pressure value during the wearing process is higher than the final values; this is consistent with our thoughts of compression perception when wearing stockings; (iv) as the stress increases, the respective pressure increases generally, indicating that the pressure is balanced against the fabric stretch in multi-directions; (v) when the wearing is complete, the stress at the bottom node 6454 is the highest; second is the middle node 2478; and then the top node 995. Correspondently, this results in graduated pressure at the three nodes.

## 20.3.2 Stress and pressure distributions

From the pressure and stress distributions resulting from the wearing simulation on male and female legs, it was found that: (i) In the two cases, the pressures show significant gradient distributions; from the ankle to the knee, the pressure value decreases; (ii) similar stress distributions in the two simulations indicate that the fabric stretch in the two stockings are roughly the same; (iii) the two pressure distributions differ from each other, the contact area on the female leg seems relatively larger than that on the male leg; therefore the pressure distributes more evenly on the whole lower leg of the female subject.



(a) Calf (male)                    (b) Calf (female)

(c) Ankle (male)                   (d) Ankle (female)
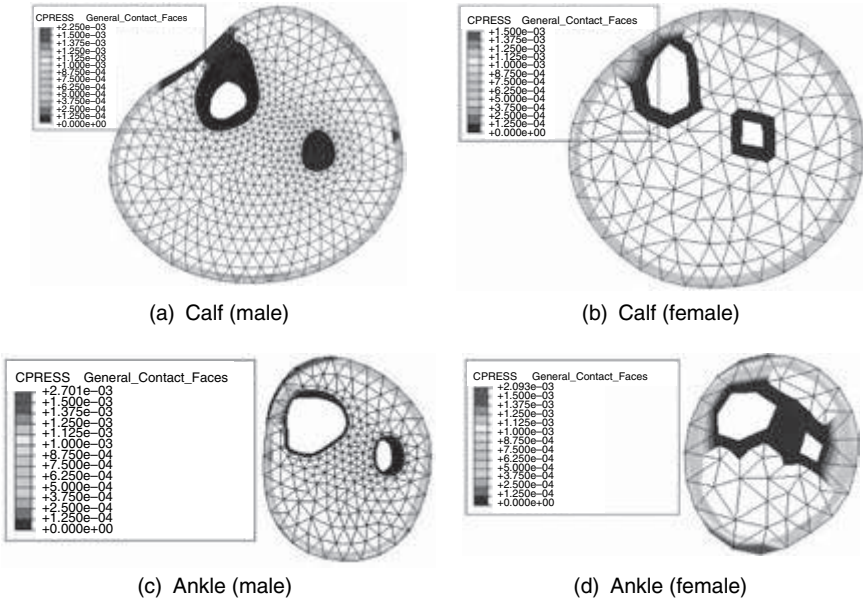
*20.5* Cross-sectional pressure distribution.

In Fig. 20.5, the cross-sectional pressure distributions at the maximum calf and at the ankle of the two legs are looked into further. At the ankle level, for leg A, the highest pressure occurs at the front, and then at the back, finally, at the two sides; for leg B, the highest pressure occurs at the back, then at the front, and finally at the two sides. At the calf level, for leg A, the highest pressure occurs at the front, then at the inner side, then the outer side, finally at the back; however, for leg B, other than the pressure value at the inner side being a little higher than at other places, the pressure distributes evenly. These observations are consistent with the measured results shown in Fig. 20.3. It can also be seen that the curvatures of calf cross-sections agree well with the respective pressure distributions. This indicates that the curvature of the lower limb surface has significant influence on the pressure.

### 20.3.3 Pressure determination

As discussed, the graduated pressure is due to the graduated stress. Table 20.3 lists the measured stretch in the cross-sectional direction at the maximum calf and at the ankle for the two subjects. The longitudinal stretch is very small for the two cases, and can be neglected. Although the stocking has a much larger stretch at the calf part than that at the ankle, the resulting stress at the calf is lower than that at the ankle. Referring to Table 20.2, it is known that this occurs due to the difference of mechanical properties of the materials for the calf part and the ankle part, especially the significant difference between the Young's modulus in the longitudinal directions. Therefore, the graduated pressure is created by using different materials (in this case, different stitches) for the ankle and the calf parts.

The above discussions make it clear that the pressure exerted on the leg by the stocking depends on the curvature of the leg surface and the stress rather than the stretch of the stocking, as has been indicated by the equation $P = K_1T_1 + K_2T_2$.[14] Here, $K_1$ and $K_2$ are the curvature of the leg surface along the cross-section direction and the length direction; $T_1$ and $T_2$ denote the stress along the two directions, respectively.
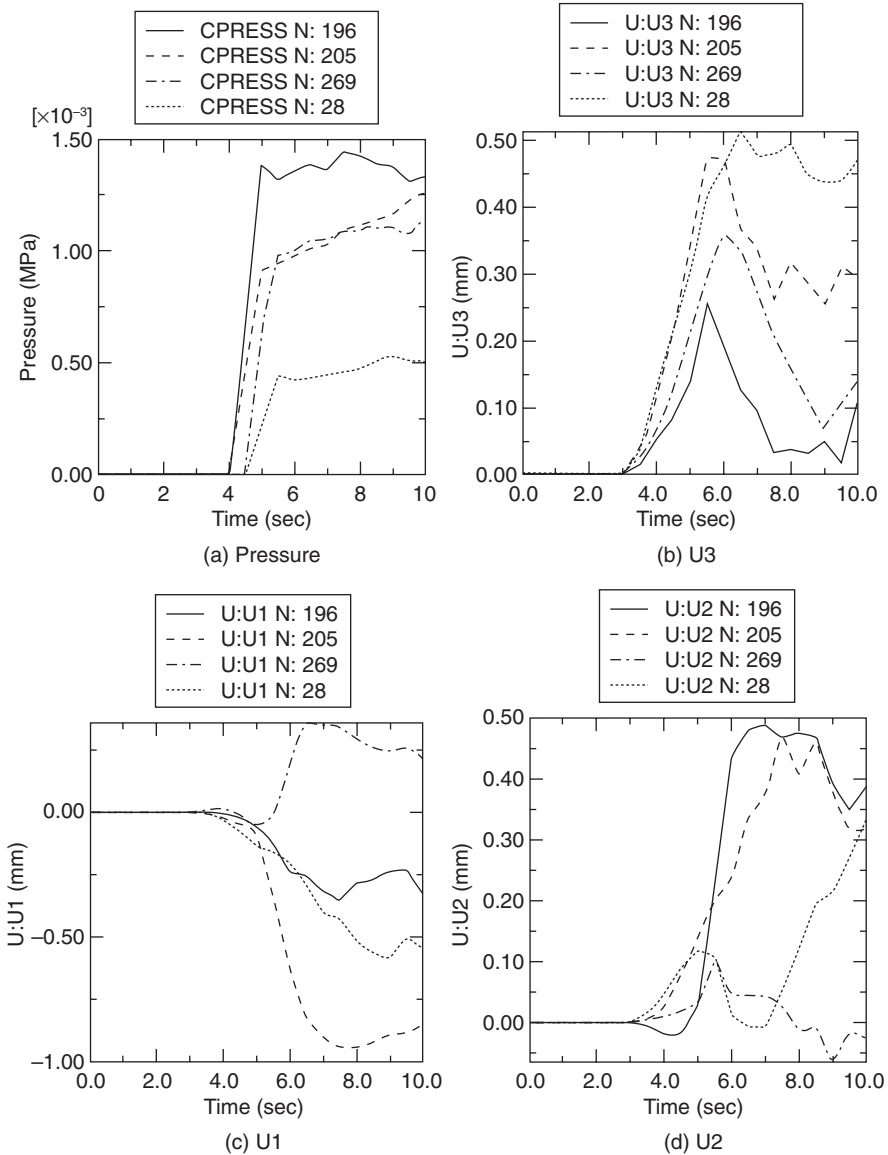
*Table 20.2* Stretch of the stockings

| Subject | Ankle | Calf |
|---------|-------|------|
| Male    | 40%   | 70%  |
| Female  | 38.5% | 75%  |

## 20.4    Investigation of the mechanism of compression therapy

### 20.4.1  Leg deformation

Fig. 20.6 shows the deformation at four feature nodes, front (196), inside (205), outside (269), and back (28) of the maximum calf contour. The



20.6 Leg displacements.

pressure plot shows that these nodes begin to be covered by the stocking at about 4.0 seconds. However, the displacements take place earlier than this, soon after that the stocking begins to come into contact with the leg. The displacements in the '3' direction (vertical) at the four nodes increase rapidly, and then decrease, vibrate, and finally reaches positive values. This indicates that during the wearing process, the whole calf is shifted upwardly due to the compression force spreading from ankle to calf. And once the upper region of the four nodes is also compressed by the stocking, the upward shift begins to recover. However, the recovery is not completed; part of the shift displacements remain, especially at the inside (205) and the central back (28).

Due to the external pressure exerted by the stocking, the calf is compressed at both sides; the displacement at the inside is greater than the outside due to the higher pressure, and both the front and the back nodes (196 and 28) are shifted toward the outside, maybe also due to the higher pressure at the inside. The displacement in the '2' direction shows more complication. The calf at node 196 seems to be stretched before it is covered by the stocking, due to the shift mentioned above; soon after that, it is covered by the stocking, at a time of about 4.0 seconds; the displacement begins to turn to become positive, meaning it is being compressed, and increases rapidly due to the higher pressure at the front. The node 205 is shifted to the back due to the pressure. The node 269 is shifted backward and then forward; finally the shift deformation almost recovers. The calf at node 28 shifts backward at first, due to the upward shifting, then recovers from the shift due to the stocking pressure; finally it turns to be shifted backward again. Since it is assumed that the soft tissue is incompressible in the simulation, the volume of the leg will remain constant during the dynamic wearing. The cross-section also tends to keep its area roughly constant. Therefore, when the calf is compressed at the front and both sides of the surface, the soft tissue is shifted toward the inner center until it reaches the fixed bone surface, and then turns toward the back side, where there is no bone, and relatively smaller pressure is exerted. However, since the whole calf is shifted upward, especially at the back and the inside, the areas of the leg cross-sections reduce to some extent. The upward shift helps the calf muscles pump. The reduction of the cross-sectional area results in the narrowing of the vein, and improvement of coaptation of the valvular cusps, which have the major positive effects of accelerating the venous flow and reducing venous reflux.
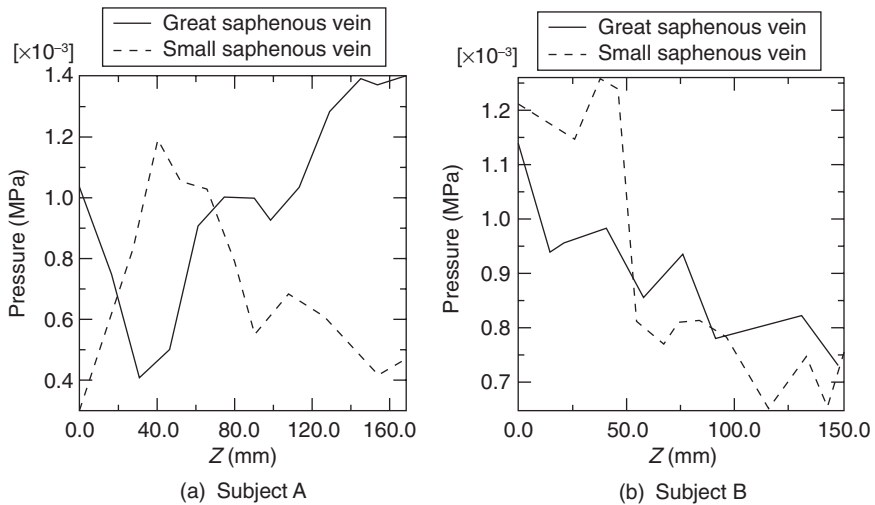
## 20.4.2 Pressure distribution along superficial veins

Venous diseases, such as varicose vein or edema, develop after long-periods of standing or sitting, due to an increase in hydrostatic pressure. One purpose

of wearing GCS is to add compression on superficial veins to bring the venous walls close together, and then to help the return of blood in the superficial venous system. Figure 20.7 shows the pressure distributions along the courses of the great and the small saphenous veins in the male and the female legs respectively. Figure 20.7b shows a trend that the pressure on the superficial veins decreases as the course goes upward from ankle to the calf. This is expected. However, in Fig. 20.7a, there is no such trend; the pressure distribution shows irregular variation. From Fig. 20.5, it can be learnt that leg B has more circular cross-sections, and is similar to a cylinder, so the gradient stress distribution in the stocking results in graduated pressure distribution on the leg surface. Leg A is of a much more irregular shape, hence the contact condition and curvature varies greatly along the vein paths from ankle to maximum calf due to the complicated geometry of the leg surface. For legs of very irregular shapes, to augment the local pressure on the veins, some compression enhancers such as pads and rolls are added over the concave areas to change the local contact condition.[15,16]

## 20.4.3 Inner leg stress

Referring to the respective cross-sectional pressure distribution in Fig. 20.5a, it is found that high pressure values induce high compression deformations (and therefore stresses) on the underlying leg surface. At the surface, normal pressure further transmits to the inner body; when going into the deeper layer of the leg, the stress decreases gradually. It is helpful to shift blood into the central compartment, and divert blood from



20.7 Pressure distribution along great and small saphenous veins.

superficial distended veins. Comparing the stresses at the calf and the ankle, it can be found that the stresses at the ankle are much higher than the respective ones at the calf. This indicates that the inner stresses decrease when going upward due to the graduated pressure distribution. The graduated stress distribution will shift blood upward, hence helping blood flow back to the heart through the veins.

Pressure sores are one of the complications of wearing compression stockings. Early researchers have concluded that if the normal capillary pressure exceeds 32 mmHg (4230 Pa),[17,18] ischemia will result, followed by occlusion or collapse of capillaries, leading to tissue destruction over a period of time. Although this limit value of 32 mmHg is questionable, and various higher or lower values have been established,[19,20] it is still the generally accepted value for relevant products. Usually, tissue interface pressure (the normal surface pressure) must be lower than 32 mmHg to prevent pressure sores. However, it is seen in simulations that, as the bones are approached, the stress increases. If the Mises stress is looked at, which is the effective stress integrating all the stress components in the three directions, the concentration of high stress at the bone prominences is significant. This is consistent with the former research findings in buttock contact simulation.[21,22] It indicates that the interface pressure is not representative of the internal mechanical state of the soft tissues involved. Pressure sores may develop easily in the deep layer, especially near the bone prominences.

## 20.5   Conclusion

Simulation demonstrates that pressure exerted on the leg by a compression stocking is induced due to fabric stretch; its value depends on fabric tension and the curvature of the leg surface. Therefore, the pressure distribution on a leg is non-uniform. Even though at the same cross-section the fabric stretch is the same, due to the irregular non-circular shape the pressure varies at different points. With the stocking-wearing model, the overall pressure distribution can be predicted in a quick and easy way. It is helpful in stocking size selection and it can aid the physician to know the inner mechanical state of leg subjected to stocking pressure. The model also enables parametrical design of gradient compression stockings.

The mechanism of compression therapy is discussed through investigating the lower leg deformation and its internal mechanical state. Reasonable correspondence between the mechanical state of the leg and the medical effects of compression exerted by the stockings is established. Since the mechanical properties of skin, fat, and muscle may vary greatly, a biomechanical leg model describing more details about the leg structure is necessary to quantitatively investigate the internal mechanical state of the leg, thus to demonstrate the medical effects of GCS. Nonlinearity of knitted

materials as well as of the soft tissue of the leg should also be taken into account.

## 20.6    Acknowledgement

## 20.7    References

1. Ramelet, A.A., Compression Therapy. *Dermatologic Surgery*, 2002. **28**: p. 6–10.
2. Lawrence, D. and Kakkar, V.V., Graduated, Static, External Compression of the Lower Limb: A Physiological Assessment. *British Journal of Surgery*, 1980. **67**: p. 119–121.
3. Porteous, L.M.J. *et al.*, Thigh length versus knee length stockings in the prevention of deep thrombosis. *British Journal of Surgery*, 1989. **76**: p. 296–302.
4. Williams, A.M. *et al.*, Knee-length versus Thigh-length Graduated Stockings in the Prevention of Deep Vein Thrombosis. *British Journal of Surgery*, 1996. **83**: p. 1553.
5. Geerts, W. *et al.*, Prevention of Venous Thromboembolism. *Chest*, 2001. **119**: p. 132S–175S.
6. Hayes, J.M., Lehman, C.A. and Castonguay, P., Graduated Compression Stockings: Updating Practice, Improving Compliance. *Medsurg Nursing*, 2002. **11**(4): p. 163–167.
7. Stolk, R. and Salz, P., A Quick Pressure Determining Device for Medical Stockings based on the Determination of the Counterpressure of Air Filled Leg Segments, in *2nd International Symposium, Compression Bandages and Medical Stockings – Clinical and Practical Results; Measuring Methods and Standards*. 1987. Zurich.
8. Momota, H. *et al.*, A Study of Clothing Pressure Caused by Japanese Men's Socks. *Journal of the Japan Research Association for Textile End-uses*, 1993. **34**(4): p. 175–186.
9. Momota, H. *et al.*, A Study of Clothing Pressure Caused by Japanese Women's High Socks. *Journal of the Japan Research Association for Textile End-uses*, 1993. **34**(11): p. 603–614.
10. Harries, C.A. and Pegg, S.P., Measuring pressure under burns pressure garments using the Oxford Pressure Monitor. *Burns*, 1989. **15**(3): p. 1879.
11. Dai, G.H., Gertler, J.P. and Kamm, R.D., The Effects of External Compression on Venous Blood Flow and Tissue Deformation in the Lower Leg. *Journal of Biomechanical Engineering*, 1999. **121**(12): p. 557–564.
12. Xiu, Y., *Advances in Sports Biomechanics*. 1998, Beijing: Guo Fang Gong Ye Press. p. 215–240.
13. Tekscan, *http://www.tekscan.com/flexiforce.html*.
14. Inoue, M., Sukigara, S. and Niwa, M., Prediction of 'Wearing Pressure' by Linearizing Method. *Journal of the Japan Research Association for Textile End-uses*, 1992. **33**(5): p. 254–260.

15. Tazelaar, D.J., Neumann, H.A.M. and De Roos, K.P., Long Cotton Wool Rolls as Compression Enhancers in Macrosclerotherapy for Varicose Veins. *Dermatologic Surgery*, 1999. **25**: p. 38–40.

16. Goldman, M.P., Sclerotherapy for Superficial Venules and Telangiectasies of the Lower Extremities. *Dermatologic Clinics*, 1987. **5**: p. 369–379.

17. Hussain, T., An Experimental Study of Some Pressure Effects on Tissues, with Reference to the Bed-sore Problem. *Journal of Bacteriology and Pathology*, 1953. **66**: p. 347–357.

18. Landis, E., Microinjection Studies of Capillary Blood Pressure in Human Skin. *Heart*, 1930. **15**: p. 209–228.

19. Defloor, T., The Risk of Pressure Sores: A Conceptual Scheme. *Journal of Clinical Nursing*, 1999. **8**: p. 206–216.

20. Young, J.B., Aids to Prevent Pressure Sores. *British Medical Journal*, 1990. **300**: p. 1002–1004.

21. Chow, C. and Odell, E., Deformations and Stresses in Soft Body Tissues of a Sitting Person. *Journal of Biomechanical Engineering*, 1978. **100**: p. 79–86.

22. Oomens, C.W.J. *et al.*, Can Loaded Interface Characteristics Influence Strain Distribution in Muscle Adjacent to Bony Promiences? *Computer Methods in Biomechanics and Biomedical Engineering*, 2003. **6**(3): p. 171–180.

# 21
## Biomechanical engineering design of socks

Y. LI[1], X-Q. DAI[1,2], M. ZHANG[1], J.T. CHEUNG[1],
AND X. ZHANG[3]
[1] The Hong Kong Polytechnic University, China
[2] Soochow University, China
[3] Xian University of Engineering Science & Technology, China

## 21.1 Introduction

### 21.1.1 Foot lesions

The human foot is an immensely practical, beautifully designed structure built to bear many times its weight, thousands of times a day and bounce back ready for more. It has been suggested that an individual takes about 8000–10 000 steps a day and in a day, the average walker generates about ½ pint of moisture through foot perspiration.[1] During walking, a foot rubs against its footwear and can be susceptible to malfunction. There are at least 300 types of foot problem. Many of them result from poorly fitting footwear. The most frequent foot problems are blisters, corns and calluses, and all of them are related to friction in shoes. Blisters are fluid-filled sacs that develop between the top layers of skin after prolonged pressure or rubbing against the skin, which causes irritation. Blisters occur most often on the heel, the toe, and the ball of the foot. Corns normally occur over toe joints, when there is friction associated with localized pressure. Calluses appear as broad areas of hardened, sometimes yellow, skin on pressure points that develop after prolonged wear-and-tear or rubbing against a shoe. Calluses usually form on the ball of the foot, the heel, and the inside of the big toe.[2]

At times, such foot problems can have life-altering consequences, especially for people with diabetes. Diabetes patients may not be able to recognize the painful event due to a condition called neuropathy. Diabetic neuropathy can cause insensitivity or a loss of ability to feel pain, heat, and cold. Diabetics suffering from neuropathy can develop minor cuts, scrapes, blisters, or pressure sores that they may not be aware of due to the insensitivity. If these minor injuries are left untreated, complications may result and lead to ulceration and possibly even amputation. Fig. 21.1 illustrates the ulcer development. Calluses occur when there is intermittent pressure at some part of the foot. This causes the outer skin to thicken and become hard, as illustrated. During rubbing, the shearing forces rupture the flesh under a callus, the outer skin becomes loose and fluid collects beneath it,
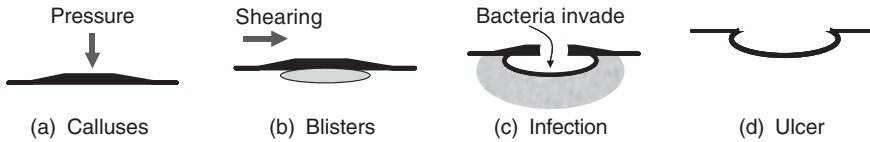
*21.1* Foot lesion development.

forming a blister. If the pressure and shearing continue, the blister breaks down and bacteria invade. The necrotic area gets infected. Finally, a deeper cavity forms as an ulcer.[3] It is reported that about 15% of diabetics will experience significant foot problems during their lives, and each year 86 000 will have a lower limb amputated because of foot complications.[4]

   Foot lesions are common and costly complications in people with diabetes.[5] Most people with diabetes are beginning to understand the importance of protecting their feet. Bad footwear has been identified as a major cause of ulceration in diabetes.[6] In a European study, footwear was implicated as being contributory to 21% of all ulcers in a large survey.[7] So an effective way to protect feet is to wear proper footwear. Actually, various preventive and therapeutic modalities, including shoes and insoles, have been developed for diabetics. Much research has been carried out to investigate the role of footwear in the prevention of foot lesions. Most of the researchers conclude that appropriate footwear helps to redistribute and reduce peak plantar pressure, which is a major cause of calluses, sores and ulcers.[5,8–14] Further research on foot care shows that good shoes and insoles are not enough, attention must also be paid to socks.[3,15,16] People with diabetes are advised that they should never wear shoes without socks. Hosiery plays a number of roles: removing perspiration from the skin, helping regulate foot temperature, providing pressure relief by increasing thickness, and protecting the skin from abrasion. However, except for a few research investigations into the effect of padded socks on plantar pressure,[15,17] research has rarely focused on socks. The part socks play in foot care remains unclear.

## 21.1.2 Socks for foot care

Compared with shoes and insoles, socks are much simpler to apply and are less expensive. However, the questions to answer are: how do socks work, and what kind of socks should people with diabetes wear? Firstly, socks should be fitted properly. Socks that are too large bunch up in the shoe; those that are too small squash the feet. During the wearing of a sock, the foot stretches the sock and, in return, the pressure induced from the sock deforms the skin and soft tissue. This mechanical interaction stimulates neurophysiological impulses of touch and pressure through the mechanical receptors in the deep layer of the skin,[1] which further induces subjective

perceptions and relevant pressure discomfort or more seriously, pain sensations. Sensitivity to pressure also differs in different small regions of the foot. For example, the absolute pressure thresholds at the hallux and the heel are higher than for the middle sole.[18] Due to difference of skin thickness, sensitivity to pressure should be higher at the instep than at the sole. However, suitable pressure is needed to keep close contact between the sock and foot. There should be no lumps or folds to irritate the foot. How to provide suitable pressure to the foot while not causing an uncomfortable compressive feeling is important in sock design and engineering.

Regarding sock materials, many people believe that natural fibers, such as cotton, are better than synthetic fibers.[5] However, other researchers disagree with this opinion. Although cotton absorbs water well, it retains it. Some researchers have found that the friction coefficients of many textile materials, especially natural fibers (cotton and silk), increase along with increase in temperature and humidity.[19] This may result in a more severe friction situation. Therefore, for sock materials, two aspects need to be considered. Firstly, wearing socks of good heat and moisture transfer, and moisture absorption properties, can help to keep the foot dry during the day, hence avoiding moist feet that tend to 'stick' to the shoe and exacerbate rubbing. Secondly, socks of low friction material can directly reduce friction. By imparting a low friction value to the contact areas, abrasion of the foot skin is diminished as well as the shearing between the contact interfaces. Friction-free technology is being developed in sock manufacture.[20] Du Pont's Teflon fibre of extremely low friction is now available for socks. How to utilize this technology in socks design for foot care is an important issue.

## 21.2  Biomechanical modeling

### 21.2.1 Model development

Various pressure measurement methods have been developed to measure static and dynamic plantar pressure.[21] There are also biomechanical foot models built for predicting the plantar pressure to aid clinical practice.[22,23] However, unlike plantar pressure that can be measured directly, there are only a few experimental devices for shear measurement.[24] Knowledge of shoe rubbing remains minimal. Since direct measurement of friction and shearing *in situ* is difficult, an approach is to build 3-D models to theoretically investigate the mechanical interactions in footwear. The focus is on normal walking rather than active sports. There is very little modeling work on foot–sock interaction reported in sock engineering. In the biomechanics research area, various 2-D and 3-D foot models using the Finite Element Method (FEM) approach have been developed, and the foot–insole interface is modeled with the aim of investigating plantar pressure and stress in

the foot during various stance phases of gait. Gefen,[25,26] Chen *et al.*,[27] and Jacob and Patil[28] developed 3-D biomechanical foot models consisting of bones, soft tissues, cartilage and ligaments and analyzed stress distribution in the foot during various stance phases of gait, mainly for clinical applications. Furthermore, Chen *et al.*,[23] and Lemmon[22] modeled the foot–insole interface to investigate the insole effect on the plantar pressure distribution. Some other researchers focused on the in-shoe pressure during walking, running or doing other sports, in order to provide guidance for sports shoes design.[29,30] There is no report on modeling foot rubbing and slippage in shoes. And since the mechanical contact between a foot and a flexible sock is difficult to model, there are also few 3-D sock models reported. A 3-D foot, sock and insole contact model has therefore been developed here to investigate the sock pressure exerted on the foot, stress in the sock, plantar pressure, plantar shearing force, and the forward slippage of the foot at push off.

## 21.2.2  Simulation of wearing a sock

*Modeling of foot and sock interaction*

Since the purpose of the foot–sock interaction model is to investigate the pressure and stress in the foot resulting from wearing socks, it is assumed that foot deformation is limited to soft tissue. Therefore, some reasonable simplification was made: all the bones and cartilages were combined as a whole skeleton and the remaining parts of the foot were considered as soft tissue. The toes were also combined as a whole. The surfaces of the foot and inner skeleton were reconstructed from Magnetic Resonance Imaging (MRI) coronal images of a male in his twenties and a solid bone and soft tissue model was created. The bone and soft tissue materials were assumed to be homogeneous, isotropic and linear elastic. For bones, the Young's modulus was taken as 7300 MPa, and Poisson ratio as 0.3, and for the soft tissue, the values were taken as 1 MPa and 0.49, respectively.[28] Since a sock takes the shape of the foot surface when it is fitted, the foot surface is used as the sock geometry. Knitted fabrics often have significantly different mechanical properties in the wale and course directions, so the materials for socks were defined as orthotropic and linear elastic shell. Two cases of a sock of crew length, worn on a foot, using two materials, nylon and cotton, were simulated. The material parameters for the sock are listed in Table 21.1, where $E_1$ and $E_2$ denote the Young's moduli in the course and wale directions respectively, $G_{12}$ and $v_1$ are the shear modulus and Poisson ratio, $W$ is the mass density and $t$ is the fabric thickness.

The interface between sock and foot is considered as surface-to-surface contact; the surfaces can undergo relatively finite sliding in relation to each

other. A penalty method is employed to enforce the kinematical constraint that the slave surface nodes (inner surface of sock) do not penetrate the master surface (foot surface); friction between the two surfaces is also taken into account. The friction coefficient is set as 0.1 in the simulation. The sock welt is often made of tightly knitted fabric to prevent slipping, so it adheres to the underlying foot surface. A tie constraint between the sock welt and the surface of the ankle was defined.

Boundary condition: Since the purpose is to investigate the pressure exerted by the sock, pressure due to the supported body weight should be avoided. Therefore, the foot is simulated as 'hung' and has no contact with other objects except for the sock. It is assumed that the bone part of the foot does not deform due to the wearing of the sock, therefore the displacements of all the nodes on the bone are constrained in all directions as a boundary condition in the simulation.

As the initial condition, the initial stress needs to be added to the sock, accounting for the sock deformation due to the wearing process. It is difficult to measure the stress in socks due to biaxial extension. However, with the Finite Element (FE) approach, the stress according to the stretch and the mechanical properties of the material can be predicted. The biaxial extension of a piece of fabric (5 cm × 10 cm rectangle) using a mesh of 4-node quadrilateral shell elements, which is the same as the sock, was

Table 21.1 Parameters of knitted fabrics

| Sock | $E_1$ (N/mm) | $E_2$ (N/mm) | $G_{12}$ (N/mm) | $v_1$ | $t$ (mm) |
|---|---|---|---|---|---|
| Nylon | 0.0446 | 0.061 | 0.02 | 0.195 | 0.5 |
| Cotton | 0.061 | 0.0728 | 0.028 | 0.155 | 0.85 |
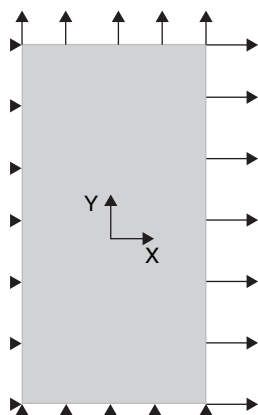


21.2 Biaxial extension of fabric.

simulated. As illustrated in Fig. 21.2, displacements corresponding to the stretch in the wale and course directions are set to the nodes on the right and top edges, while the displacements of the nodes on the left edge are constrained in the $X$ axis direction and those on bottom edge are constrained in the $Y$ axis direction. The resulting stresses in the two directions are taken as initial stresses for the sock in the wale and the course directions. A non-linear general static analysis is performed for the bi-extension simulation.

For each sock case, static general nonlinear analysis was performed in ABAQUS/Standard using the Newton–Raphson method.

*Experimental results and discussions*

Both of the two sock samples have foot-like shapes. Therefore, the sock model is divided into four parts and it is assumed that the fabric is evenly stretched in each part. Then, according to the sock sizes and the dimension of the subject's foot, it is calculated that the fabric stretches in two directions for each part. The stress in the nylon sock is found to be higher than that in the cotton sock. Before numerical analysis, the sock is in an unbalanced state, but after the numerical analysis, the sock stress is balanced by the contact pressure and frictional force due to the interaction between sock and foot, and reaches a balanced redistribution.

The stress in the sock, pressure on the foot, and stress in the foot show significantly different distributions. The Mises stress in the cotton sock varies from 0.0043 to 0.0347 MPa, and that in the nylon sock varies from 0.00625 to 0.0399 MPa. This indicates that the sock is stretched everywhere and no part rests on the foot surface. Higher stress concentrates at the heel part. The stretched sock induces pressure on the underlying foot. From the pressure distributions, it was noticed that the pressure does not distribute uniformly over all the foot. The pressure range for the cotton sock was 0–0.0039 MPa, and for the nylon sock 0–0.0046 MPa. Zero pressure indicates 'no contact' between the foot and sock. Due to the complicated geometrical feature of the foot surface, as well as the tightly-stretched state of fabric, the sock is not in contact with the underlying foot everywhere: only the convex surface of positive Gaussian curvature supports the sock, and the concave surface of negative Gaussian curvature does not contact the sock. Moreover, high pressure occurs where the curvature of the foot surface is high, such as the end of the toes, and the two lateral sides of the foot. As a whole, the two socks result in similar pressure distributions. The pressure on the foot deforms the foot. The stress in the foot caused by the cotton sock ranged from 0–0.00299 MPa, and the nylon sock from 0 to 0.00399 MPa. High stress concentrates at the toe part.

Comparing the two socks, it was found that the stress in the nylon sock is higher than that in the cotton sock. As a result, it was found that the stress

and pressure in the foot for the nylon sock are also higher than those for the cotton sock, especially at the toe part. These distributions demonstrate that the pressure depends on the curvature of the body surface and the stress in the fabric. This observation has been confirmed by Inoue *et al.*'s work,[31] in which reasonable pantyhose pressure was predicted according to the body curvature and the biaxial extension of fabrics, and was compared with subjective test results. However, it is difficult to calculate the curvature of the body surface as it is often of complicated shape. Therefore, in that work, the thigh was simplified as a cylinder and was focused upon.

*Comparison with measured results*

Pressure measurement was carried out by using an apparatus developed in the laboratory of the Institute of Textiles and Clothing at The Hong Kong Polytechnic University, in which the sensor 'Flexiforce Sensor Model A201'[32] was used as a pressure receptor. According to reference 33, the pressure was measured at the following positions: Malleolus medialis (Mm), Malleolus lateralis (Ml), Instep (Ins), Ball of foot (Ba), facies mediales of the Digitus 1 (D1), facies lateralis of the Digitus 5 (D5), facies mediales of the Planta (Pl), and facies posterior of the Calx (Ca). These points are the characteristic points of the foot surface geometry; the curvatures at these points are relatively high. At these points, the pressure is the highest within the vicinity around them. The measured results are shown in Fig. 21.3, and 'M' and 'S' means 'measured' and 'simulated', respectively.
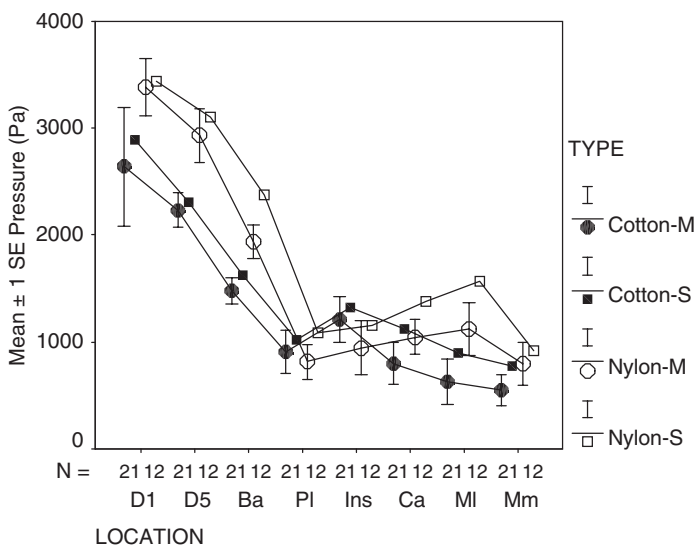


*21.3* Pressure in the sock.

Both of the socks showed the same trend of pressure change: the highest pressure occured at D1, then D5. These pressures were greater than the rest. This trend is consistent with that reported in references 33, 34. When comparing the two socks, it was found that the pressure in the nylon sock was significantly higher than that in the cotton sock due to the higher strain, especially at D1. The simulated pressure results agreed roughly with the respective measured ones. The difference between the simulated and measured results, especially at the positions, where the pressure is low, is considered to be because the measure positions in simulation and in reality may not be exactly the same; and the measurement error also accounts for the difference. The error of stretch measurement for each sock part is also a main factor causing the difference between the simulation results and the actual state of the sock. The agreement between real measurement results and simulated ones confirms that the model is useful in predicting the pressure on the foot caused by wearing the sock. By using the model, not only the pressure values of several feature points, but also the overall pressure distribution in a sock of complicated geometry can be predicted.

*Pressure control*

To avoid causing uncomfortable compressive feelings, the high pressure at the toe part needs to be reduced. However, lumps or folds resulting from loose-fitting socks may irritate the foot. A certain pressure is necessary to provide tight contact at the sole. However, both the socks show lower pressure at the facies mediales of the Planta (Pl). An ideal design for a sock provides tight contact at the sole part and relatively loose contact at the toe part. Using higher Young's moduli for the sole part and lower Young's moduli for the toe part, and assuming the sock has uniform stretch, the initial stress distribution can then be obtained. After the numerical simulation, the stress is redistributed so that the higher pressures concentrate at the sole and instep rather than the toe; stress in the toe part is also reduced. The simulation indicated that it is easy to predict the overall pressure distribution exerted by a sock assembled by various materials, by using the foot–sock contact model.

## 21.2.3 Dynamic walking simulation

*Modeling of foot, sock and insole interaction*

During walking, the gait cycle is usually subdivided into a stance phase and a swing phase. The swing phase is the period of time when the foot under consideration is not in contact with the floor. The stance phase is the period of time when the foot under consideration is in contact with the floor. The

stance phase can be further subdivided into five stages: heel-strike (initial foot-floor contact), foot-flat, mid-stance, push-off, and toe-off. According to our perception, slippage takes place easily when the phase turns from foot flat to mid-stance, and then to push-off. Therefore, the phase transition from foot-flat to push-off is simulated. Since the shoe is not the focus of this study, only a barefoot or a foot wearing a sock standing upon an insole lain over a supporter is simulated rather than in a shoe.

To allow bone deformation, proper partition is performed on the skeleton, and the thinner pieces between parts are defined as soft cartilages. The bone, cartilage, and soft tissue materials are assumed to be homogeneous, isotropic and linear elastic. The Young's moduli, Poisson ratios, and mass densities for these materials are listed in Table 21.2.

For the loads on the foot, the loads at the mid-stance phase are used. According to reference 28, only ankle joint force and the forces of several major muscles are considered. The muscle forces include triceps surae (TS), reaction at the medial pulley due to the muscles flexor hallucis longus (FHL), flexor digitorum longus (FDL), tibialis posterior (TP), reaction at lateral pulley due to muscles peroneus longus (PL), peroneus brevis (PB), and flexor hallucis longus (FHL).

Three computational experiments were carried out: one barefoot and two sock simulations. There are several objects involved in the mechanical system: bone, tissue, insole, support and in some cases, sock. In the barefoot simulation, there is only a pair of surfaces involved in the contact problem: the foot surface and the top surface of the insole. The friction coefficient is set as 0.5. In the sock simulation, there are two pairs of surfaces involved: the foot surface and the inside of the sock; and the outside of the sock and the top surface of the insole. It has been reported that the friction coefficient between skin and Teflon fabric can be as low as 0.04 while that between skin and cotton fabric is as high as 0.54.[35] These two friction coefficients are chosen in the simulation. Two cases differing in friction arrangements are simulated: in case I, the coefficient of the friction between sock and foot is set as 0.54, and that between sock and insole is set as 0.04; in case II, the two friction coefficients are arranged *vice versa*. Usually, the soft tissue

*Table 21.2* Material properties of foot and insole

| Parameters | Soft tissue | Bone | Cartilage | Supporter | Insole |
|---|---|---|---|---|---|
| Young's modulus (MPa) | 1.0 | 7300 | 10 | 50 | 0.5 |
| Poisson ratio $v_1$ | 0.49 | 0.3 | 0.4 | 0.36 | 0.85 |
| Mass density (kg/m³) | $9.37 \times 10^3$ | $1.5 \times 10^3$ | $2.0 \times 10^3$ | $5.0 \times 10^3$ | $2.0 \times 10^3$ |

adheres tightly to the underlying bone; the two objects are not free from each other in motion. A tie constraint between the surface of the skeleton and the inside of the soft tissue model is defined, and also the interface of the insole and the supporter is defined as a tie constraint.

The simulation is divided into two steps: the first step is to calculate the sock–foot interaction, and reach a stable mechanical state of sock on foot; the second step is to simulate the phase change from mid-stance to push-off. The time period is set as 0.5 second and 0.75 second for the two steps, respectively. To make the simulation results comparable, the step set for the bare foot simulation is the same as the one for the foot wearing the sock. During the first step, no foot load is added, and the foot is fixed at three points. At the end of this step, the initial stress is redistributed in the sock and is balanced by the contact pressure, indicating that the sock is worn on the foot. In this simulation, it is assumed that the fabric is stretched evenly all over the sock, and the obtained stresses in the wale and the course directions are 0.03 MPa and 0.04 MPa respectively. In the second step, the loads mentioned above are added to the foot to simulate the foot phase change from mid-stance to push-off. Since the stress distribution in the bones is not examined as in reference 28, to simplify the calculation the loads are applied at single points rather than in areas. The magnitudes of loads are listed in Table 21.3. To allow for the foot motion during the phase changing from mid-stance to push-off, the constraints on the foot length direction at the fixed three points are released.

*Simulation results*

The frames taken from the bare-foot simulation were examined. The foot is flattened and then turns to take off. There was a similarity between the stress distributions and the respective pressure, demonstrating that the high pressure induces high stress in the foot. However, the pressure only occurs where the foot sole comes into contact with the insole: the stress distributes on larger regions than the pressure does, indicating that the mechanical response to pressure spreads to large areas on foot.
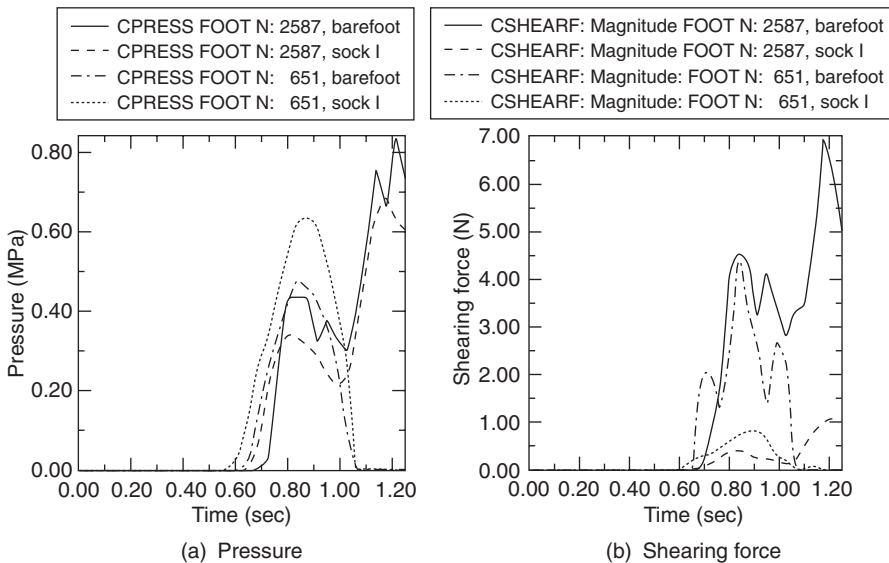
The sock simulation at the end of the first step was also examined. The uniform initial stress is redistributed in the sock and is balanced by the contact pressure. The pressure does not distribute uniformly; the pressure
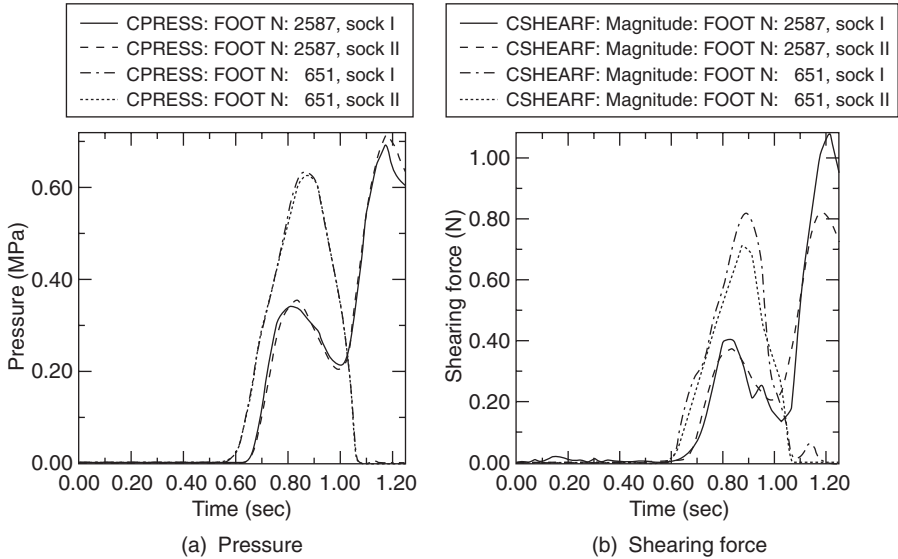
*Table 21.3* Loads on foot skeleton

| Positions | L1 | L2 | L3 | L4 | L5 |
|---|---|---|---|---|---|
| Load | 1800 N | 1200 N | 850 N | 200 N | 100 N |

magnitude varies from 0 to 0.005 MPa. The foot displacement in the simulation of foot wearing the sock I is compared with that in the barefoot simulation. Significantly, the foot wearing the sock slips to a larger distance upon the insole. In Fig. 21.4, it can be seen that the shearing force distributions in the two simulations are similar while the magnitudes of the shearing forces differ greatly. Fig. 21.4a shows the change of pressure on foot at two nodes, 651 at the heel, and 2587 at the forefoot; the pressure values peak in these vicinities. When the foot phase turns from mid-stance to push-off, the heel lifts up, only the forefoot is in contact with the insole, and the decrease of contact area leads to the increasing of pressure at the forefoot. The peak forefoot pressure is also higher than at the heel. It is consistent with many measurement results.[36] Compare the two simulations: at the forefoot, the plantar pressure reduces for the foot wearing the sock while the situation is the converse at the heel. This observation needs to be confirmed by further experimental measurement. Some former research has shown that a peak plantar pressure of larger than 12.3 kg/cm²(12.05 MPa)[37] has the highest specificity in identifying patients at risk of foot ulceration, while a recent piece of research regarded 6 kg/cm²(0.588 MPa) as a threshold.[38] No matter what the exact value of the threshold is, the pressure change plot will be helpful in identifying the risk.

In the simulated distribution of the shearing force on the foot sole, the shearing force occurring accompanied by the pressure showed a significant difference between the barefoot and the foot wearing the sock I. Both at



21.4 Changes of pressure and shearing force at two foot nodes.

| CPRESS: FOOT N: 2587, sock I | CSHEARF: Magnitude: FOOT N: 2587, sock I |
| CPRESS: FOOT N: 2587, sock II | CSHEARF: Magnitude: FOOT N: 2587, sock II |
| CPRESS: FOOT N:  651, sock I | CSHEARF: Magnitude: FOOT N:  651, sock I |
| CPRESS: FOOT N:  651, sock II | CSHEARF: Magnitude: FOOT N:  651, sock II |

(a) Pressure                    (b) Shearing force

*21.5* Comparison between two socks.

the heel and at the forefoot, the shearing force reduces dramatically for the foot wearing the sock. Although the magnitude of the shearing force depends on the pressure, its change trend is not always the same as the pressure. Comparing Fig. 21.4a with b, at the heel node, the shearing force for the foot wearing the sock reduces significantly while the pressure change increases.

In Fig. 21.5a, the two simulated results for the two socks are compared. The plots of plantar pressure are almost the same for the two cases, indicating that the difference in friction arrangements have no influence on the plantar pressure. Figure 21.5b shows that the shearing force for sock II is significantly lower than that for sock I: at the heel, the peak shearing force reduces from 0.84 N to 0.71 N, and at the forefoot, it reduces from 1.09 N to 0.78 N.

The change of foot and sock displacement is further looked into in Fig. 21.6, which shows the changes of the displacements along the foot length direction of the forefoot node (2587) and the sock node (5050) initially close to it. In the two sock simulations, the foot has the same slippage distance of 9.8 mm, while the barefoot has a very smaller displacement (1.34 mm). The slippage difference is 8.46 mm. At the node 5050, sock I has the same displacement as the underlying foot node, indicating that the foot adheres to the sock due to the high friction (0.54), and they slip upon the insole together. However, sock II has no forward displacement, indicating that it sticks to the insole, and the foot slips in the sock due to the low friction (0.04). The different foot movement in the sock results in completely
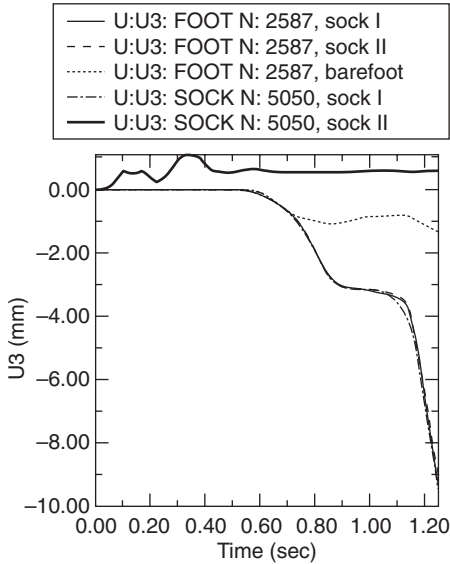
*21.6* Displacement of foot and sock.

different stress distributions in the two socks. Due to the high friction between the sock and the skin of the foot, sock I adheres to the underlying foot during the phase changing, and slips together with the foot upon the insole. Therefore, the differences of displacement for different regions of the sock sole are not significant. The stress in the sock shows a similar distribution to that of the shearing force and the change of the stress in the sock also shows the same trend with the respective change of the shearing force, indicating that the sock stress is increased to balance the shearing force resulting from the friction against the foot as well as the insole. The situation for sock II is completely different. On the one hand, as demonstrated in Fig. 21.6, the sock sticks to the insole at the metatarsal heads during the phase changing of the foot. On the other hand, pushed by the advancing toes of the foot sliding inside the sock during walking, the sock at the toe part is stretched. Hence, the stress of the sock toe increases, accompanying the foot slippage.

*Plantar pressure measurement*

Besides the numerical simulation, a plantar pressure measurement using the pedobarograph (Tekscan, Inc, Boston, USA) was carried out. The subject whose foot is used in the simulation walks on the sensor mat with bare feet or wearing polyester socks of lower friction. The plantar pressures of the bare feet were consistent with the patterns shown in the simulated values

while the magnitude was lower due to the sensor losing accuracy. The slippage distance of the foot was further investigated. A peak phase pattern was used to show the largest measured values of each sensing point. The pattern illustrates the accumulated contact area during walking. The difference in the length between the peak pattern of barefoot and that wearing the socks is taken as the difference of slippage distance between the two walking situations. The length is calculated through the ASCII data file, in which the pressure value of each sensing points is recorded in a fixed rectangular array. The range of the non-zero column is counted and converted to length. The resulted difference was 9.04 mm. It is close to the simulated results of 8.46 mm.

## 21.3    Implications in sock design

### 21.3.1  Sock pressure

In days gone by, socks were something that were kept going for as long as possible. Today, the main consumer purchasing considerations are fit and comfort. For people with diabetes, socks are essential medical devices for foot care. We have seen some of the foot problems that may be caused by high sock pressure. To choose socks of the correct size and that fit the feet properly is very important.

### 21.3.2  Plantar pressure and shearing force

Through the numerical experiment, it was demonstrated that high plantar pressure and shearing force occur at the forefoot and heel during walking. The magnitudes of the plantar pressure and shearing force are large at the forefoot as well as at the heel. Since the tissue thickness at the forefoot is smaller than that at the heel, blisters and ulcers form more easily at the forefoot. The shearing force distribution at the forefoot compares with the blister and ulcer areas. To avoid foot ulceration, reducing the plantar shearing force is as important as reducing the plantar pressure. Soft and thick padded soles are often used to reduce the plantar pressure. To reduce the shearing force, an easy and effective approach is to wear socks of low friction.

The barefoot simulation demonstrated that high friction between the foot skin and the insole make the barefoot stick to the insole easily, and that this sticking leads to extremely high shearing forces. Due to the foot load, there is a potential for forward slipping in the shoe. If the slipping is completely resisted by rubbing against the insole and the shoe sides and tops, the high pressure and shearing force will soon results in calluses and blisters, especially at the forefoot. If the foot is allowed to slide upon the insole to a

certain distance, the shearing force will be reduced, hence reducing the potential for the formation of various foot lesions. This demands both a low friction and a certain space kept in the shoe to allow the foot to slide. Wearing a sock can reduce friction and allow the foot to slide upon the insole, hence reducing the shearing force.

Friction between the shoe insole and the sock or foot can influence a walkers' definition of comfort and the risk of injury. If it is too low, the foot will move easily in the shoe. But excessive movement gives rise to a feeling of underfoot insecurity, and may well generate pressure and rubbing between the top and upper part of the foot and the shoe.[39] Rubbing in the shoe includes friction between the foot and the inner surface of the sock, and that between the outer surface of sock and shoe. Friction that is too low in both of the interfaces may lead to excessive movement of the foot in the shoe, and cause discomfort and feelings of insecurity. An ideal way is to allow low friction on one side to allow foot sliding, and high friction on the other side to provide an appropriate level of resistance to avoid excessive movement. The numerical simulations demonstrated that this is more effective by reducing the plantar shearing force in the sock II simulation with low friction set against the foot skin than that in the sock I simulation with high friction set against the foot skin. This consideration has been confirmed by the socks using the low friction Teflon fiber.[20] By keeping the Teflon fiber against the skin to reduce rubbing between the foot and the sock's inner surface, and using high friction to provide the required resistance between the outside of the sock and the insole to prevent excessive movement of the foot in the shoe, the socks reduced the occurrence of blisters by around 90 percent in athletes.[40] The benefit of this technique in diabetic foot care needs to be confirmed in clinical practice. However, as observed above, the toe part of sock II shows large alternating stretch and recovery due to the foot sliding inside the sock during walking. This deformation and recovery may cause the fabric at this part to get looser or wear out easily. So, in sock design using friction-free fibres, a material of good elasticity and stretch recovery is necessary for the sock, especially at the toe.

## 21.3.3 Sock design

For different end uses, there are large variations of functional requirements. For each foot part, there are also different requirements. For normal use, the sole needs to be soft and durable; the instep of the sock can be loose-fitting to reduce the pressure where the skin is thin and the pressure threshold is relatively lower. For athletes, it is important to reduce calluses and blisters, and prevent tendons from injury. Sports socks often have thick cushioned soles, and reinforced elastic material to fully encompass the arch

and instep for a snug fit and support and also to protect the Achilles tendon. For diabetic patients, any tiny lesion will lead to ulceration. There should be no elastic or tight welt which can interfere with blood flow. There should also be no seam felt. Any holes in the sock can be a source of additional friction. There should be no lumps or folds to irritate the foot.

Regarding sock material, it must be able to wick moisture away from the foot leaving skin dry and reduce sticking. Materials such as Coolmax™ have been used in sock manufacture. For the foot arch part, reinforced elastic materials such as Lycra™ have been used to support and protect the foot arch. For the sock sole, soft and thick cushioning is necessary to reduce plantar pressure; 'friction free' construction, such as the use of Teflon™ fiber, needs to be imparted to the forefoot and heel to reduce rubbing. For the sock instep, loose fit can help reduce the sock pressure for comfort.

The present biomechanical foot, sock and insole interaction model can help us to design a sock of complicated structure and material assembly, and predict the pressure and shearing. Further development of the model can be focused on sock thickness, to quantitatively investigate the effect of thickness on plantar pressure. Integration with the shoe model is also expected, in order to study the mechanical interaction of footwear systematically.

## 21.4   Acknowledgement

## 21.5   References

1. Anon., Hot under the Foot. *World Sports Activewear*, 1999. **5**: p. 58.
2. Anon., *Skin and Toenail Problems*. Foot Care Basics, A Special Health Report from Harvard Medical School, 2001: p. 21–27.
3. Phillips, P., Evans, A. and Popplewell, P., Diabetic Foot Ulcers, A Guide to Treatment. *American Journal of Clinical Dermatology*, 2000. **1**(2): p. 117–123.
4. Anon., *Foot Care Basics*. Foot Care Basics, A Special Health Report from Harvard Medical School, 2001: p. 1–2.
5. Litzelman, D.K., Marriott, D.J. and Vinicor, F., The Role of Footwear in the Prevention of Foot Lesions in Patients with NIDDM. *Diabetes Care*, 1997. **20**(2): p. 156–162.
6. Apelqvist, J., Larsson, J. and Agardh, C.D., The Influence of External Precipitating Factors and Peripheral Neuropathy on the Development and Outcome of Diabetic Foot Ulcers. *Journal of Diabetes Complications*, 1990. **4**: p. 21–25.
7. MacFarlane, R.M. and Jeffcoate, W.J., Factors Contributing to the Presentation of Diabetic Foot Ulcers. *Diabetic Medicine*, 1997. **16**: p. 867–870.

8.  Perry, J.E. *et al.*, The Use of Running Shoes to Reduce Plantar Pressures in Patients Who Have Diabetes. *The Journal of Bone and Joint Surgery*, 1995. **77-A**: p. 1819–1828.
9.  Boulton, A.J.M. and Jude, E.B., Therapeutic Footwear in Diabetes. *Diabetes Care*, 2004. **27**(7): p. 1832–1833.
10. Lord, M. and Hosein, R., Pressure Redistribution by Molded Inserts in Diabetic Footwear: A Pilot Study. *Journal of Rehabilitation Research and Development*, 1994. **31**: p. 214–221.
11. Maciejewshi, M.L. *et al.*, Effectiveness of Diabetic Therapeutic Footwear in Preventing Reulceration. *Diabetes Care*, 2004. **27**(7): p. 1774–1782.
12. Mueller, M., Strube, M.J. and Allen, B.T., Therapeutic Footwear Can Reduce Plantar Pressures in Patients with Diabetes and Transmetatarsal Amputation. *Diabetes Care*, 1997. **20**(4): p. 367–371.
13. Praet, S.F.E. and Louwerens, J.W.K., The Influence of Shoe Design on Plantar Pressures in Neuropathic Feet. *Diabetes Care*, 2003. **26**(2): p. 441–445.
14. Viswanathan, V. *et al.*, Effectiveness of Different Types of Footwear Insoles for the Dianetic Neuropathic Foot. *Diabetes Care*, 2004. **27**(2): p. 474–477.
15. Scheffler, N.M., All about Socks. *Diabetes Forecast*, 2001. **54**(9): p. 78,80–81.
16. Mayfield, J.A. *et al.*, Preventive Foot Care in People with Diabetes. *Diabetes Care*, 1998. **21**(12): p. 2161–2177.
17. Veves, A. *et al.*, Use of Experiment Padded Hosiery to Reduce Abnormal Foot Pressures in Diabetic Neuropathy. *Diabetes Care*, 1989. **12**: p. 653–655.
18. Dohi, M., Mochimaru, M. and Kouchi. M., The Tactile Sensitivity and the Elasticity of the Sole of the Foot as Factors of the Shoe Comfort, in *IEA2003*. 2003.
19. Morooka, H. *et al.*, Relationships of Slip in Shoes to Frictional Property and Cloth Thickness of Men's Socks. *Journal of the Japan Research Association for Textile End-uses*, 1994. **35**(12): p. 682–689.
20. Anon., More Comfort from Socks with Low-friction Teflon. *Textile Magazine*, 1999. **28**(2): p. 8–9.
21. Cavanagh, P.R., Hewitt, F.G.J. and Perry, J.E., In-shoe Plantar Pressure Measurement: A Review. *Foot*, 1992. **2**: p. 185–194.
22. Lemmon, D., The Effect of Insoles in Therapeutic Footwear – A Finite Element Approach. *Journal of Biomechanics*, 1997. **30**(6): p. 615–620.
23. Chen, W.P., Ju, C.W. and Tang, F.T., Effects of Total Contact Insoles on the Plantar Stress Redistribution: A Finite Element Analysis Clinical Biomechanics. *Clinical Biomechanics*, 2003. **18**: p. s17–s24.
24. Hosein, R. and Lord, M. A Study of in-shoe Plantar Shear in Normals, *Clinical Biomechanics*, 2000. **12**, p. 46–53.
25. Gefen, A., Biomechanical Analysis of the Three-dimensional Foot Structure During Gait: A Basic Tool for Clinical Applications. *Journal of Biomechanical Engineering*, 2000. **122**(12): p. 630–639.
26. Gefen, A., Stress Analysis of the Standing Foot Following Surgical Planter Fascia Release. *Journal of Biomechanics*, 2002. **35**: p. 629–637.
27. Chen, W.P., Tang, F.T. and Ju, C.W., Stress Distribution of the Foot during Mid-stance to Push-off in Barefoot Gait: A 3-D Finite Element Analysis. *Clinical Biomechanics*, 2001. **16**: p. 614–620.

28. Jacob, S. and Patil, M.K., Three-dimensional Foot Modeling and Analysis of Stresses in Normal and Early Stage Hansen's Disease with Muscle Paralysis. *Journal of Rehabilation Research and Development*, 1999. **36**(3).

29. Aguinaldo, A. and Mahar, A., Impact Loading in Running Shoes with Cushioning Column System. *Journal of Applied Biomechanics*, 2003. **19**(4): p. 353–360.

30. Geil, M.D., The Role of Footwear on Kinematics and Plantar Foot Pressure in Fencing. *Journal of Applied Biomechanics*, 2002. **18**: p. 155–162.

31. Inoue, M., Sukigara, S. and Niwa, M., Prediction of 'Wearing Pressure' by Linearizing Method. *Journal of the Japan Research Association for Textile End-uses*, 1992. **33**(5): p. 254–260.

32. Tekscan, *http://www.tekscan.com/flexiforce.html*.

33. Momota, H. *et al.*, A Study of Clothing Pressure Caused by Japanese Men's Socks. *Journal of the Japan Research Association for Textile End-uses*, 1993. **34**(4): p. 175–186.

34. Momota, H. *et al.*, A Study of Clothing Pressure Caused by Japanese Women's High Socks. *Journal of the Japan Research Association for Textile End-uses*, 1993. **34**(11): p. 603–614.

35. Buirski, Just Slip into Something a Little More Comfortable. *World Sports Activewear*, 2000. **6**(4): p. 49–50.

36. Caselli, A. *et al.*, The Forefoot-to-Rearfoot Plantar Pressure Ratio is Increased in Severe Diabetic Neuropathy and Can Predict Foot Ulceration. *Diabetes Care*, 2002. **25**(6): p. 1066–1071.

37. Veves, A. *et al.*, The Risk of Foot Ulceration in Diabetic Patients with High Foot Pressure: A Prospective Study. *Diabetologia*, 1992. **35**: p. 660–663.

38. Pham, H. *et al.*, Screening Techniques to Identify People at High Risk for Diabetic Foot Ulceration: A Prospective Multicenter Trial. *Diabetes Care*, 2000. **23**(5): p. 606–611.

39. Draper, D., Coming down to Earth. *World Sports Activewear*, 1999. **5**(1): p. 53–55.

40. Delporte, C., New Socks Offer Relief, Blister Guard System with Teflon Reduces Friction between Foot and Sock. *America's Textiles International*, 1997. **26**(12): p. K/A 10.

# 22
## Biomechanical engineering of footwear

A. LUXIMON AND M. ZHANG
The Hong Kong Polytechnic University, China

## 22.1   Introduction

It is not very clear why or when humans started wearing footwear. Many scientists believe that the first shoe, probably a bag-like wrapping made from animal skins,[1–3] was used to protect against the cold temperatures during the Ice Age about 500,000 years ago.[4] Ever since people started to wear footwear, there has been a constant progression in its use and design. The impact and influence of footwear have changed over the years. During the Stone Age, footwear was probably used to protect the feet against rocks, thorns, and harsh weather, whereas in the ancient Egyptian time, footwear depicted rank and was a status symbol.[4] Initially, footwear production was completely manual. Then, during the Industrial Revolution, the mechanization of the footwear industry started after the invention of sewing machines and equipment to roll sole-leather.[5] From that time, the number and variety of footwear have drastically increased. Foot coverings have become increasingly specialized for a variety of tasks and functions. For example, nowadays it is not surprising to have more than 200 models of running shoes.[6] Since footwear has become an integral part of our daily life, it is nearly impossible for many people to go out without footwear or even to stay in their room without some sort of foot covering.

During most of the early years of footwear development, style and fashion have played a huge part in the design of footwear. Since designs were based on aesthetic and sensual appeal rather than scientific studies, it is not surprising to find several examples of beautiful but 'badly-designed' footwear. In the Middle Ages, men were wearing long-toed footwear called *poulaine* to show their masculine sexuality;[4] however, the toe extensions were so long that it made walking almost impossible. Similarly, during the fifteenth century, beautifully decorated *chopine* footwear was designed to increase the height of ladies. It was short-lived because ladies could easy fall over while wearing it, resulting in miscarriages.[4] Furthermore, *chopine* footwear caused changes in posture and eventually the start of medical interest in problems with
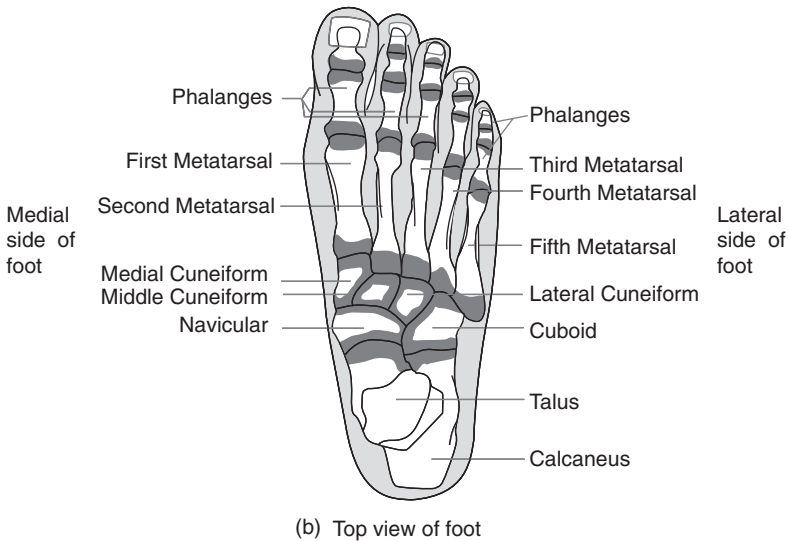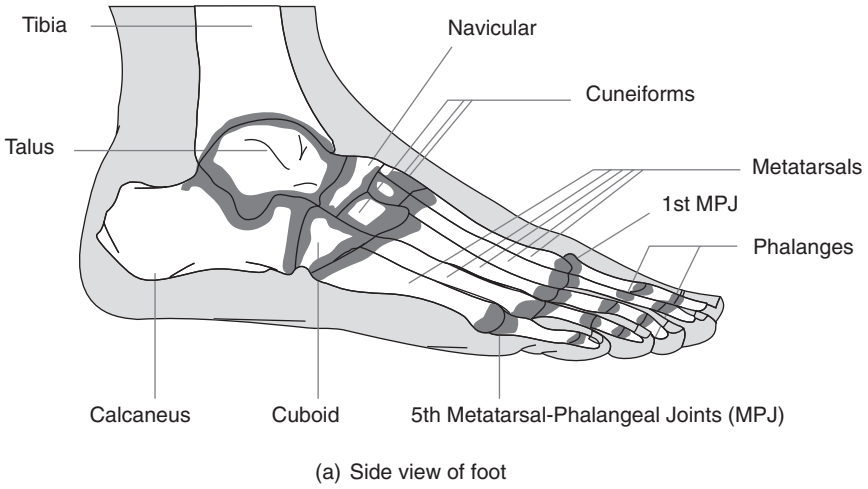
elevated footwear. Although we cannot find *chopine* footwear today, a variation of it, the high heel, is widely available. As a result, there is still medical interest in elevated footwear. Of course, there are other parameters of footwear design that are of medical interest. Another classic example of 'beauty footwear' occurred during the tenth century (continuing until 1911) in China. In the name of beauty, Chinese female children's feet were bound with cloth to stop them from growing. The aim of the foot binding was to obtain feet resembling a 'three-inch golden lotus' and the women would be able to wear tiny footwear. Foot binding causes damage to the foot structure resulting in severe life-long disability for many elderly Chinese women.[7] Today, there are no extreme cases of foot torture such as foot binding; however, the incompatibility of footwear and the feet usually causes some sort of foot injury and illness. This chapter provides some basic information on the feet and footwear, so that footwear is designed to have aesthetic as well as fit, comfort, and functional design elements.

## 22.2    The human foot

Humans have evolved and have adopted an upright posture by walking on their hind-limbs and leaving the fore-limbs free for other uses. The development into bipedalism was a major step in human evolution, as many things associated with being human became possible – including fine manipulation with the hands and more mobility.[8] During the developmental stages, the foot lost the climbing ability and evolved into an organ of weight bearing, support, and locomotion. In early hominids or humans, the weight was carried along the side of the foot, while now the body weight is transmitted internally from the heel along the outside (lateral) of the foot. Also, in early hominids the body was pushed forward through the middle of the toes, while now the push-off is made generally by the big toe. This is a much more efficient arrangement for striding.[8] The detailed discussion of the development of hominids falls outside the scope of this chapter; instead, the foot structure of the 'modern' human foot is discussed in more detail.

### 22.2.1  Foot skeletal structure

The human foot (Fig. 22.1), an unsymmetrical object, comprises a complex arrangements of 26 bones, cartilage, muscles, tendons, ligaments, nerves, and blood vessels, and has evolved from a generalized grasping organ to an organ specialized in weight bearing, locomotion, and support.[9] The 26 bones are divided into three major groups: hind-foot (tarsal), mid-foot (metatarsals), and fore-foot (phalanges). The hind-foot consists of seven short bones (calcaneus, talus, navicular, cuboid, medial cuneiform, lateral cuneiform, and intermediate cuneiform) as shown in Fig. 22.1. The calcaneus, also

Tibia

Navicular

Cuneiforms

Talus

Metatarsals

1st MPJ

Phalanges

Calcaneus    Cuboid    5th Metatarsal-Phalangeal Joints (MPJ)

(a) Side view of foot

Phalanges

Phalanges

First Metatarsal

Third Metatarsal

Fourth Metatarsal

Second Metatarsal

Medial
side of
foot

Lateral
side of
foot

Fifth Metatarsal

Medial Cuneiform
Middle Cuneiform

Lateral Cuneiform

Navicular

Cuboid

Talus

Calcaneus

(b) Top view of foot

*22.1* Basic foot structure.

known as the heel bone, carries a large proportion of the body weight. The talus is connected to the tibia and fibula (leg bones), and helps to distribute the weight of the body on the foot. The mid-foot consists of five metatarsals. The first three metatarsals are joined to the cuneiform bones (lateral, medial, and intermediate), while the last two metatarsals are joined to the cuboid. The fore-foot consists of fourteen phalanges that form the toes. Even though the three-section classification of the foot is more prevalent, some studies have separated the foot into four groups[10] for biomechanical

purposes. The four foot sections are: hind-foot (calcaneus and talus); mid-foot (navicular, cuboid, medial cuneiform, lateral cuneiform, and intermediate cuneiform); fore-foot (5 metatarsals); and phalanges (14 phalanges).

The bones are joined together at joints where some degree of motion is possible. The main foot joints are the ankle joint, the subtalar joint, the midtarsal joint, the metatarsal-phalangeal joint, and the phalangeal-phalangeal joints. The ankle joint is between the tibia and the talus. The subtalar joint involves talus, calcaneus, and navicular bones, whereas the midtarsal joint involves the talus, calcaneus, and cuboid bones. The ankle, metatarsal-phalangeal joints (MPJ) and phalangeal-phalangeal are hinge-type joints. At the joints, cartilage covers the ends of the bones and acts as a shock absorber. Cartilage also allows motion at the joints while being lubricated by synovial fluid. In order to have movement at the joints, muscles attached to the bones by tendons are used to create the pulling force. These muscles are stimulated by nerve endings through voluntary, involuntary or reflex actions. Ligament attaches a bone to another bone and thus restricts the bone motion resulting in enhanced support and locomotion. The complex arrangement of bones, muscles, ligaments, and other tissues are enclosed in a protective layer – the skin. The skin has nerve endings, blood vessels, sweat glands, and hair follicles, to enable its function of protection, temperature control and the sense of touch. Due to the complexity of the foot structures, the human foot has wide variations in size, shape, and proportion, within and between persons under different conditions, which affect the footwear fit.[11]

*Within-subject variation*

For a given person, the feet are different between the right and the left foot. Individuals working with their right hand have the tendency to use the left foot as a support. Thus, some people assume that the left foot might be longer. Rossi[12] reported that differences between the feet are prominent, based on a study using 6800 participants. Rossi states that 'no individuals are likely to have two feet exactly alike in terms of size, shape or proportions'. There are differences of 5 to 10% between the right and left foot. Similarly, several studies have found differences between the left and right foot of individual people; however, some people will have their right foot longer than their left foot and some *vice versa*. On average, there is no *overall* difference between right and left feet. Since previous studies have only considered length and width dimensions, more studies are required to look into the 3-D shape differences between the left and the right feet.

For an individual, in addition to differences in left and right feet, the feet undergo changes under different conditions such as loaded versus unloaded; functionality; and thermal conditions.[12] The foot normally increases in shape

and size when moving from no-load to semi-load to full-load weight bearing. A no-load, unloaded or no-weight condition is when the foot does not carry any body weight. This situation can be obtained by sitting and removing all weight from the foot. The semi-load, half load or semi-weight bearing condition is when one foot carries half of the body weight. This situation occurs while standing normally. The full-load, loaded, or full-weight bearing situation is when the foot is subjected to the full weight of the body. This situation can be obtained while the person is standing on one foot.

When comparing both feet in a fully loaded state, one foot elongates more than the other for 80% of people.[12] For example, this foot stretches half a shoe-size (1/6 inch) more than the other for about 85% of women, while it stretches 1 shoe-size (1/3 inch) or more for the rest. Since both the length and width increases in dimension under loading condition, fitting trials must include wearing both shoes and testing the fit under different weight-bearing conditions.[13] The foot shape is also different under different functions.

The foot functions can be separated into two main conditions: static and dynamic. Previous sections have considered the foot in static conditions (standing and sitting). Dynamic conditions include walking, running, jumping, other such activities; and the foot shape is different depending on the functions. The foot shape is different due to several motions at the joints, notably the ankle, the sub-talar, the mid-tarsal, the metatarsal-phalangeal and the phalangeal-phalangeal joints. These joints allow a different range of motion and thus the foot shape changes. At the ankle joint, a hinge type mechanism allows dorsiflexion (upward movement) and plantarflexion (downward movement) as shown in Fig. 22.2. The sub-talar and the mid-tarsal joints, located below the ankle, play a major role in supination and pronation.[14] Pronation is composed of three movements: eversion, abduction and dorsiflexion (Fig. 22.2), and it results in an upwards and inwards movement; while supination, the opposite of pronation, is composed of inversion, adduction and plantarflexion, and it results in a down and outwards movement. Furthermore, the metatarsal-phalangeal joints (MPJs) and the phalangeal-phalangeal joints (PPJs) are hinge joints. The MPJ allows dorsiflexion and plantarflexion of the toes, while the PPJ permits toe grasping. During any given dynamic condition, heat, friction, and sweat are produced which change the interior-shoe condition. The foot shape is also influenced by changes in environmental conditions.

The foot shape is affected by interior-shoe conditions such as heat, friction, humidity, and moisture. The foot volume changes by 5% at the end of the day compared to early morning, due to these thermal conditions.[12] Perspiration plays a major role in controlling body temperature. When the body becomes heated from muscular activity an even larger quantity of moisture is produced.[14] During perspiration, the sweat glands produce half
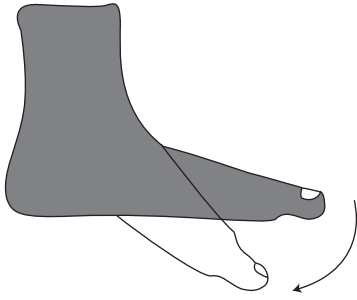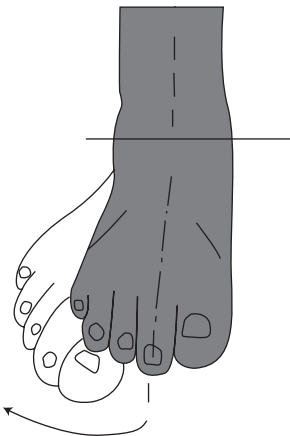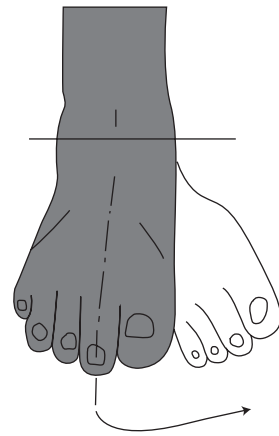
Dorsiflexion
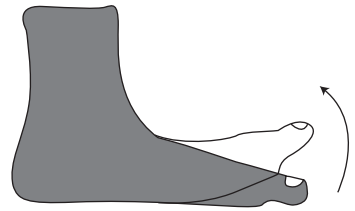
Plantarflexion

Inversion

Eversion

Abduction

Adduction

*22.2* Foot dynamics.

a pint of moisture, salts, and acid into the shoes each day, changing the interior-shoe conditions drastically. So far the inter-subject variations have been considered: in contrast the between-subject variations are larger.

*Between-subject variation*

There are variations between people depending on gender, age, and race.[14] The mean length of the female foot is about 92% of the mean length of the male foot, while the mean volume of the female foot is about 81% of the mean volume of the male foot.[15] Even when comparing children between the ages of 6 to 11, boys have consistently a larger foot length and foot breadth than girls.[16] As far as the age variation is concerned, the foot stops growing after 14 years in boys and 13 years in girls even though the height is still increasing.[15] Dahlberg and Lander[1] studied men's feet as they aged between 17 and 47, and found that there were no differences in 18 foot-measurements showing that the feet had stopped growing. It is very evident that the foot size (length and width) changes for children, but does the foot shape change proportionately? This remains to be seen. In addition to gender and age, the feet are also different among different races.

Cheskin[14] grouped the feet into 3 main groups: Negroid foot; Oriental foot; and Caucasian foot. The Negroid foot is broad at the forepart and narrow at the heel. The oriental foot is short and broad in the forepart and heel. The Caucasian foot is broad with straight toes. There have been several studies on age and gender; however, studies on racial differences are few. Thus, a comprehensive study to quantify the racial differences would be useful.

## 22.2.2  Foot classification

Human feet have wide variations and, in order to simplify analysis, feet have often been classified according to arch height;[14,17,18] flare angle;[19,20] rear foot position[21] and big toe length.[17]

*Arch height*

When considering arch height, the foot can be grouped as high arched (Pes Cavus), normal arched and low arched (Pes Planus) as shown in Fig. 22.3. Figure 22.3 also shows typical plantar pressure distribution for feet with different arch heights. Pes Cavus and Pes Planus (flat foot) are developed when the balance between the muscles and ligaments of the foot is somehow disrupted.[18] In the high arched foot, the forefoot and the heel generally carry more weight, while for the normal arched foot the body's weight is distributed evenly throughout the foot.[14] However, in the low arched foot,
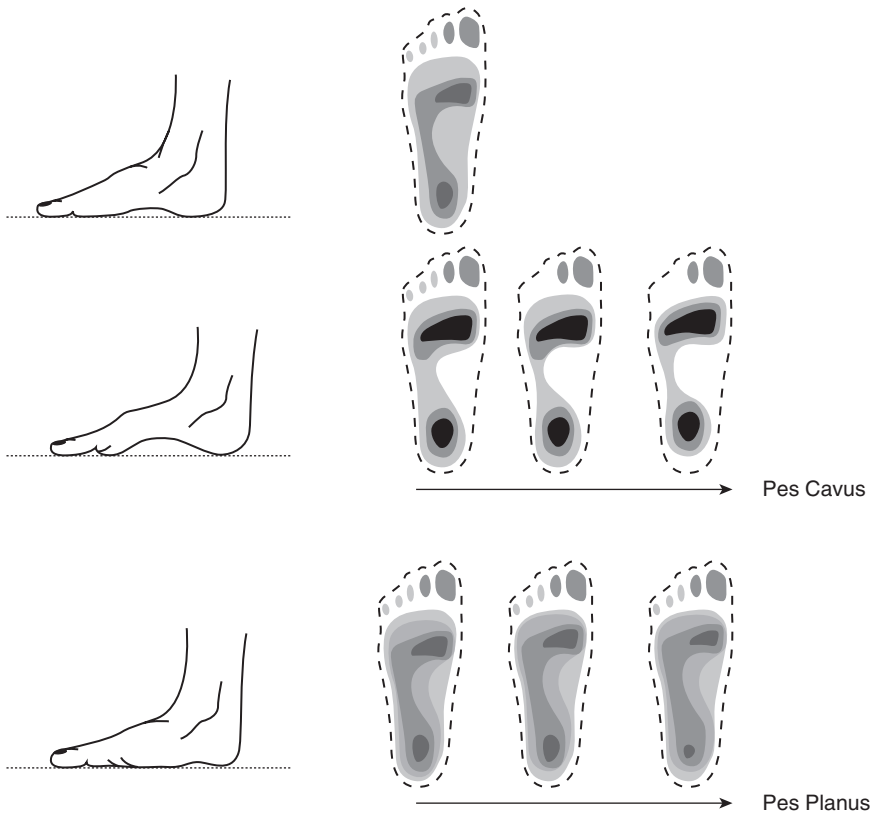
*22.3* Classification based on arch height.

the weight is distributed over the total area of the foot. This causes extra pressure on the outside border areas, especially the medial side of the foot, resulting in pain, discomfort and decrease in function. The percentage of different arch types may vary between races but all types are found in all races.[14] The arch height can be determined from footprints. The various stages of the development of the Pes Cavus and Pes Planus are also shown in Fig. 22.3. Since Pes Cavus and Pes Planus feet are structurally weak, there have been several methods developed to quantify the percentage or degree of flat footedness. A simple method involves measuring the arch height[22] while others involve taking measurement from the plantar pressure prints.[23] The results obtained from the measurement techniques can vary for different conditions, e.g. static and dynamic; or loaded versus unloaded. In other words, an accurate method for quantification of flat footedness should account for age, gender, race, and different conditions, and existing results should be used with caution.

*Foot flare*

The foot can be classified as based on foot flare, which is a measure for the planter curvature of the foot similar to last flare (discussed in later sections). In order to calculate the amount of foot flare, we need to define a flare axis. For the purpose of calculating foot flare, the heel center line has been used. Freedman *et al.* (1946) have defined foot flare as the ratio of the horizontal distance between the heel center axis and the medial ball point to the foot width (horizontal distance between the heel center axis and the medial ball point + horizontal distance between the heel center axis and the lateral ball point). According to this definition, a straight foot is one which has a ratio of 50%, an out-flared foot is one which has a ratio of less than 50%, and an in-flared foot is one which has a ration greater than 50%. Goonetilleke and Luximon[20] used principal component analysis and found that the foot center is located at approximately 52% of the foot length, and that Hong Kong males have a mean in-flare of 3.2 degrees (standard deviation 2.73). According to Goonetilleke and Luximon's method, a negative angle value shows in-flare, while positive values show out-flare. Their method has higher sensitivity and is highly correlated with Freedman's ratio measure.

*Rear foot position*

Nigg[21] classified the foot according to rear foot position (Fig. 22.4). If the foot rear position is 0° to 6° toward the medial side, it is called a normal foot. If the foot is inclined more than 6° toward the medial side, it is called Pes Valgus. It is called Pes Varus if it is inclined toward the lateral side. In most cases, Pes Valgus occurs in combination with Pes Planus; thus some



Normal          Pes Valgus          Pes Varus
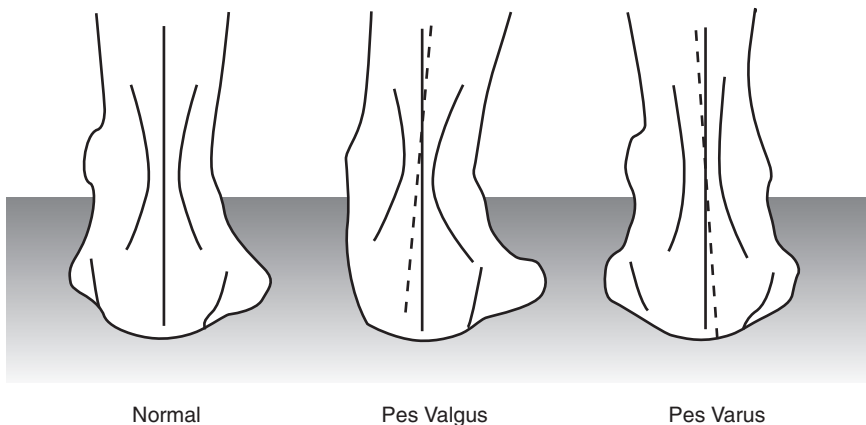
*22.4* Classification based on rear foot position.

people use the measurement of the rear foot angle to quantify the degree of flat footedness.

*Toe length*

Feet can be classified in terms of big toe length, as shown in Fig. 22.5.[24] If the big toe length is the longest compared to the other toes, then the foot is called an Egyptian foot. If the second toe is the same length as the big toe, then the foot is called a Square foot. However, if the second toe is longer than the big toe, the foot is called a Greek foot. Kaplan[25] has attributed the differences in toe length to genetics, with long toe lengths being recessive. Due to the different toe lengths, the walking pattern and foot pressure of these different types changes. Figure 22.5 shows the typical pressure print of the three types of feet. For extreme cases of Greek feet (i.e. when the second toe are significantly longer), plantar pressure is higher at the second MPJ location. This might result in pain, discomfort, and skin break down.

### 22.2.3 Human gait

After considering the variation in feet and foot classification, the foot primary function is now considered. The foot is used primarily for walking and the human walking gait is very important. Foot, limb, and other muscu-



Egyptian foot                Square foot                Greek foot
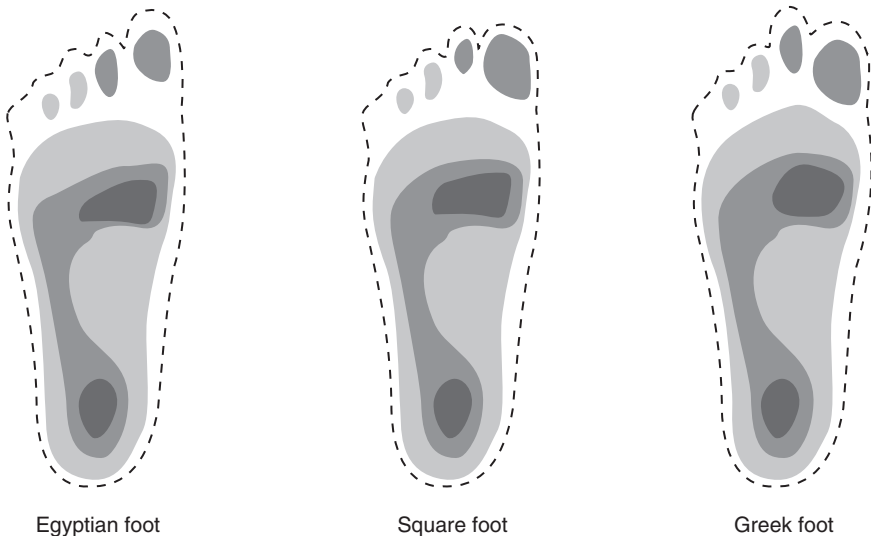
*22.5* Classification based on toe length.

loskeletal problems can be identified by gait cycle evaluation. The gait cycle begins when one foot touches the ground and ends when the same foot touches the ground again (Fig. 22.6). The gait cycle is divided into two main phases, the stance phase and the swing phase. The stance phase is when the foot is touching the ground, while the swing phase is while the foot is not touching the ground and is in motion. The stance swing phase starts when the foot touches the ground, usually at the heel (heel strike), and ends when the foot leaves the ground, usually at the toe (toe off). During the stance phase, three periods can be identified: initial double limb support, single limb support, and terminal double limb support. Each double limb support period accounts for about 10% of the gait cycle (20% total), while the single limb support is 40% of the gait cycle. During the double limb support, the two limbs usually do not share equal load. There is always a shift of load from one foot to the other during the gait cycle. The swing phase for the same limb is the remaining 40% of the gait cycle. For different walking



| Right heel contact | Left toe-off | | | Left heel contact | Right toe-off | | | Right heel contact | Left toe-off |
|---|---|---|---|---|---|---|---|---|---|
| Both foot support | | Right foot support | | Both foot support | | Left foot support | | Both foot support | |
| Right foot stance phase | | | | | | Right foot swing phase | | | |
| Left foot swing phase | | | | Left foot stance phase | | | | | |
| Cycle (stride) duration | | | | | | | | | |
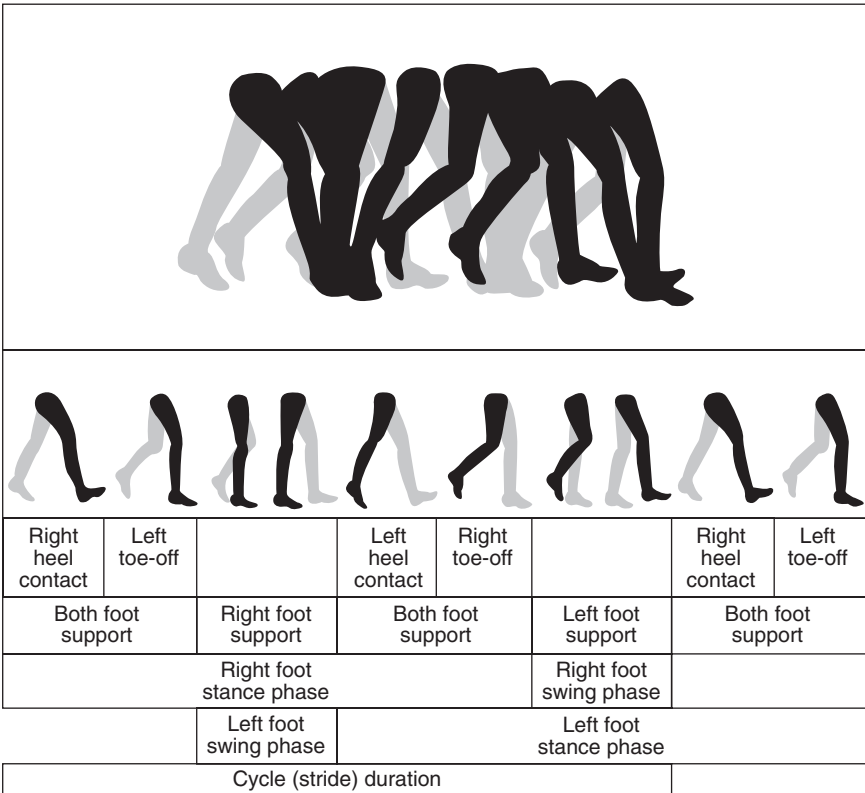
*22.6* Gait cycle.

speeds, there are slight variations in the percentage of stance and swing phases. Also, when changing from walking to running, the duration of double limb support decreases until it is eliminated while running. A stride or gait is the interval between sequential initial floor contacts by the same limb (Fig. 22.6). A step is recognized as the interval between sequential floor contacts; thus, two steps make up each gait cycle.
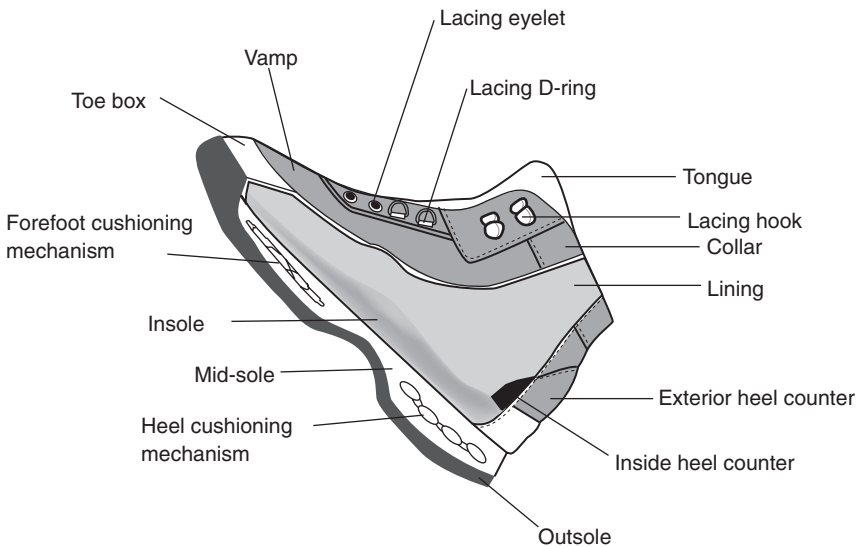
## 22.3   Footwear

In today's society, footwear has become increasingly specialized for a variety of tasks and functions. There are shoes for most sports, ranging from running to golf. Footwear design and manufacture have been influenced by function but also by fashion and technology. In the following sub-sections, the main components of footwear (Fig. 22.7) and footwear manufacturing will be discussed.

### 22.3.1  Anatomy of footwear

*Shoe upper*

The shoe upper includes toe box, vamp, tongue, lining, collar, and fastening mechanisms (lacings, zipper, etc). The toe box covers the toe region and affects the fit at the toes. The function of the toe box is to protect the toes,



*22.7* Anatomy of footwear.

allow their movement, and retain the shape of the shoe around the toe. The toe box may include a metal toecap in order to protect the toes against injury, especially in working boots. The vamp covers the dorsum of the foot including the tongue piece and superior aspects over the toes. This section is reinforced to give the shoe its shape as well as protection. The vamp is often made of more than one piece, creating a decorative pattern. There are various types of vamps suited for different styles of shoes.

The construction of shoe upper depends on style and fashion; however, the shoe *last*, a 3-D mould that represent the foot shape, determines the shape of the shoe upper. The uppers are made with leather or synthetic materials such as polyurethane-coated fabrics (PUCFs), polyvinyl chloride coated fabrics (PVC-CFs) or leather-like materials called poromerics. Leather, due to its inherent properties such as plasticity and breathability, is a better choice for the shoe upper and has been used through the ages. Leather can easily take the shape of the foot after sometime in use. It can also absorb perspiration and allow air-flow from the surrounding. This provides good aeration and can keep a suitable climate inside the shoe. Even though leather seems to be the perfect choice for shoe upper, PUCF, PVC-CF, and poromerics are also used because of cost and fashion trends. Synthetic uppers are cheaper and are used in most mass-produced footwear. PUCF is soft, light and comfortable to wear, but not so durable. PVC-CF is cheap, easy to clean, durable, but not breathable and does not change shape to fit the foot. Poromerics, even though synthetic, have leather-like properties. They are used widely as a leather substitute.

*Shoe sole*

The main components of the bottom are the outsole, the mid-sole, and the insole. The outsole is designed to give durability and traction but also contributes to shock absorption. The mid-sole is designed exclusively for shock absorption. Sometime a wedge is added at the heel for shock absorption and heel lift. The insole board is covered with a thin layer of material called a 'sock-liner' or an insole. This provides some cushioning, but its importance is during lasting (pulling the upper part of the shoe on the *last* and sticking on the insole board). Since many sports movements produce forces of considerable magnitude, most sports footwear has some sort of cushioning mechanism making use of air or gel.

Common soling materials are leather, rubber, polyvinyl chloride (PVC), ethylene vinyl acetate (EVA), and polyurethane (PU).[26] EVA is light weight and has good cushioning abilities. PU is heavy and inflexible, though it is more durable than EVA and still has cushioning abilities.

## 22.3.2 Shoe last

The word *last* (Figure 22.8) comes from the old Anglo-Saxon word *laest*, meaning a footprint or foot track. While shoemaking is an age-old craft rich in tradition, heritage and prestige, the foundation of shoes – the *last* – has been recognized as an important fashion and health factor only within the past few decades.[5] The *last* is the very heart, the single most important element, of the shoe.[12] It is the most scientific and complex part of the whole shoemaking process and it is the foundation upon which much shoe-related foot health depends.[27] It is responsible for the size, fit, shape, feel, wear, style, tread, and even the making of the shoe.[28]

The *last* is a reproduction, generally in maple wood, of the approximate shape of the human foot over which a shoe is produced which, when properly constructed, furnishes support and protection without undue pressure,
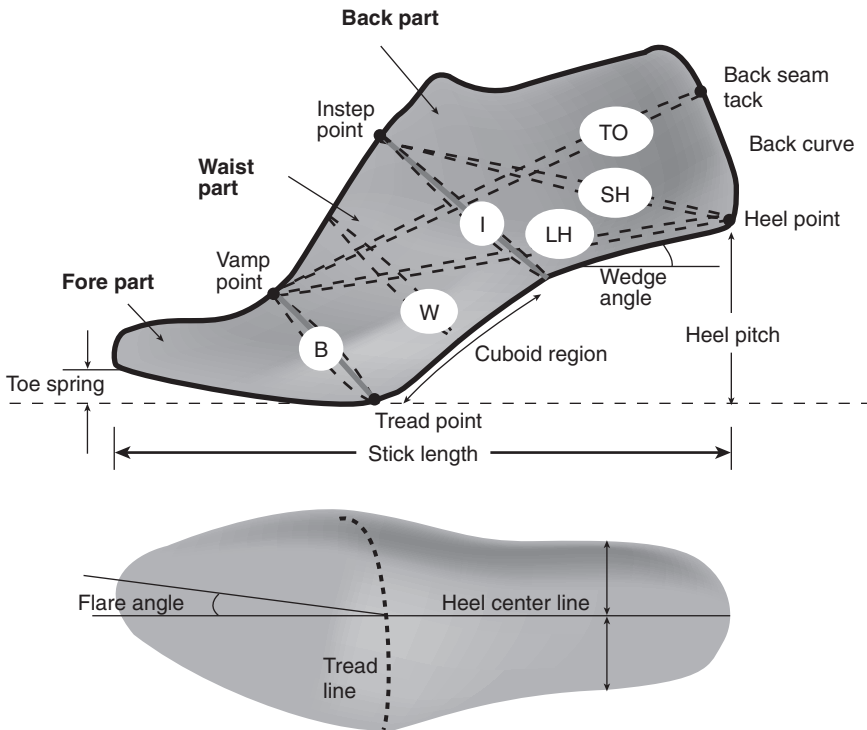


Note:
I : Instep girth        W : Waist girth        B : Ball girth
LH : Long heel girth    SH : short heel girth    TO : Throat opening

*22.8* Ladies shoe-last with basic last measurements.

binding or constriction at any point.[5] The first *last* maker in the USA whose name is on record was William Young of Philadelphia, Pennsylvania, who was granted a patent for a minor *last* improvement in the year 1807. In 1840, *lasts* were slightly improved. By adding a pad over the front of the shoe they created two sizes called 'slim' and 'fat'. Now, shoes are made on *lasts* graded in width from AAA (small) to EE (large) (The widths are AAA, AA, A, B, C, D, E, EE).

During the 19th century until about the time of the American civil war, the same wooden *last* was used in the construction of both right and left shoes. The *lasts* were straight in shape with no allowance for the foot contour. The shoes could be swapped from left to right. Before 1880, shoes were made in full sizes and seldom more than three widths. After 1880, half sizes were introduced. In the twentieth century, quarter sizes were introduced but were unsuccessful due to inventory costs.

In 1815, Thomas Blanchard, Sutton, Massachusetts invented a lathe for the turning of irregular shaped objects. It was first used for turning out gunstocks but was later adopted for *lasts*. The Gilman lathe, now used throughout the *last* industry, was an improvement on the Blanchard lathe. By reason of the fact that no feet are exactly alike, one can readily appreciate the necessity of making shoes on scientifically designed *lasts* – *lasts* that will conform to the great majority of feet of any given type.[5]

Even after 60 years, most master *lasts* are still made by a master *last* maker, who uses his/her artistic skills to generate a *last* using few foot parameters. Currently, wood, aluminum, or plastic (high density polyurethane) are used for shoe *lasts*. The wooden *last*, which has a high price and low durability, is the traditional material for *last* making. It has the disadvantage of changing its shape due to temperature and humidity. Currently, it is usually used for the model, master or designer's *last*. However, the plastic *last* is widely used. It has a medium durability, but it is difficult to handle due to its heavy weight. Aluminum *lasts* are relatively cheap and have high durability, however, their shape is temperature dependent.

*Difference between foot and last*

It is essential to understand the difference between a *last* and a human foot. The *last* has a smooth surface to enhance the appearance of the shoe and enable the upper to be moulded more easily to shape. The surface of the foot is irregular and varies with individuals. The outline of a *last* is regular and continuous with a sharp featheredge around the seat and forepart to assist lasting and give a clear defined edge to the finished shoe. The foot has no featheredge. The *last* is hard and firm, while the foot is softer and more flexible. The foot has separate toes, while the toe end of a *last* is solid. The heel curve is greater on the *last* to help the shoe grip the foot. Heel pitch

is present in the *last* but not on the foot. The front part of the *last* is thinner to help the shoe to grip the foot around the quarters. The *last* length is greater than the foot to prevent pressure on the foot. Toe spring is not present on foot but is on the *last.* Girth and size intervals are regular on *lasts* but irregular on feet. The dimensions are identical on a pair of *lasts* but rarely identical on a pair of feet. At the toes, the *last* increases gradually in height from the feather line, but not in the foot. The *last* is for shoe making while the foot is used for weight bearing and locomotion.

### Basic last measurements

The American Footwear Manufacturers Association (AFMA) defines as many as 61 terms related to *last* dimensions. However, there is no direct mapping from the foot to the *last*. The model maker rarely starts from scratch. A previous *last* is used as a starting point, and thus foot studies have little impact on *last* making.[17] Although the *last* is a complex 3-D shape with no straight lines on it, the *last* maker first marks the four points vamp, instep, ball break, and heel point as the reference points[17] as shown in Fig. 22.8. Then only six dimensions are used to guide the last maker in the *last* making process. Five of the six measures are circumference measures: ball girth, waist girth, instep girth, long heel girth, and short heel girth. The final measurement is the overall heel-to-toe length on the *last*, which is also called stick length. The model maker shapes, sands and files until the six measurements match and the model 'looks right'.[17] The way the model has been sanded will affect the fit. The *last* making is evolved on a man's size 9D *last* or a woman's size 7D *last*. The other sizes are generated by a procedure known as grading.[28]

It is important to note that the stick length used in *last* making is dependent upon heel height, toe spring, and toe style. The degree of toe spring in a *last* depends on several factors, namely the heel height, the shoe style, the upper material and the general flexibility of the shoes. When the heel height is high, the toe spring is lower. Stiff upper material requires more toe spring. Furthermore, toe spring depends on the purpose of the footwear. Normally, walking shoes need more toe spring than dress shoes, while ballet shoes do not have toe spring.

### Sizing and grading

Sizing basically involves the construction of footwear of different sizes in order to *fit* the selected population. A *last* is measured by the 'stick length' shoe size. The exact sizing of footwear in order to have perfect physical *fit* is complicated since there is a large range of variations in the dimensions

of the human foot. In order to make the sizing simple, a combination of foot length and foot width is used. However, the size markings are rarely exact.[26] Foot length is measured as the maximum distance from the heel point to the toes. Foot measuring devices such as the Brannock, the Ritz stick, and the Scholl have concentrated on two areas by measuring the length along the foot and the maximum width around the MPJ joint area.

In the US and British systems, the shoe size length changes by 1/3″ (8 mm) per size and the girth by 1/4″ (6 mm) per size. In addition there is an increase in 1/4″ (6 mm) between different width grades. For example, from shoe size 9D to shoe size 10D the length will increase by 1/3″ (8 mm) while the girth will increase by 1/4″ (6 mm). However, from shoe size 9D to shoe size 9E the girth increases by 1/4″ (6 mm) while the length is not increased. Apart from the US and British systems, most European countries use the French system, also known as the continental system or the Paris points. The ratio of length increase to girth increase is the same as in the other two systems. However, the metric increment is not the same. The length grade is 2/3 cm and the girth grade is 1/2 cm between sizes. The Mondopoint system is a foot sizing system proposed by the International Standards Organization (ISO). This uses the metric system for sizing the length and the width dimensions.[29] Different from the other system, the projected length of a foot, around which the shoe should *fit*, is used for sizing.

There are three types of grading system: the arithmetic grade, the geometric grade, and the proportional grade. In an arithmetic grade, the increment of a dimension per increase in foot size is a constant.[28] The arithmetic grade is currently used for US and British shoe standards. In the geometric grade, the increment per size and/or width of any dimension is a specified percentage of the dimension. Proportional grading is a system in which the increments of all dimensions per size within a size run are a constant.

*Different last shape*

There are an enormous number of shoes, but most of them can be classified into six toe types. These are square, oblique, round, circle, oval and crescent (Fig. 22.9). Moving from round to crescent passing through circle and oval, the toe shape becomes more pointed. The square shape shoe *last*, as the name suggests, does not have a rounded toe box. The oblique toe box provides more space at the big toe and less space at the fifth toe. If properly designed, it can provide the best comfort. In addition, the shoe-last can be different based on different toe heights, as shown in Fig. 22.9. Due to the shape of the *last*, especially at the toe, shoes of the same size may not have the same length and width. As a result, shoes manufactured with different shoe-last do not have the same *fit*.

Square        Oblique        Round        Circle        Oval        Crescent

(a) Different toe shape

Pointed                              Bump

(b) Different toe height
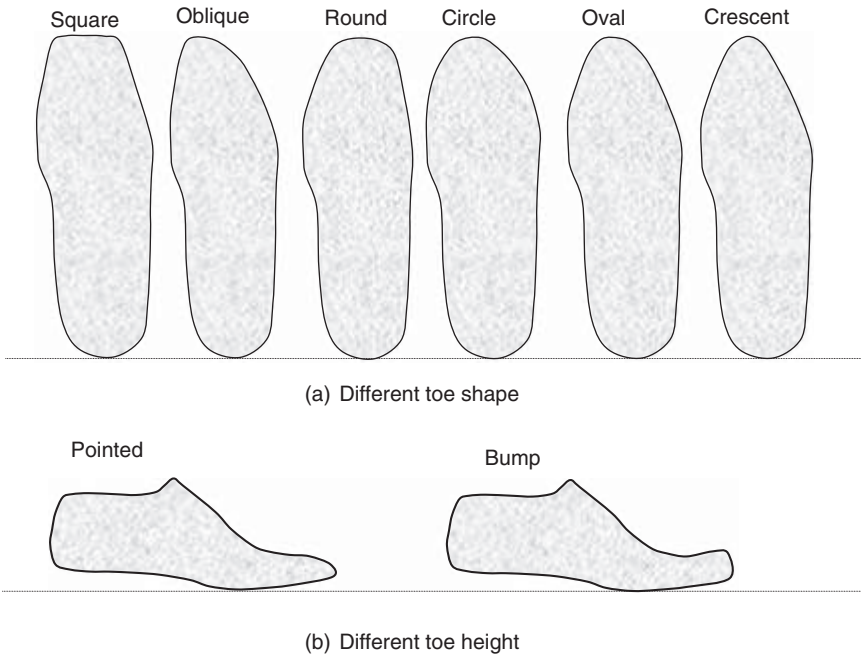
*22.9* Shoe-last shapes.

*Curve and straight last*

In addition to *last* shape, shoe-lasts can have different plantar curvature (Fig. 22.10). The shoe 'curvature' or flare can be seen while looking at the shoe outsole or the bottom of a *last*. The flare can be quantified as an angular measure,[19] ratio,[30] or an angular measure with a center.[20] Most *lasts* have a distinct inward turn towards the medial side of the foot and are known as curved, racing or inflared *lasts*. Most shoes have a 6 degrees inflare.[31] The flare angle, which is typically 3 degrees for a straight *last*, can be up to 12 degrees.[17] Different shoe manufacturers build-in different flares in their shoes (Fig. 22.10); thus different shoes with the same size can have different fittings.

## 22.3.3 Footwear manufacturing

SATRA[26] provides 12 simple steps to make footwear. The first step in shoe production is to have a shoe *last*. The *last* is covered with paper tape and a pattern is drawn on it. The tape is then removed from the *last*. Various allowances are added. The patterns are then encoded into knives and cutters. This can be used in a press to cut the leather or synthetic material. After
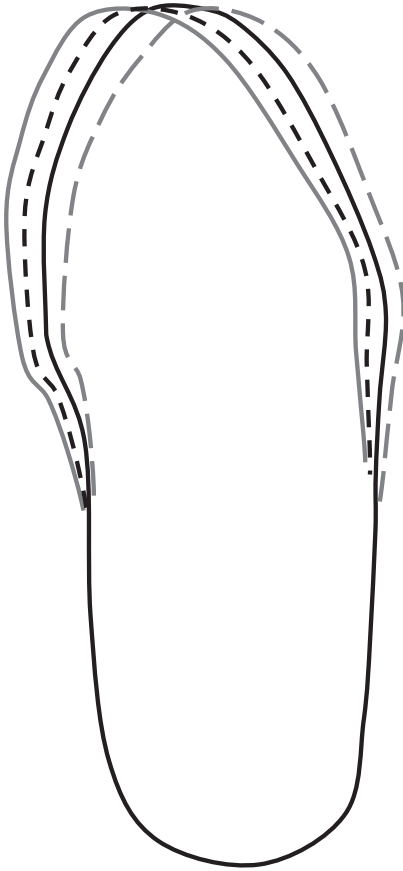
*22.10* Shoe-last with different curvatures.

the upper material is cut, it is stitched together to form the upper part of the shoe. The upper part may include toe puffs and heel stiffeners. The insole is attached to the *last*. The upper part is lasted. Lasting is basically the pulling of the upper part and sticking in on the insole attached to the *last*. The sole unit is attached. In some cases the sole and heel are attached. The shoe is cleaned and sprayed. The shoe is checked and dispatched. This procedure is for the cemented shoe construction method, the most common shoe manufacturing method (Table 22.1). There are different types of shoe construction based on shoe style, cost and quality.[32]

*Shoe classification*

There are numerous shoe styles and new styles of footwear are created every day. Independent of the number of shoes in the market, there is a fixed shoe

*Table 22.1* Type of shoe construction

| Name | Construction method |
|------|---------------------|
| Cemented | Most shoes are constructed using this method.<br>– The insole is attached using staples or adhesives to the last bottom.<br>– The shoe upper is placed on top of the last.<br>– The free ends of the upper are pulled, turned on the insole and glued.<br>– The outsole is cemented to the bottom of the lasted shoe upper.<br>– The heel is attached if needed. |
| Veldtschoen stitch down | The upper is flanged outwards and stitched to the insole. The outsole is cemented to the lasted shoe. |
| Welted | A special insole with a rib or wall is used. The upper is attached to the ribs usually by wires or staples. The sole is then stitched to the upper. This method is usually used to make better grade men's dress shoes and requires high skills, especially if manual. |
| Slip-lasted | The last is placed inside after the upper has been stitched with the insole and a sock or cover. Most infant shoes and slippers are constructed using this method. |
| String lasted | A strong string is used to stitch the edge of the upper. The upper is fitted to the last and then the string is drawn and its ends tied. Then the soles are attached. |
| Vulcanized | Usually the upper is made of canvas and the insole is attached to the canvas by sewing.<br>– The last is forced inside the upper.<br>– The sole and mud-guard rubber foxing are attached.<br>– The shoe is vulcanized (placing the lasted shoe in a vulcanization tank which is set to a temperature of 150 °C, pressure 3 kg/cm³ for about 50 minutes.)<br>For some shoes, such as work shoes and outdoor boots, the outsole is directly vulcanized and moulded to the shape of the sole. |
| Injection | Soles are directly heat-sealed to the upper by machine. |

classification system. In general, seven categories are used, except in Hong Kong where ten categories are used for footwear classification. The categories, as shown in Fig. 22.11, are Oxford, pump, boot, sandal, mule, clog, moccasin, infant (Hong Kong classification), children (Hong Kong classification), and sports (Hong Kong classification). Figure 22.11 also provides a simple drawing for each shoe category. Traditionally, Oxford was worn by men only; however, this trend has changed. Now even ladies wear Oxford shoes. Pump, mule and clog are usually worn by ladies, while Oxford, boots, moccasin, sports shoes, and sandals are worn by both ladies and gentleman. Babies' and children's footwear need to have allowance for foot growth and should also include attractive components (lights, sounds, and attractive colors).

| Oxford | | For many people, Oxford shoes are basically dress shoes and are worn by men, ladies and children. Oxford shoes can be sub-categorized into Balmoral Oxford, Blucher Oxford, Saddle Oxford, Derby, Work shoe, Loafer, and Monk shoe. |
|---|---|---|
| Boot | | Worn by men, ladies, children and infants. This footwear covers the ankle and was designed for industrial and military work, and outdoor activities. These days, it is worn for all purposes. Boots can be further categorized into Desert boot, Wellington boot, Work boot, Military boot and Cowboy. |
| Moccasin | | Shoe constructed with leather wrapped around the last to form the bottom, sides and upper. Include Deck shoes. |
| Sandal | | Sandals are worn by men, ladies and children. Sandals are open shoes which consists of a decorative or functional arrangement of straps. These include Casual sandals, Sport sandals and Thong sandals. |
| Pump | | Pumps are ladies' shoes. They include Pump, Sling-back court, Open Shank court, Open back court, Open toe court, and Platform court. |
| Mule | | These are shoes without a back strap and slippers with or without heel. |
| Clog | | Clogs are shoes with thick wooden soles. |
| Infant | | Shoes designed for young children. These are soft, with lots of room for the foot to move and grow. |
| Children | | These shoes may have special design for beauty and fun such as sounds and lights. |
| Sport | | There are more and more specific shoe designs for different sports such as Badminton, Baseball, Basketball and others. Since these sports have different dynamics, the shoes are designed to enhance performance and reduce injury, as well as to provide comfort. |

*22.11* Shoe classification.

## 22.4    Foot and footwear interface

The interface between the foot and the shoe determines the footwear fit and comfort. When there is a mismatch between the foot and the shoe, the foot is deformed resulting in injury and foot-related illness. It has often been stated that babies are born with perfect or near perfect feet, and many of the foot deformities are due to ill-fitting footwear.

## 22.4.1  Foot problems

Some of the foot deformities related to footwear are hallux valgus, ankle valgus, hallux rigidus, lesions, corns, calluses, blisters, chilblains. Hallux valgus is associated with abnormal pressure at the MPJ joint of the great toe.[33] The joint is enlarged and there may be formation of a bursa sac of fluid at the joint. In advanced cases, the first toe can overlap or underlay the second toe and the first metatarsal may be deflected away from the other metatarsals. In addition, the MPJ may dislocate and the metatarsal head can be exposed. Moreover, the bursa can be inflamed and it is then known as a bunion. Hallux valgus is caused by footwear that is too narrow or too short. The footwear squeezes the toes together. Ankle valgus (pes valgus) may not be painful in itself. It is caused by the inward rotation of the back of the foot such that the body weight falls on the inner side of the foot, causing the arch to flatten. The condition is self-aggravating, since the more the foot twists the more the weight is on the inner side of the foot. Hallux rigidus include deformities such as hammer toe, clawed toe, retracted toe, mallet toe. It occurs when the footwear is too short and thus limits the movement of the toe at the joints. Calluses, corns, blisters and chilblains belong to the deformities known as lesions. Calluses occur when there is intermittent pressure on some part of the foot. This causes the outer skin to thicken and become hard. Usually, there is pain and a burning sensation when the calluses are under pressure. Corns normally occur over toe joints, when there is friction associated with localized pressure. Blisters are caused by friction. During friction, the outer skin becomes loose and fluid collects beneath it. If the friction continues, the blister breaks, causing an inflamed area. This occurs normally at the back of the heel due to heel slip. Chilblains are caused by pressure, normally at the back of the heel in cold weather.

  Many deformities can be eliminated if the offending footwear is discarded early enough. For mild cases, custom insoles, wide toe-box shoes, and arch supports can be used, while surgery might be needed for severe cases.

## 22.4.2  Consumer consideration

Several surveys have shown that footwear *fit* is a very important factor when purchasing footwear. The characteristics that may affect the choice of footwear depend upon footwear related factors (material, weight, quality, durability, flexibility, traction, shock resistance, etc.), society related factors (fashion, style, brand, store, peer pressure, self esteem, etc.), and foot related factors (comfort, fit, function, softness, cushioning, perceived flexibility, breathability, etc.).[33] Furthermore, subjects rate *fit*, minimal perspiration, good thermal insulation, sole flexibility, upper flexibility, and protection

against the elements as the main elements of comfort (Bolanger, 1974, cited in reference 17). According to Clarks,[28] major consumer needs are appearance and fashion content, *fit* and comfort, price, quality and store. Chong and Chan,[2] in a footwear survey using 70 subjects, required the subjects to rank the importance of six factors (attractive style, function, affordable price, famous brand, material quality, and comfort) when buying a pair of shoes. 27.8% of the subjects gave the highest rating to comfort. When computing the weighted average from Chong and Chan's study,[2] Luximon and Goonetilleke[34] found that comfort was rated higher than quality, price, function, and brand. Since comfort is affected by *fit*, it can be deduced that *fit* is an important factor. The footwear fit can be quantified using dimensional differences between footwear and foot.[34] Fit is just one of the consumer considerations; the whole footwear has to be assessed to select a proper choice for a given function.

## 22.4.3 Footwear assessment

Experienced fitters check 14 points when fitting footwear.[11] Most of the *fit* trials show that the toes and the ball areas are the most critical to an individual's perception of *fit*. In addition to footwear fit, comfort, flexibility and cushioning have also been evaluated subjectively and objectively.[35] Luximon[33] has considered comfort and fit at the toe box, waist, instep region, and heel region. Table 22.2 shows the different parameters and the footwear regions that can be used to assess footwear comfort, fit, and function.

*Table 22.2* Footwear assessment

| Footwear region | Parameters | | |
|---|---|---|---|
| Toe region or toe box | Width | Height | Volume |
| MPJ region | Width | Height | Girth |
| Instep region | Width | Height | Girth |
| Arch | Height | | |
| Topline or Collar | Height | Comfort | |
| Heel | Width | Back curve | Heel cup fit |
| Sole | Flexibility | Flexion point | Tread pattern |
| | Overall cushioning | Cushioning at heel | Cushioning at forefoot |
| | Traction | Comfort | |
| General | Flexibility | Material | Construction |
| | Overall comfort | Fastening mechanism | Stability |

## 22.5    Biomechanical model

Due to the advancement of technology, it is possible to generate a complex 3-D biomechanical model of the foot including its structures. Generally, the 3-D model of the human foot and ankle is generated from coronal sections of MRI images. Zhang *et al.*[36] used MRI images at 2 mm intervals to create a 3-D geometrical accurate ankle–foot model using MIMICS™ (Materialise Inc., Leuven, Belgium) and SolidWorks 2001™ (SolidWorks Corporation, Massachusetts). Then, ABAQUS™ (ABAQUS Inc. Pawtucket: Rhode Island, USA), a Finite-Element (FE) analysis software, was used for FE mesh generation and subsequent FE analysis.[36] The FE model consisted of 28 distinct bony segments and all major ligaments embedded in homogenous soft tissue.[37] In order to simplify, as well as to have computational convergence, all elements had homogeneous, isotropic, and linearly elastic material properties. The bony structure had a Young's modulus of 10 000 MPa and the Poisson ratio was 0.34, while the plantar soft tissues had a Young's modulus ranging from 0.05 MPa to 0.3 MPa and a Poisson ratio of 0.49.[38] The foot biomechanical model, together with mechanical models of insole,[39] *last*, and footwear,[40] can be used to evaluate internal stresses/strains of the ankle–foot complex. FE analyses can be used efficiently to determine design parameters of footwear without the need for expensive experimental study. In addition, the material properties of the insole and foot model can be varied to study the impact on the foot.

## 22.6    Conclusion

Footwear has become an integral part of our life and it will remain so for many years to come. Although, footwear has become very sophisticated, footwear comfort and fit has often been neglected. This might be due to the wide variation in feet and the cost of production. It is very expensive to produce individual footwear, so footwear is produced in different sizes. In addition, shoes are produced in different styles depending on fashion. This might further aggravate footwear comfort and fitting. As people become more health conscious, more research is being undertaken into understanding the human foot and its biomechanics. Several biomechanical models are being constructed to help design better footwear. In addition, advancement in technologies will reduce the cost of production; thus perfect fitting footwear will be possible. In conclusion, footwear design should consider fashion and style as well as fit, comfort, and function.

## 22.7    References

1. Dahlberg, G. and Lander, E. (1948). Size and form of the foot in men. *Acta Genetica*, **2**(I): 8–162.

2. Chong, W.K.F. and Chan, P.P.C. (1992). *Consumer Buying Behaviour in Sports Footwear Industry*. Hong Kong, Business Research Centre: Hong Kong Baptist College.
3. Carlson, M. (2001). Footwear of the Middle Ages. *http://www.personal.utulsa. edu/~marc-carlson/shoe/SHOEHOM1.HTM*.
4. Kippen, C. (2004). The History of Footwear. *http://podiatry.curtin.edu.au/history. html*.
5. Quimby, H.R. (1944). *The Story of Lasts*. New York, National Shoe Manufacturers Association.
6. Luximon, A. and Goonetilleke, R.S. (2001). A fit metric for footwear customization. *World Congress on Mass Customization and Personalization*, Hong Kong.
7. Cummings, S.R., Ling, X. and Stone, K. (1997). Consequences of foot binding among older women in Beijing, China. *American Journal of Public Health*, **87**, (10): 1677–1679.
8. Hunt, K.D. (1994). The evolution of human bipedality: Ecology and functional morphology. *Journal of Human Evolution*, **26**, (3): 183–202.
9. Morton, D.J. (1935). *The Human Foot*. New York, Columbia University Press.
10. Abboud, R.J. (2002). Relevant foot biomechanics. *Current Orthopaedics*, **16**, (3): 165–179.
11. Rossi, W.A. (1988). The futile search for the perfect shoe fit. *Journal of Testing and Evaluation*, **16**: 393–403.
12. Rossi, W.A. (1983). The high incidence of mismated feet in the population. *Foot and Ankle*, **4**, (2): 105–112.
13. Tsung, Y.S. (2003). *Insole design based on pressure distribution and foot shape under different weight bearing conditions*. Hong Kong, The Hong Kong Polytechnic University.
14. Cheskin, M.P. (1987). *The Complete Handbook of Athletic Footwear*. New York, Fairchild Publications.
15. Kouchi, M. and Mochimaru, M. (2002). *Japanese Body Dimensions Data 1997–1998*, Digital Human Research Center, National Institute of Advanced Industrial Science and Technology.
16. Malina, R.M., Hamill, P.V.V. and Lemeshow, S. (1973). Selected measurements of children 6–11 years. *Vital Health Statistics, Series 11*. Washington, DC., USDHHS, US Government Printing Office.
17. Cavanagh, P.R. (1980). *The Running Shoe Book*. Mountain View, CA, Anderson World.
18. Palastanga, N., Field, D. and Soames, R. (1989). *Anatomy and Human Movement: Structure and Function*. Oxford, Heinemann Medical Books.
19. Freedman, A., Huntington, E.C., Davis, G.C., Magee, R.B., Milstead, V.M. and Kirkpatrick, C.M. (1946). *Foot Dimensions of Soldiers*. Fort Knox, Kentucky, Armored Medical Research Laboratory.
20. Goonetilleke, R.S. and Luximon, A. (1999). Foot flare and foot axis. *Human Factors*, **41**, (4): 596–607.
21. Nigg, B.M. (1986). *Biomechanics of Running Shoes*. Champaign, Ill, Human Kinetics Publishers.
22. Clarke, H.H. (1933). An objective method of measuring the height of the longitudinal arch in foot measurements. *Research Quarterly*, **4**: 99–107.
23. Cavanagh, P.R. and Rodgers, M.M. (1987). The arch index: A useful measure from footprints. *Journal of Biomechanics*, **20**, (5): 547–551.

24. Kreighbaum, E.F. and Smith, M.A. (1996). *Sports and Fitness Equipment Design*. Champaign, Ill., Human Kinetics.
25. Kaplan, A.R. (1964). Genetics of Relative Toe Lengths. *Acta Genet. Med. Gemellol*, **13**: 295–304.
26. SATRA (1993). *How to Fit Footwear*. UK, Shoe and Allied Trades Research Association (SATRA), Footwear Technology Centre.
27. Rossi, W.A. (1980). The Last: Heart of the Shoe. *Journal of American Podiatrist Association*, **70**: 533–534.
28. Clarks (1989). *Manual of shoe making*. UK, Training Department Clarks.
29. ISO9407 (1991). *Shoe Sizes – Mondopoint System of Sizing and Marking*. Switzerland, International Organization for Standardization.
30. Yavatkar, A.S. (1993). *Computer aided system approach to determine the shoe-last size and shape based on statistical approximated model of a human foot*. Medford MA, Tufts University.
31. Holscher, E.C. and Hu, K.K. (1976). Detrimental results with the common inflared shoe. *Symposium on Pitfalls in Foot Surgery*: 1011–1018.
32. Hong Kong Productivity Council (2001). *Information Handbook for Merchandisers of the Hong Kong Footwear Industry*. Hong Kong, Publisher Hong Kong Productivity Council.
33. Luximon, A. (2001). Foot shape evaluation for footwear fitting, in *Industrial Engineering and Engineering Management*. Hong Kong, Hong Kong University of Science and Technology.
34. Luximon, A. and Goonetilleke, R.S. (2003). A 3-D methodology to quantify footwear fit (Chapter 28), in *The Customer Centric Enterprise – Advances in Customization and Personalization*. M.M. Tseng and F. Piller (eds). New York, Berlin, Springer: 491–499.
35. Mundermann, A., Stefanyshyn, D.J. and Nigg, B.M. (2001). Relationship between footwear comfort of shoe inserts and anthropometric and sensory factors. *Medicine and Science in Sports and Exercise*, **33**, (11): 1939–1945.
36. Zhang, M., Cheung, J.T.M., Fan, Y.B. and Leung, A.K.L. (2002). Development of 3D finite element model of human foot and ankle. *IVth World Congress of Biomechanics*, Calgary, Canada.
37. Cheung, J.T.M. and Zhang, M. (2004). A 3-D finite element model of the human foot and ankle for insole design. *Archives of Physical Medicine and Rehabilitation*: Accepted 2004.
38. Gefen, A., Megido-Ravid, M. and Itzchak, Y. (2001). *In vivo* biomechanical behavior of the human heel pad during the stance phase of gait. *Journal of Biomechanics*, **34**, (12): 1661–1665.
39. Cheung, J.T.-M., Zhang, M. and Luximon, A. (2004). *Computational Model for Foot Orthosis Design*. 11th *World Congress of International Society for Prosthetics and Orthotics*, Hong Kong.
40. Luximon, A., Cheung, J.T.M. and Zhang, M. (2004). Biomechanical effects of shoe last design on the ankle–foot structures, *International Society for Prosthetics and Orthotics*, Hong Kong.

# 23
## Biomechanical engineering of aerobic sportswear

A. WONG[1], Y. LI[1], E. NEWTON[1] AND X. ZHANG[2]

[1] The Hong Kong Polytechnic University, China
[2] Xian University of Engineering Science & Technology, China

## 23.1 Introduction

In relation to clothing construction, Kirstein *et al.*[3] stated that the term 'fit' means to adjust the measurements of a garment to those of the body. Zhang *et al.*[15] stated that garment pressure is closely related to the space allowance between the body and the garment during body movement. When a garment girth measurement is smaller than the human body, the space allowance between body and garment is less than or equal to zero, hence pressure is generated. Skin is extremely sensitive to pressure and, under ideal conditions, skin displacement that is less than 0.001 mm can result in a sensation of pressure or touch.[9] Denton[2] found the level of clothing pressure discomfort to be in the range 20 to 40 g/cm$^2$, depending on the individual and the part of the body concerned. According to Pratt and West,[8] there are three factors influencing the pressure exerted by garments: (i) shape of the body parts, the greater the degree of curvature, the greater the pressure exerted; (ii) type of fabrics used; and (iii) design and fit of the garment. A badly designed garment may lead to the body suffering by perceiving unnecessary pressure.

In general, investigations of pressure distribution on the human body can be classified into two categories: experimental and numerical. The experimental category, can be divided into psychological and physical sections. Morooka *et al.*[7] found that perception of clothing pressure of females in their forties was twenty percent less than for females in their teens and twenties. Furthermore, the influence of leg circumference on the clothing pressure tended to become lower with increasing age. Zhang *et al.*[11–14] carried out a series of investigations in relation to pressure by using the force–deformation of relationship fabric bagging – a planar fabric being forced to conform to a spherical surface. Mitsuno *et al.*[6] used a hydrostatic pressure-balanced method to measure clothing pressure qualitatively. Makabe *et al.*[5] investigated clothing pressure developed by a girdle. They found that subjects perceived pressure discomfort mainly on the front waist

line and the thigh base. They also noticed that when clothing pressure reached more than 30 to 40 mm Hg, subjects began to complain of pressure discomfort. The previous chapter investigated the psychological pressure perception of tight-fitting sportswear in young adults.[10] A group of subjects wearing different sets of tight-fitting sportswear and required to perform different postures gave scores at nine pressure points on the perception of pressure comfort on the body after each posture. The results show that subjects perceived most pressure discomfort around the thigh. We also carried out a physical pressure distribution investigation, when five female subjects participated in a wear trial.[10] Each subject was connected to nine pressure sensors, which were placed between the subject's skin surface and the inner layer of the garment at nine different body locations. By assuming different postures, the results show that subjects perceived most pressure at the side waist while they were standing, arm-lifting and stretching. However, subjects perceived most pressure at the front waist while they were curling-up their legs.

Although these experimental results indicate that there are differences in the pressure perception, they do have disadvantages, including: (i) many subjects have to be used in order to obtain a reliable result, (ii) subjective judgments may be influenced by many psychological factors, which vary from person to person, and (iii) the variations in subjects' body curvatures influence the placement of pressure sensors. Cheng *et al.*[1] stated that the distortion degree of sensor insertion and the degree of accuracy of the sensor used were found to be important factors influencing the measured level of garment pressure. These experiments provide evidence and clues on what factors influence the garment pressure and the perception of pressure comfort. However, they cannot explain the physical mechanisms involved.

Theoretical investigations can be carried out to develop an understanding of the mechanisms by establishing mechanical–mathematical models on the basis of physical laws. The models can be solved by numerical computation, and can be used for numerical simulation of the wear process. In the numerical simulation, the 3D human body model can be generated through a commercially available virtual human model or a scanned human body, and pressure distributions of a garment can be predicted on the basis of fabric properties. A series of biomechanical models have been developed by Zhang *et al.*[15] and Li *et al.*[4] to investigate the dynamic interactions between the human body and garments in various wear situations, such as a bra and tight-fitting trousers, by considering the biomechanical structures of the human body, and the contact mechanics between body, garment and 3D garment constructions.

In this chapter, a theoretical investigation of garment pressure comfort is conducted by applying a dynamic model for the numerical simulation of

pressure in tight-fitting garments during wear. By analyzing the contact characteristics between a human body and a tight-fit garment, the process of a female body wearing three well-fitting tight-fit garments, which have the same design but are made from different fabric, is simulated. The predicted pressure distributions are compared with the objective garment pressure measurements and psychological pressure perception ratings.

## 23.2    Biomechanical modeling

Clothing pressure is a combination of garment, human body and the mechanical interactions between them. Denton[2] stated that true fitting to the body shape can only be achieved by the use of stretch fabrics that can expand and contract without buckling or wrinkling to accommodate body movement. Zhang et al.[15] held that garment pressure is closely related to the space allowance between body and garment when the body is moving. Furthermore, Zhang classified garment into three categories on the basis of space allowance.

Therefore, the assumption of stretch-to-fit garment is to be a thin elastic shell with material linearity and geometric non-linearity, and the human body to be a rigid body. The stress in the direction of fabric thickness is assumed to be zero. This simulation only considers the female body in a steady standing state. All the garments have the same style but are made of different materials.

Figure 23.1 shows the model developed by Zhang et al.,[15] which describes the interaction between human body and a tight-fit garment. During wear, mechanical interaction occurs at the contact areas between the body and the garments. The figure shows the external forces on the tight-fit shorts during wear, including an interactive contact force $q_c$ in the normal direction to the contact surface, the friction $q_f$ as the garment slips on the surface and the gravity $q_g$ on the garment. The external forces will be balanced by fabric internal stresses (tension, shearing and bending) and the inertia force $q_I$ of the garment during a dynamic deformation process.

In the simulation of a human body, three major components (skin, soft tissue and bone) were considered. A human body is constructed from a skeleton covered by a layer of skin, which is the largest organ in a human. Between the skeleton and skin is a layer of tissue. A 3D finite element model of a female human body was developed on the basis of a commercially available virtual human model.

The process of a female human body wearing a pair of tight-fit shorts from the foot level to the waist was simulated. The process was divided into three steps: (i) the waistline of the garment just reaching the subject's shank; (ii) the waistline of the garment reaching the subject's pelvis; and (iii) the garment completely fitted to the subject. In practice, a human's body and
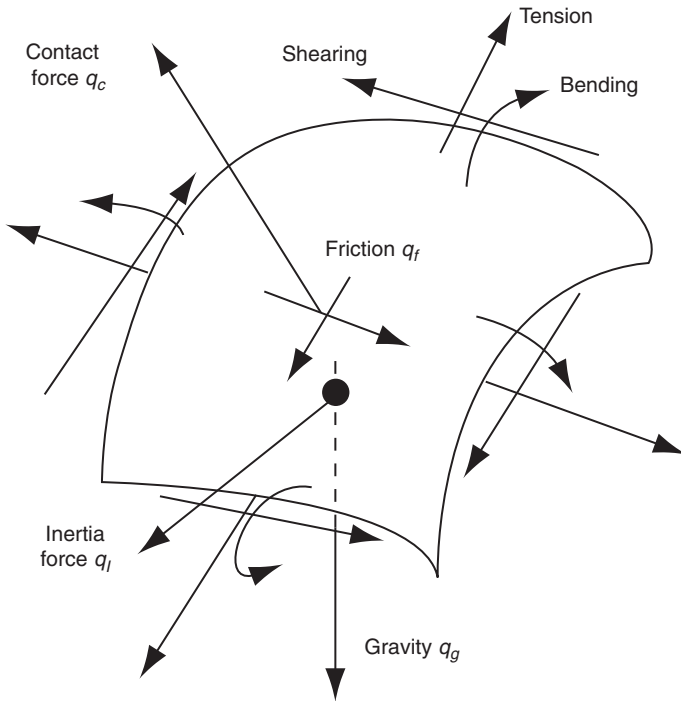
*23.1* External forces on tight-fit shorts during wear.

legs are moving continuously during the wearing process. This might cause external force to be applied to the shorts, which begin to deform. As the amount of force acting on the shorts is unknown, therefore, the female body was assumed to remain still in the standing position throughout the wearing process. It was also assumed that the frictional force between body skin and the shorts is negligible.

## 23.3    Physical properties of aerobic wear

The physical properties of the two tight-fit garments used in this study are shown in Table 23.1. Two fabrics made of different fibres with completely different mechanical properties were selected in order to study the influence of the garments on dynamic clothing pressure distribution. Each fabric sample was kept in a conditioned room for more than 24 hours with temperature and humidity of $20 \pm 2\,°C$ and $65 \pm 3\%$, respectively. In order to test the mechanical properties of the garments, which relate to the development of the numerical model, the KES tensile and shear tester, KES-FB-1, was used. The mechanical parameters of both tests were modified from the

original setting of the machine. The maximum force was set at 50 gf/cm, the sensitivity was $5 \times 5$, the tensile speed was 0.1 mm/sec, and the size of the fabric was $20 \times 20\,cm^2$. The characteristic property values and the measurement conditions for these parameters are listed in Table 23.2.

## 23.4   Biomechanical simulation

### 23.4.1  Simulated pressure changes at measured body locations

Dynamic pressure changes of two garments, C98L2 and P98L2, at seven pressure points during the wearing process were simulated. A positive pressure value indicates the force in the garment moving towards the skin when the garment does not contact the body at a particular point. A negative

*Table 23.1* Basic description of selected garments

| Garment | Thickness (mm) | Weight (g/m²) | Fibre content (%) | Construction |
|---|---|---|---|---|
| C98L2 | 0.73 | 179.00 | Cotton (98) & Lycra™ (2) | Plain knitted |
| P98L2 | 1.27 | 220.00 | Polyester (98) & Lycra™ (2) | Rib knitted |

*Table 23.2* Tensile and shear properties of selected garments

| Property | Symbol | Unit | Garment | |
|---|---|---|---|---|
| | | | C98L2 | P98L2 |
| Tensile | LT | – | 0.83 ± 0.15 | 0.78 ± 0.11 |
| | WT | gf/cm · cm² | 3.76 ± 1.62 | 6.28 ± 1.58 |
| | RT | % | 57.26 ± 12.17 | 54.02 ± 15.10 |
| | EMT | % | 24.56 ± 6.12 | 56.40 ± 37.90 |
| Shear | G | gf/cm · degree | 0.77 ± 0.02 | 0.46 ± 0.10 |
| | 2HG | gf/cm | 2.21 ± 0.14 | 1.47 ± 0.18 |
| | 2HG5 | gf/cm | 2.47 ± 0.22 | 1.57 ± 0.19 |

LT = Linearity of load–extension curve
WT = Tensile energy
RT = Tensile resilience
EMT = Tensile strain
G = Slope measured between $\phi = 0.5$ and 5.0 degrees
2HG = Hysteresis of Fs at $\phi = 0.5$ degrees
2HG5 = Hysteresis of Fs at $\phi = 5.0$ degrees

pressure value indicates that pressure on the body is induced by the garment. The pressure distribution at individual pressure points among the two garments was similar. For the pressure points on the waist girth, the pressure changes had an increasing trend until the garment passed through the hip and the trend began to decrease until the garment was totally fitted onto the body. On the other hand, the changes of pressure on garment side pelvis and thigh girth points had relatively flat and stable trends, which began to increase when the garment passed through the hip. The maximum pressures on the waist were 29 and 30 gf/cm$^2$ for garments C98L2 and P98L2, respectively.

## 23.4.2  Maxima of the predicted garment pressure measurements

Figure 23.2 compares the maxima of the predicted garment pressure measurements at different locations on the two garments. The general patterns of the two garment trends are similar. It appears that the maximum garment pressure of C98L2 is greater than P98L2 for most of the body locations except back waist. C98L2 has a lower value of tensile strain than P98L2, suggesting that more force has to be applied in order to put on C98L2 during the wear process, especially when the waist girth of the shorts passes through the pelvis of the simulated body.
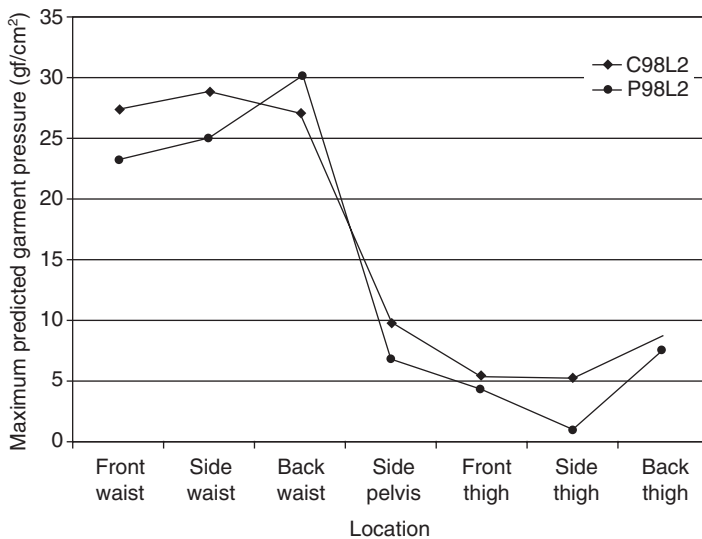


23.2 Predicted garment pressure, maximum measurements.

### 23.4.3 Simulated pressure distribution in 3D

The simulated pressure distributions of C98L2 and P98L2 from the front and back in the fitted position were determined. Based on the contour plot, the simulated pressure acting on the subject body was not uniformly distributed and was within the range of 6 to $30\,gf/cm^2$. High-pressure zones were observed on the waist girth for both garments, with a range between 18 and $30\,gf/cm^2$.

## 23.5    Validation of the model

### 23.5.1 Objective measurements of pressure distribution

Figure 23.3 compares the objective pressure measurements for the two tight-fit garments. Among the three pressure locations on the waist girth, back waist has least pressure for both garments. The subjects perceived significantly greater pressure at the front waist with C98L2 than P98L2. On average, the pressure at the waist girth is greater than at the thigh girth. ANOVA shows that there is a significant difference ($p < 0.05$) between pressure measurements of the two garments, suggesting that these two garments, which were made of different type of fabrics, provided significantly difference objective garment pressure to the wearers. In Chapter 6, the detailed ANOVA table shows that garments have a significant influence on garment pressures. Location also has a significant ($p < 0.05$) influence on this.
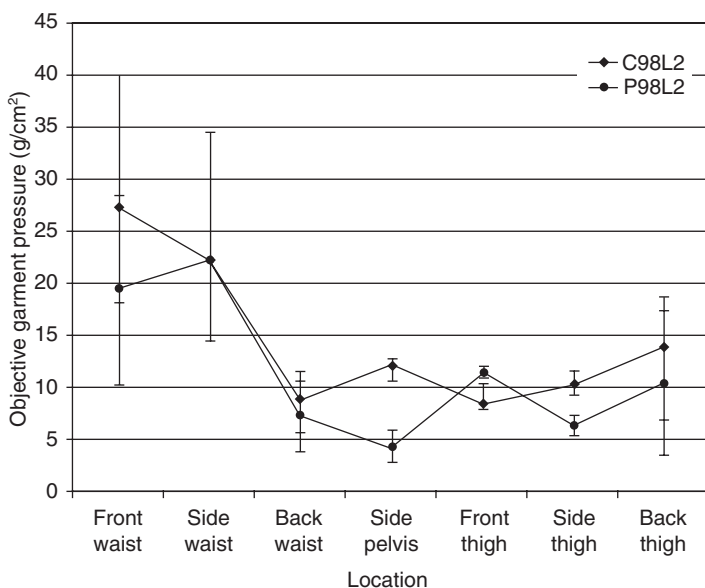


*23.3* Objective pressure measurements on two garments.

### 23.5.2  Subjective assessments of pressure distribution

Figure 23.4 compares the subjective pressure comfort rating of two tight-fit garments. It is obvious that subjects are more comfortable with C98L2 than with P98L2 when comparing the pressure comfort rating around the thigh girth. The subjective clothing pressure comfort rating and objective clothing pressure measurement have relatively larger variations at the front and side waist than other body locations. This might be explained by the variation of the subjects' waist measurements. In other words, the difference in waist measurement is larger than thigh measurement for the objective clothing pressure measurement. Furthermore, the skin sensitivity also has to be taken into account for the subjective clothing pressure comfort rating.

### 23.5.3  Comparison between experimental and simulated pressure distribution

The experimental and simulated pressure distributions of both garments were compared at seven pressure points. The trends of experimental and simulated pressure distributions are similar for both garments over the seven body locations except at the back waist. At the back waist, predicted garment pressure was higher than the measured values for
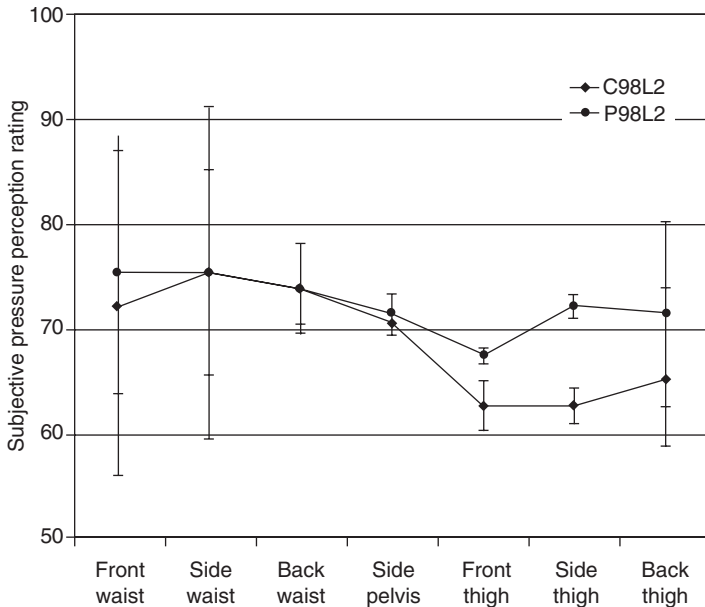


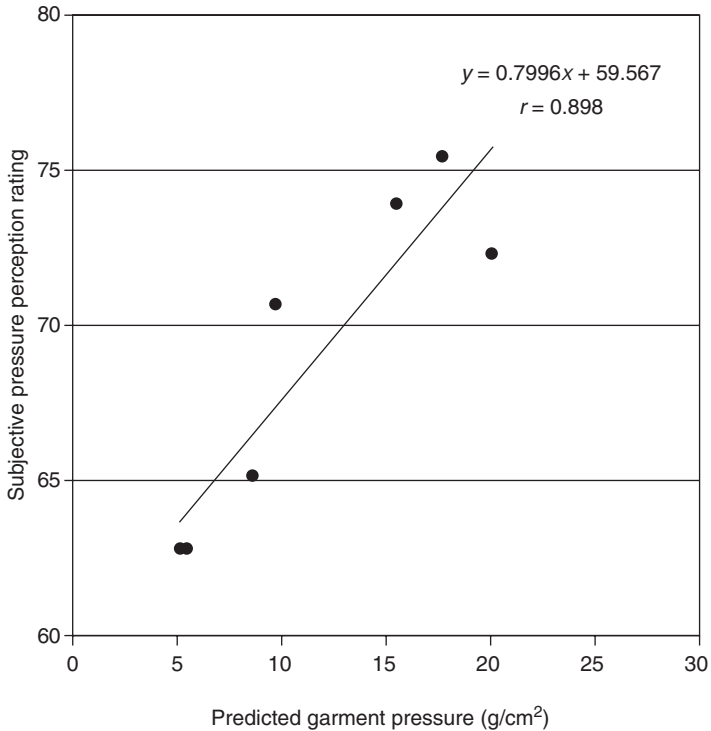*23.4* Subjective pressure perception rating of two garments.

both garments. This might be explained by the difference in the geometric contours between the simulation and the experiment. Practically, there is a hollow place between the skin and garment at the back waist, the depth of which varies from person to person. Hence, the contact force and area between skin and garment are expected to be small. However, the simulated body has no such variation, as the depth is small and garment is closely contacted with skin. Therefore, the predicted garment pressure was greater than experimental garment pressure measurement in both garments. In C98L2, both subjective pressure perception rating and predicted garment pressure measurement peaked at the front waist, followed by the points at the side waist. On the other hand, subjective pressure perception rating and predicted garment pressure measurement of P98L2 peaked at the side waist and the back waist, respectively.

### 23.5.4  Relationship between subjective garment pressure perception and predicted garment pressure measurement

Figures 23.5 and 23.6 illustrate the relationship between subjective pressure perception ratings and predicted garment pressures. Positive linear relationships between subjective rating and predicted pressure distribution are observed for both garments. For the garment made of cotton and Lycra™ (C98L2), the correlation between the two sets of data has $r = 0.90$, significant at the 0.05 level. For the garment made of polyester and Lycra™ (P98L2), the correlation between the two has $r = 0.78$ at a significance level of 0.05. This suggests that the predicted pressure of C98L2 has a slightly closer linear relationship with the subjective pressure perception rating than the predicted pressure measurement of P98L2.

The gradients of two slopes is different due to the fact that the garments are made of two different types of fabric, the mechanical properties of which are different, although the design and size are the same for both garments in the wear trial and simulation process. This suggests that the mechanical properties play an important role in clothing pressure. The measuring conditions and physical parameters of the two garments are shown in Table 23.2.
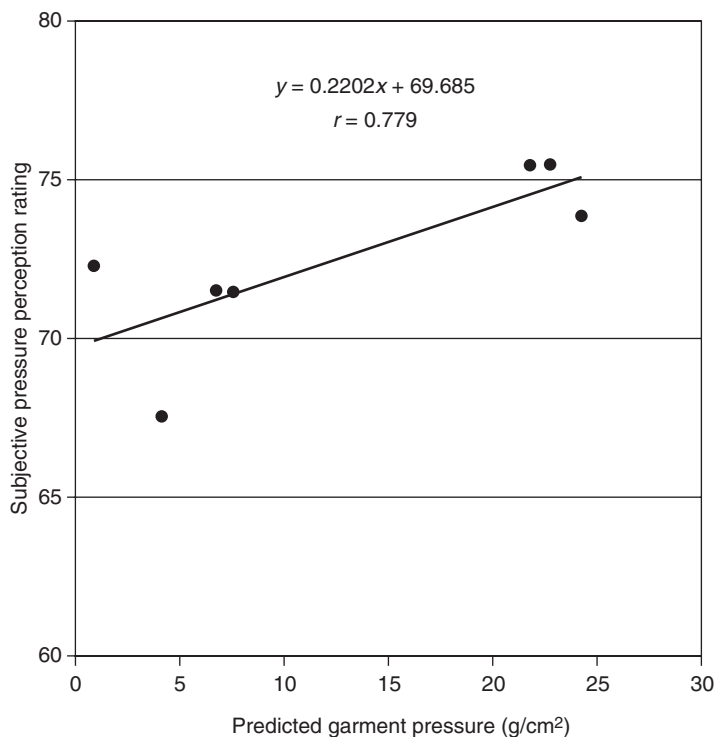
The significant relationship between subjective pressure perception and predicted pressure shows: (i) theoretical modeling is effective for prediction of pressure comfort; (ii) the physical mechanisms developed in the model are valid for the description of the perception of pressure comfort; and (iii) fabric mechanical properties influence the garment pressure distribution, and thus the subjective pressure comfort perceptions.

*23.5* Relationship between subjective pressure perception rating and predicted garment pressure (cotton/Lycra™ garment).

## 23.6   Conclusion

Clothing pressure distributions of two sets of tight-fit sportswear have been investigated by theoretical modeling and simulation. In the numerical simulation of clothing pressure, we found that pressure increased more at the waist girth than at other body locations. The pressure begins to decrease when the waist girth passes through the pelvis. Meanwhile, pressure at side pelvis and thigh girth begins to increase during the wearing process. Based on the pressure contour plot on the subject body, pressure was not uniformly distributed and a high-pressure zone was found on the waist girth for both garments. Garments made from different fibres have different pressure distributions during wear and pressures are significantly different at different body locations. Good correlations were observed between subjective pressure perception rating and predicted garment pressure, indicating that the physical mechanisms proposed in the model are valid in describing the dynamic mechanical interaction between body and garments so as to predict garment pressure comfort. Fabrics with different mechanical

*23.6* Relationship between subjective pressure perception rating and predicted garment pressure (polyester/Lycra™ garment).

properties influence the dynamic pressure distributions at contacts with the body during wear. Good agreement was found between predicted and measured garment pressure.

## 23.7   Acknowledgement

## 23.8   References

1.  Cheng, J.C.Y., Evans, J.H., Leung, K.S., Clark, J.A., Choy, T.T.C., and Leung, P.C. Pressure Therapy in the Treatment of Postburn Hypertrophic Scar – A Clinical Look into Its Usefulness and Fallacies by Pressure Monitoring. *Burns*, 1984. **10**(3): p. 154–163.
2.  Denton, M.J., Fit, Stretch, and Comfort, in *Textiles*. 1972. p. 14.
3.  Kirstein, T., Krzywinski, S. and Rodel, H., Fit optimization for close-fitting garments with regard to material properties. *Texsci-'98*, 2001. **3**: p. 398–403.

   4.  Li, Y., Zhang, X. and Yeung, K.W., A 3D Bio-Mechanical Model for Numerical Simulation of Dynamic Mechanical Interactions of Bra and Breast during Wear. *Ergonomics*, 2001.

   5.  Makabe, H., Momota, H., Mitsuno, T. and Ueda, K., A study of clothing pressure developed by the girdle. *Journal of the Japan Research Association for Textile End-Uses*, 1991. **32**: p. 424–438.

   6.  Mitsuno, T., Makabe, H., Momota, H. and Ueda, K., Studies on the Clothing Pressure (Part 1) – Measurements by a Hydrostatic Pressure-Balanced Method. *Journal of the Japan Research Association for Textile End-Uses*, 1991. **32**: p. 362–367.

   7.  Morooka, H., Nakahashi, M. and Morooka, H., Compressive property of legs and clothing pressure of pantyhose from the view point of difference in age. *Journal of the Japan Research Association for Textile End-Uses*, 1997. **38**: p. 324–332.

   8.  Pratt, J. and West, G., *Pressure garments – A manual on their design and fabrication*. 1995: Butterworth Heinemann.

   9.  Schiffman, H.R., The Skin, Body, and Chemical Senses, in *Sensation and Perception*, R.L. Gregory and A.M. Colman, Editors. 1995, Longman: London and New York. p. 70–96.

   10. Wong, A.S.W., Li, Y. and Zhang, X., *Influence of fabric mechanical property on clothing dynamic pressure distribution and pressure comfort on tight-fit sportswear.* Sen-i Gakkaishi, 2004. **60**(10): p. 293–299.

   11. Zhang, X., Li, Y., Yeung, K.W., Miao, M.H., and Yao, M., Fabric Bagging: Distribution of Stresses of Isotropic and Anisotropic Fabrics. *Journal of Textile Institute*, 2000. **91**(4): p. 563–576.

   12. Zhang, X., Li, Y., Yeung, K.W. and Yao, M., Fabric Bagging Part I: Subjective Perception and Psychophysical Mechanisms. *Textile Research Journal*, 1999. **69**(7): p. 511–518.

   13. Zhang, X., Li, Y., Yeung, K.W. and Yao, M., Fabric Bagging, Part II: Objective Evaluation and Physical Mechanism. *Textile Research Journal*, 1999. **69**(8): p. 598–606.

   14. Zhang, X., Li, Y., Yeung, K.W., Miao, M.H. and Yao, M., Fabric Bagging: Simulation and Test Method. *International Journal of Clothing of Science and Technology (submitted)*, 1998.

   15. Zhang, X., Yeung, K.W. and Li, Y., Numerical Simulation of 3D Dynamic Garment Pressure. *Textile Research Journal*, 2002. **72**(3): p. 245–252.